THE CHARACTERISTICS OF TITANIUM TETRACHLORIDE PLASMAS IN A TRANSFERRED-ARC SYSTEMS

a

THESIS

by

Panayotis G. Tsantrizos

Department of Chemical Engineering - McGill University

Under the Supervision of Dr. W.H. Gauvin

Submitted to the Faculty of Graduate Studies
and Research of McGill University in partial
fulfillment of the requirements for the
degree of Doctor of Philosophy

McGill University
Montreal, Canada

March 1988

ISBN 0-315-45931-X

THE CHARACTERISTICS OF TITANIUM TETRACHLORIDE ARCS

to my parents

who loved and toiled

for my creation

THE CHARACTERISTICS OF TITANIUM TETRACHLORIDE PLASMAS IN A TRANSFERRED-ARC SYSTEM

by

B. Tsantrizos

ABSTRACT

A stable transferred arc was produced with plasmagas containing up to 20 percent molar $TiCl_4$ in argon, helium and argon/hydrogen mixtures. This was achieved by replacing the commonly-used thoriated tungsten cathode tip with a tantalum carbide tip. Thus, corrosive reactions at the cathode surface, which were shown to be the cause of the observed instability, were prevented. This allowed the characteristics of stable titanium tetrachloride plasmas in a transferred arc reactor to be investigated.

Furthermore, an investigation was conducted into the feasibility of collecting titanium metal from the dissociated $TiCl_4$ molecule in the plasmagas. The titanium metal was collected in a molten bath, which also served as the anode in the transferred arc system. Three anode bath compositions were used in this study. Two of them, namely titanium and zirconium, were not able to reduce recombined titanium subchlorides in the bath. The third aluminum, was a reducing bath. When aluminum was used, about 60 percent of all titanium fed into the reactor was collected.

Finally, phenomena occurring on the surface of a thoriated tungsten cathode were studied in a transferred-arc reactor using argon or helium as the plasmagas. The effect of cathode geometry on the rate and mechanisms of cathode erosion were investigated. It was shown that the surface temperature of flat-tip cathodes operating in argon is near the melting point of tungsten. On the other hand, the surface temperature of flat-tip cathodes operating in helium and pointed-tip cathodes operating in either helium or argon are near the boilint point of tungsten. Some of the material vapourized from the cathode was redeposited on the cathode surface, forming crystals whose morphology and composition depended on their distance from the arc root and the plasmagas composition.

Being a seeker of truth is not just a matter of having the right ideas. It is a journey of the whole person which requires just the perfect blend of tolerance, scepticism, and reflection. It is the discovery of a virgin world within as it may have existed prior to the alterations imposed by the ego.

seeker of truth

follow no path

all paths lead where

truth is here

poem by: e.e. cummings

LES CARACTÉRISTIQUES D'UN PLSMA DE TETRACHLORURE DE TITANE DANS UN ARC TRANSFÉRÉ

par:

P. Tsantrizos

RÉSUMÉ

Un arc transféré d'excellente stabilité contenant jusqu'à 20 pourcent de tetrachlorure de titane dans des plasmas d'argon d'hélium ou d'un mélange d'argon et d'hydrogène, a été obtenu en remplaçant la pointe en tungstène thorié de la cathode par du carbure de tantale. Ceci a démontré que l'instabilité notoire en présence du tungstène était due à des réactions corrosives sur la surface de la cathode. La stabilité ainsi obtenue a permis l'étude des caractéristiques de plasma de $TiCl_4$.

Une investigation a aussi été conduite sur la faisabilité de récupérer du titane métallique à partir de vapeur de $TiCl_4$ dissociée dans un plasma d'argon, en utilisant des bains de métaux fondus comme anodes dans le système d'arc transféré. Des bains de titane ou de zirconium n'ont pas été capables de réduire les sous-chlorures de titane. Un bain d'aluminium, d'un autre côté, étant un bon réducteur, a réussi à collecter environ 60% du titane injecté dans le réacteur.

Finalement, les phéhomènes ayant lieu à la surface d'une cathode de tungstène thorié ont été étudiés dans un réacteur utilisant des arcs transférés d'argon ou d'hélium. L'étude a surtout porté sur la géométrie de la cathode et le taux et mécanisme d'érosion de cette dernière. Il a été démontré que la température d'une cathode au bout aplati opérant dans de l'argon était proche du point de fusion du tungstène, tandis que dans l'hélium ou avec des bouts pointus dans l'argon ou l'hélium, la température était proche du point d'ébullition. Une partie du métal vaporisé au pied de l'arc était redéposé sur la surface de la cathode, formant des cristaux dont la morphologie et composition dépendaient de la distance du pied de l'arc et de la nature du gaz formant le plasma.

ACKNOWLEDGEMENTS

A thesis represents not only what the author has contributed to his field of studies but also what life has contributed to the author. Unfortunately, acknowledging individually all those who have contributed to my life, my parents, wife, children, friends, relatives, teachers, scientists and poets, would be an overambitious task. I must, therefore, thank all of these contributors collectively and limit individual acknowledgements to those who have directly contributed to the preparation of this document and the execution of the research reported within.

First of all, I would like to thank my friend and colleague V. Jariwala who made important contributions to this thesis in general and to the study of cathode deterioration in particular. I also would like to thank all the members of the McGill plasma group and especially Prof. R.J. Munz, Prof. D. Burk, P. Patterson, E. Chin, Dr. J.-L. Meunier, R.N. Szente and P. Stuart, who along with Prof. J.M. Dealy and Prof. J.H. Vera, and friends N. Poirier and J. Fallavollita contributed their time and effort in so many relevant discussions.

Special thanks to A. Krish and the Chemical Engineering Workshop staff including A. Gagnon and J. Dumont without whose contribution this experimental work would not have been possible.

I also would like to thank G. Bata and the staff of the Industrial Materials Research Institute who supported my research and contributed their resources and ideas to it. I am especially thankful to J. Tremblay who typed and edited this thesis and M. Lapalme who made similar contributions during the preparation of the proposal for this research.

Finally, I would like to thank four very special people who helped and helped and helped. Dr. W.H. Gauvin, Prof. M. Weber (McGill University), Dr. M.G. Drouet (Hydro-Quebec Research Institute) and Holly (my wife) thank you so much. This task could not have been completed without you.

TABLE OF CONTENTS

GENERAL INTRODUCTION

PART I. STABILITY AND OPERATING CHARACTERISTICS OF A TITANIUM TETRACHLORIDE TRANSFERRED-ARC

PART II. CATHODE DETERIORATION PHENOMENA IN A TRANSFERRED-ARC REACTOR

PART III. AN ASSESSEMENT OF THE POTENTIAL OF RECOVERING TITANIUM METAL IN THE MOLTEN ANODE OF A TRANSFERRED TITANIUM TETRACHLORIDE ARC

LIST OF FIGURES

GENERAL INTRODUCTION

PART ONE

PART II

PART THREE

LIST OF TABLES

GENERAL INTRODUCTION

PART ONE

PART TWO

PART THREE

GENERAL INTRODUCTION

INTRODUCTION

Titanium is truly a progeny of the 20th century, a structural metal of great potential with unique physico-chemical and mechanical properties. Its high strength-to-weight ratio offers ideal applications in the aerospace industry, while its oustanding corrosion resistance, particularly inorganic chlorides which attack stainless steel, offers distinct advantages for the fabrication of equipment for water desalination plants, the marine industry, the production of ferric and cupric chlorides, and the paper, plastics and detergent industries. Reviews of the applications of titanium are given by Kane and Boyd (1981), Farthing (1985), and Froes (1987).

The reserves of titaniferous ores in the earth's crust are quite considerable, making titanium potentially one of the most widespread commercial metals. It is the ninth most abundant element in the lithosphere and accounts for 0.63 % of the total. Of all structural metals only aluminum, iron and magnesium are more common. Titanium-containing minerals such as ilmenite ($FeTiO_3$) and rutile (TiO_2) are found in many parts of the world including Australia, Norway, Canada, the U.S.A. and the U.S.S.R. (Energy, Mines and Resources Canada, 1984).

Despite the metal's exceptional properties and relative abundance, the applications of titanium have been limited by the high processing cost and severe operating problems associated with its production. A brief look at the economics of producing titanium based on the cost of the ore and intermediate compounds is given in Table I. Over half of the cost of titanium can be attributed to the consolidation of the sponge into dense metal. Only 3 % of the total cost is attributable to the ore. Substantial reductions in production costs would dramatically improve titanium's competitiveness in areas where its properties would be desirable and increase its rate of consumption. Figure 1 gives comparative annual production rates of aluminum, magnesium and titanium, on a semi-logarithmic scale. As shown in the graph, the commercial use of titanium has a relatively short history and is still in the growing stage, albeit at a much lower rate than its two competitors.

Most of the titanium metal produced today is obtained by first chlorinating titanium oxide (rutile) to titanium tetrachloride and then reducing the chloride to the metal. A simplified flowsheet of the process is shown in Figure 2. Titanium tetrachloride is made by the thermal chlorination of rutile in the presence of carbon according to the equation:

$$2TiO_2 + 4Cl_2 + 3C \rightarrow 2TiCl_4 + 2CO + CO_2$$

$$(\Delta F^\circ = -45.6 \text{ kJ/mol at } 1{,}000^\circ\text{C})$$

TABLE I. ECONOMICS OF TITANIUM PRODUCTION

COMPOUND	PRICE (US$/kg)	VALUE OF CONTAINED TITANIUM (US$/kg)	% OF TITANIUM METAL PRICE
TiO_2 (rutile ore)	0.56 [1]	0.93	4
$TiCl_4$ (tech. bulk)	0.66 [2]	2.61	12
Ti sponge (99.3%)	9.13 [3]	9.19	43
Ti metal (comm. pure)	21.45 [3]	21.45	100

Notes: [1] Effective: Sept. 1986 Engineering and Mining Journal

[2] Effective: Oct. 1986 Chemical Marketing Reporter

[3] Effective: Oct. 1986 American Metal Market

FIGURE 1

WORLD PRODUCTION OF ALUMINUM, MAGNESIUM AND TITANIUM

Source: Ikeshima (1985)

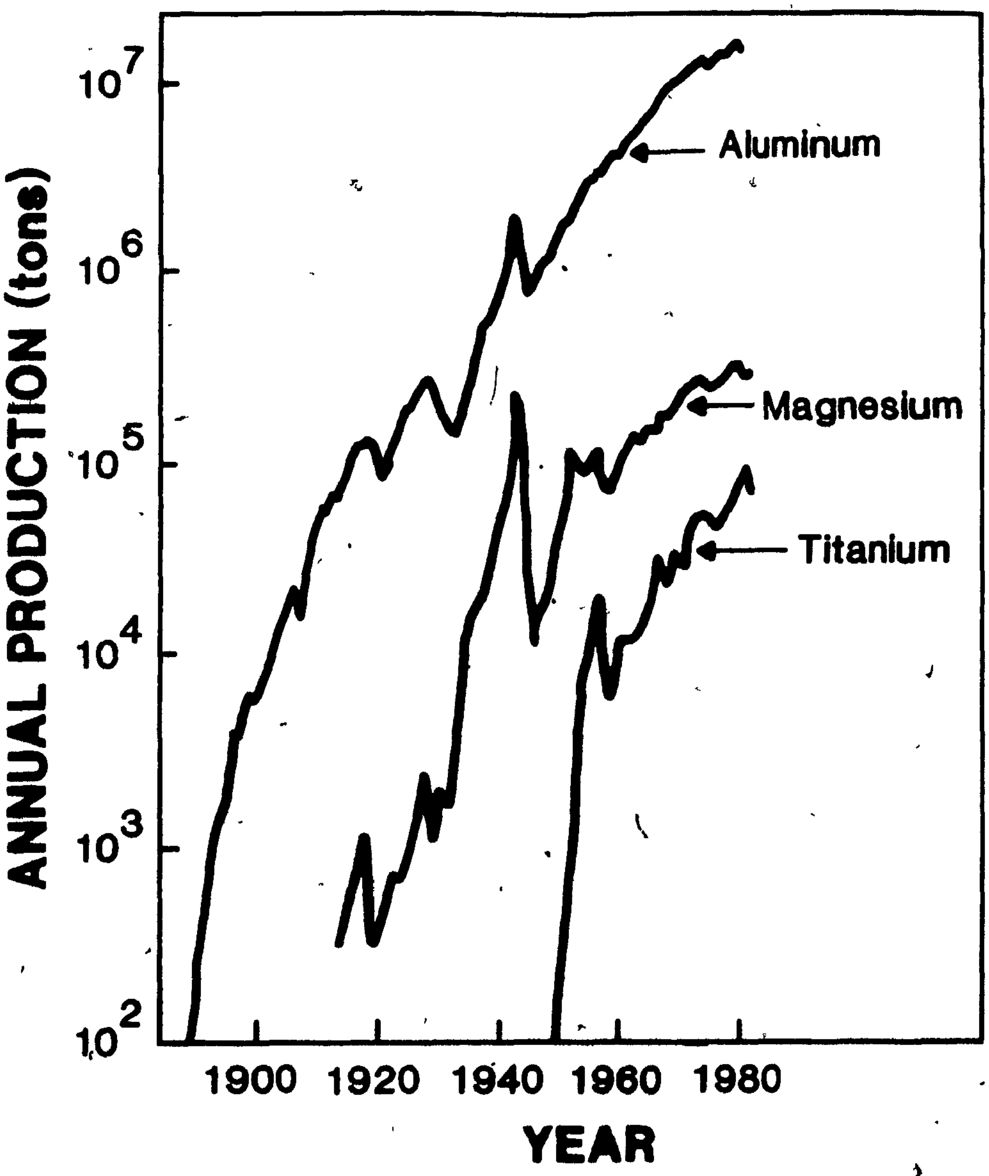

ANNUAL PRODUCTION (tons)
10^7
10^6
10^5
10^4
10^3
10^2
1900
1920
1940
1960
1980
YEAR
Aluminum
Magnesium
Titanium

FIGURE 2

TITANIUM PRODUCTION - THE KROLL PROCESS

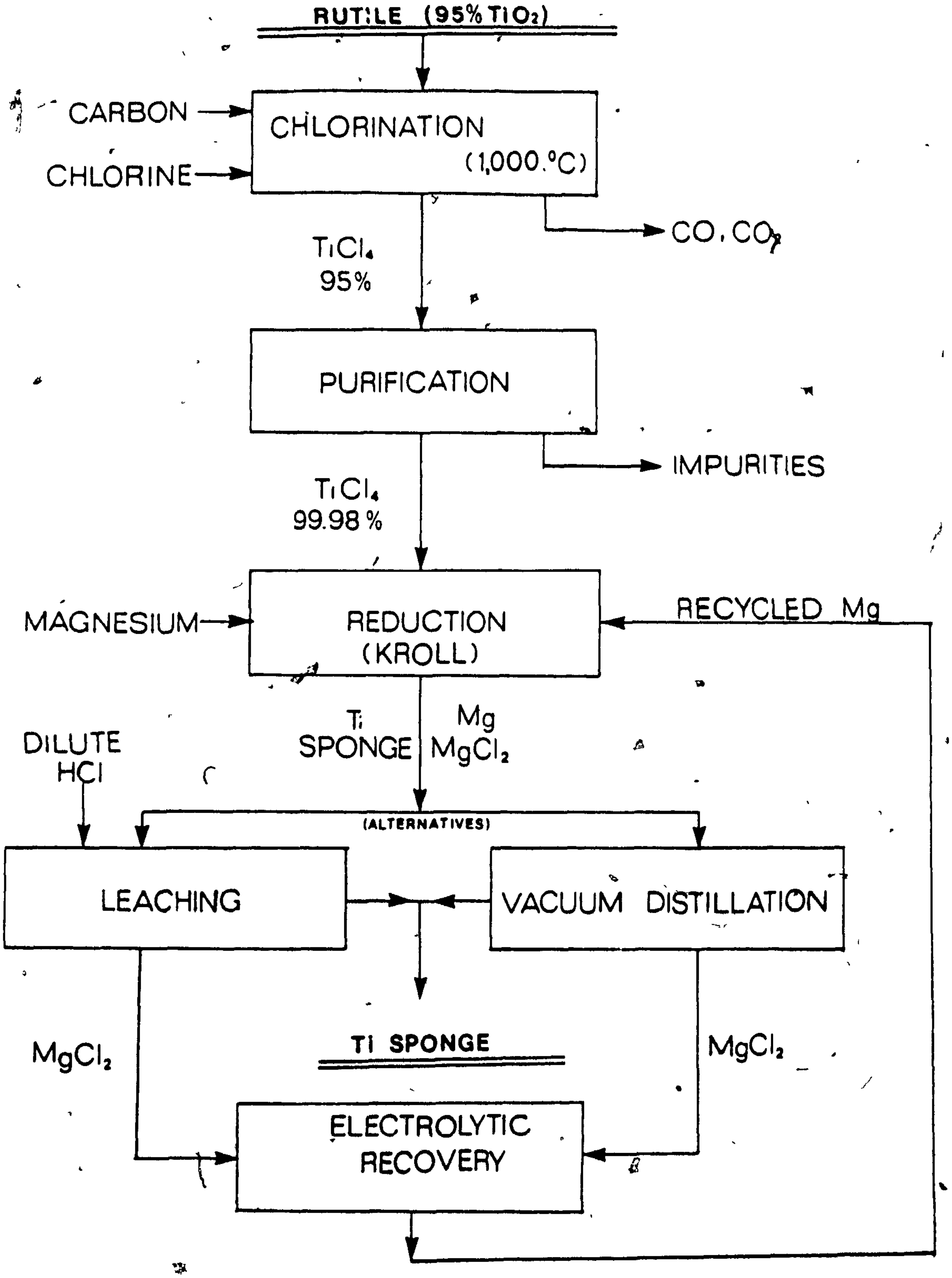
RUTILE (95% TiO_2)
CARBON
CHLORINE
CHLORINATION
(1,000 °C)
CO, CO_2
$TiCl_4$
95%
PURIFICATION
IMPURITIES
$TiCl_4$
99.98 %
MAGNESIUM
REDUCTION
(KROLL)
RECYCLED Mg
Ti
SPONGE
Mg
$MgCl_2$
DILUTE
HCl
(ALTERNATIVES)
LEACHING
VACUUM DISTILLATION
$MgCl_2$
TI SPONGE
$MgCl_2$
ELECTROLYTIC
RECOVERY

The crude titanium tetrachloride (containing impurities such as silicon and carbon tetrachloride, vanadium oxychloride, and ferric and aluminum chlorides) is first purified and then reduced to titanium metal using sodium or magnesium as a reducing agent. The sodium reduction, known as the Hunter process (Hunter, 1910) occurs at a temperature of 700°C according to the equation:

$$TiCl_4 + 4Na \rightarrow Ti + 4NaCl$$

$$(\Delta F^\circ = -946\ 420 + 65.2T\ \mathrm{J/mol},\ T\ \mathrm{in\ K})$$

Both, the Hunter and the Kroll processes produce titanium sponge which must be first separated from the respective chlorides and then consolidated to its valuable dense metal form. Table II lists the production capacity and method of titanium sponge production in some titanium-producing companies. An extensive review of the reserves, uses and production of titanium is given by Barksdale (1966). Further details on the metallurgy of titanium is provided by McQuillan and McQuillan (1956).

The cost and operating difficulties associated with both the Hunter and the Kroll processes have encouraged metallurgists to search for alternative methods of producing the metal. Some of these methods involve the direct reduction of titanium dioxide to the metal. Others have proposed an electrolytic process using a bath of fused salts to reduce titanium tetrachloride to titanium metal. These processes and

TABLE II. PRODUCTION CAPACITY OF TITANIUM SPONGE (tons/yr)

JAPAN		
Osaka Titanium	18 000	Mg Reduction - Vacuum Distillation
Toho Titanium	12 000	Mg Reduction - Vacuum Distillation
Nippon Soda	2 400	Na Reduction - Leaching
Showa Titanum	2 000	Mg Reduction - Vacuum Distillation
Total	34 400	
U. S. A.		
TIMET	14 500	Mg Reduction - Leaching
RMI	8 600	Na Reduction - Leaching
OREMET	4 100	Mg Reduction - He Sweeping
International Titanium	3 600	Mg Reduction - Vacuum Distillation
Teledyne Wah Chang	1 400	Mg Reduction - Vacuum Distillation
Total	32 200	
U. K.		
Deeside Titanium	5 000	Na Reduction - Leaching
Total	5 000	
U.S.S.R.	45 000	Mg Reduction - Vacuum Distillation
CHINA	3 000	Details not known
World Total	**119 600**	

Source: Ikeshima (1985).

others are thoroughly reviewed by Barksdale (1966) and Ikeshima (1985). The most successful of these new processes is employed by Albany Titanium Inc. It produces titanium sponge continously from ilmenite, using a process developed by Occidental Research Corp. (American Metal Market, 1983). The process reacts ilmenite with sodium fluorosilicate to form sodium fluorotitanate which is then reduced with aluminum-zinc alloy, producing titanium-zinc alloy,from which, by evaporating zinc, titanium sponge is obtained (Hard et al., 1983)

A process of particular interest to this study involves the direct reduction of $TiCl_4$ to the metal in high temperature plasmas. The basic idea in this process is to thermally dissociate the $TiCl_4$ molecule into its monoatomic constituents and capture the titanium before it can recombine with the chlorine. An extensive review of efforts relative to this process is given as background information in Part III (An Assessment of the Potential of Recovery Titanium Metal in the Molten Anode of a Transferred Titanium Tetrachloride Arc) of this thesis.

The present thesis is divided into three main parts, each covering specific areas of the study. Part I deals with the stability, voltage-current and energy distribution characteristics of transferred arc plasmas which utilize mixtures of $TiCl_4$ with hydrogen, argon and helium as the plasmagas. Part II focuses on the thermal erosion of a thoriated tungsten cathode in a transferred arc reactor which utilizes argon or helium as the plasmagas. Finally, Part III assesses the technical feasibility of producing titanium by dissociating the $TiCl_4$ molecule in a hot plasma and recovering the metal in a molten bath anode. Each of the three parts is "self-standing" and includes the relevant sections of literature review, experimental results, discussion and conclusions. The experimental apparatus used in the study is common to all parts and is described fully in Part I. A brief review of the chemistry of titanium and its halides is considered relevant and is thus included in Appendix I. General reviews of plasma phenomena and plasma generating devices are also included as background information.

PLASMA PHENOMENA AND PLASMA DEVICES

Definition of Plasma

Matter can exist in nature in four different states: solid, liquid, gas, and plasma. When enough energy is added to a gas, the kinetic energy of the molecules increases and molecular impacts become so intense that dissociation into atoms occurs, followed by the separation of one or more of the electrons in specific orbits around the atom nucleus. When enough atoms are thus ionized, the free charges (ions and electrons) cause significant changes in the physical properties of the particular matter, and the gas is said to have changed into the plasma state. Thus, a plasma is a mixture of positively charged, negatively charged and neutral particles. It is on the average neutral since the density of the positive charges is equal to that of the negative charges.

Up to 99 percent of the matter in the universe exists in the plasma state, making plasma by far the most common form of matter. It is also the most energetic state. While a body requires only an average of 10^{-2} eV per particle to change its state from solid to liquid or from liquid to gas, it requires from 1 to 30 eV per particle to change from gas to plasma (Kettani and Hoyaux, 1973).

Plasmas have been conveniently classified into two broad categories. The first is known as cold or low-pressure plasmas and includes the Towsend or dark discharge, which carries currents up to 10^{-6} A, and glow discharge, which carries currents from 10^{-6} A to 10^{-1} A (Howartson, 1976). The second category is known as the hot or thermal plasma which operates at or above atmospheric pressure and carries currents higher than one ampere. In these plasmas, local thermodynamic equilibrium (LTE) often exists among the electrons, atoms and ions, thus making it possible to characterize them in terms of transport and energy-temperature relationships. Thermal plasmas formed by electrical discharges typically have temperatures between 2 500 and 30 000 K and ionization levels greater than 0.1 percent (Howartson, 1976). Thermal plasmas, also known as arcs, have been used in a number of high-temperature, chemical and metallurgical processes and they are the only ones relevant to this study. For this reason, all further discussion will be restricted to this type of plasma.

Electric Features of Arc Plasmas

When an electric current is to be passed between two electrodes in a gas, three processes must take place:

a. The current must be transfered across the cathode-gas junction.

b. The current must be conducted through the body of the gas. For this to be possible, the normally neutral gas must be rendered conducting by the introduction of charged carriers, or by their creation within it, or both.

c. The current must be transferred across the gas-anode junction.

In the electric arc, three distinct regions can be recognized, corresponding to the three processes listed above. A schematic representation of the conventional arc displaying in addition the voltage distribution along the length of the arc is shown in Figure 3. The three regions are known as the cathode fall, the anode fall and the arc column. Phenomena relevant to the cathode and anode fall regions have been discussed respectively in Parts II and III of the present thesis. Only some general characteristics of the arc column will be mentioned in this section.

FIGURE 3

SCHEMATIC REPRESENTATION OF THE ARC AND CHARACTERISTIC VOLTAGE DISTRIBUTION

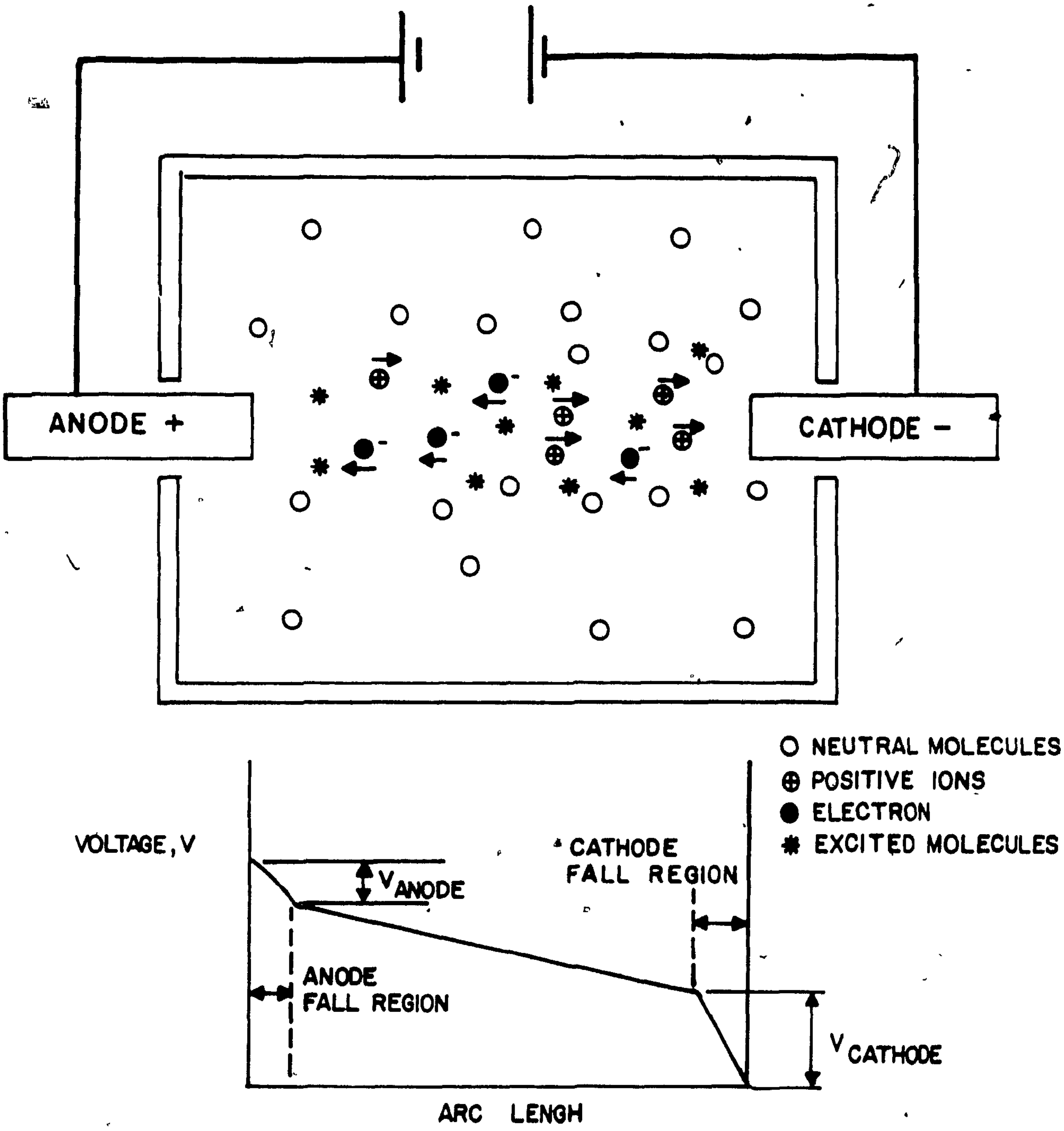
ANODE +
CATHODE -
○ NEUTRAL MOLECULES
⊕ POSITIVE IONS
● ELECTRON
✱ EXCITED MOLECULES
VOLTAGE, V
V ANODE
CATHODE FALL REGION
ANODE FALL REGION
V CATHODE
ARC LENGH

The Arc Column

The arc column constitutes the major component of a transferred arc and it is the region best understood by the researchers in this field. Extensive reviews of the phenomena and parameters occuring in the column can be found in the theses of Choi (1981) and Mehmetoglu (1980). Also the texts by Somerville (1959) and Hellun (1961) are very useful in explaining the basic concepts.

The arc column is hotter than the regions in the immediate neighbourhoods of the two electrodes. The column conducts because of the presence of charge carriers of both signs within it. The composition and temperature of the column are a function of the net energy input, the nature of the gas and the gas pressure. It is important to note that the number densities of electrons and positive ions must always be approximately equal. The charge neutrality can be explained by the fact that if a predominance of one charge existed the whole column would be disrupted by the repulsive forces existing between charges of the same sign (Coulomb repulsion). Therefore, in order to have electrostatic stability it is required that the arc column be quasi-neutral.

The presence of quasi-neutrality does not mean that electrons and ions carry equal amounts of energy to the column. Although both electrons and ions fall through the same potential, the electrons do it much more quickly due to their smaller mass. The main carrier, therefore, by which the external electrical supply feeds power to the arc column is the electron constituent of the plasma. Equation (1) expresses the arc-current density (**j**) as the sum of the electron current and ion current (Somerville, 1959):

$$j = n_e ev_e + n_i ev_i \text{ (A/cm}^2\text{)} \tag{1}$$

In the above equation **n_e** and **n_i** are the electron and ion number densities, respectively, and have typical values in the range of 10^{12} - 10^{15}/cc (Hellund, 1961). The magnitude of the charge of either electrons or ions is **e**, and **v_e** and **v_i** are the electron and ion drift velocities, respectively. Normally, the ion drift velocity is smaller by a factor of the order of several hundreds (Somerville, 1959) than the drift velocity of electrons. Thus, it can be seen that the current is carried mainly by the electrons.

The different components of the plasma, namely the electrons, positive ions and neutral molecules, are not in thermal equilibrium. The reason for this is that the ions do not pick up energy from the field as readily as electrons due to their greater mass. Hence, the electrons are always at the highest temperature in the arc plasma, the ions are cooler and the neutral molecules are at the lowest temperature. The degree of departure from thermal equilibrium depends on the gas pressure and temperature. High pressure plasmas are normally close to ideal equilibrium and their state is denoted as "Local Thermodynamic Equilibrium" or LTE.

Plasma Devices

A number of reviews have been published on the different types of available plasma-generating devices and their applications. The interested reader is referred to a thorough review published recently by the U.S. National Materials Advisory Board (1985). In general thermal-plasma-generating devices have been divided into three categories: the induction torch, the d.c. jet torch and the transferred arc. Variations of these three devices have been used in laboratories and in industry.

i. The Induction Torch

These types of plasma generators are electrodeless as compared to the d.c. torch and the transferred arc, where the plasma operates between electrodes. The energy is transferred to the gas from a high frequency (1-10 Mhz) source by a coil, resulting in an inductive coupling between the electric and magnetic fields (Munz 1974).

Most laboratory induction plasma torches consist of a multi-turn, water-cooled copper induction coil surrounding a quartz tube which contains the plasma. The quartz tube can be air or water-cooled, depending on the power at which the torch is designed to operate.

The absence of electrodes avoids contamination of the plasma system from the possibly evaporating electrode material and permits the use of highly corrosive gases, such as chlorine, as the plasma constituent (Biceroglu, 1978). Since they were first described by Reed (1961), induction torches have found applications as light sources, in spheroidization, crystal growing, and chemical synthesis. A review paper by Eckert (1974) and a book by Baddour and Timmins (1967) describe a large number of such applications. The use of an induction torch in the production of an argon plasma containing 1 percent titanium tetrachloride was investigated by Miller and Ayen (1969).

ii. The d.c. Plasma Torch

The d.c. plasma torch consists of a conical, water-cooled cathode surrounded by an annular water-cooled anode, which is terminated by a constricting nozzle. The arc is struck between the electrodes and ionizes the plasmagas which flows between the electrodes and exits through the nozzle as a high temperature jet. The axial temperatures attainable in this type of torch can range between 9 000 and 30 000 K.

Lewis and Gauvin (1973) found the temperature in the cone of an argon plasma, using a d.c. torch, to be about 13 000 K. The plasma flame from these torches is characterized by very high velocities, steep velocity and temperature gradients, and high turbulence, although a long laminar flame can also be produced under certain operating conditions.

Hamblyn (1977), and Bokhari and Boulos (1980) give a review of the different modifications made to the basic d.c. torch in order to improve its efficiency and stability. Still, a number of limitations are inherent in this type of plasma-generating device. The high currents used in the d.c. torch can cause a rapid erosion of the electrodes, contributing considerably to the total operating cost. Furthermore, due to corrosion problems at the electrodes, only inert gases such as argon, helium and nitrogen, or reducing gases such as ammonia and hydrogen, can be used. Nonetheless, the d.c. plasma torch is used extensively by industry for spraying, cutting and welding.

In general, the d.c. torch is simple in construction, reliable in operation and its steep temperature gradient at the arc can be useful in homogeneous reactions where a rapid quench is required. In the McGill Plasma Laboratoy, the d.c. plasma torch has been used for a number of studies on heat and momentum transfer to particles (Kubanek and Gauvin, 1968), (Lewis and Gauvin, 1973), (Katta and Gauvin, 1973). More recently, d.c. torches have been used at McGill to superheat steam which in turn was used either as the drying medium for the spray-drying of non-heat-sensitive meterials (Amelot, 1983) or as a reactive medium in the gasification of peat (Grosddier, 1982) and the hydrocracking of heavy oils (Kubanek, 1985).

iii. The Transferred Arc

The transferred arc differs from the d.c. torch in a number of important ways. In this device, the arc is struck between two widely separated electrodes. Most often the largest dissipation of energy here is at the anode face. Therefore, if the anode is made the work piece, as it is in the case of metal cutting, or the reactant, as in the case of a pool of molten metal, the energy efficiency can be made quite high.

In the basic design of a transferred-arc system, a conical, cooled cathode is closely surrounded by a conical nozzle. The plasma-forming gas is injected through the gap between the nozzle and the cathode tip, as a high velocity stream, into the arc column (Sheer et al., 1969). The cathode tip is cooled internally through a water-cooling system and externally by the injected gas through convection. This tends to minimize material losses from the cathode. This type of configuration is known as the Fluid Convective Cathode (FCC). It was also found that the imposed electric field in the arc column creates a continuous discharge resulting in a high current flow which gives rise to a magnetic field. The plasmagen is drawn into the arc and forms a high-temperature, high-velocity jet (the so-called cathode jet) travelling along the arc axis, and impinging on the anode in relatively short arcs. The pressure gradient around the cathode can be calculated by the magneto-hydrodynamic theories (MHD), and is called the "Maecker Effect" (Somerville, 1959).

Sheer et al. (1974) in a later publication described a double shrounded FCC for the injection of reactive gases and for particles into the arc column. While non-reactive gases such as argon, helium and nitrogen, are fed through the inner nozzle to protect and cool the cathode, the reactive gases and/or particles are fed through the outer annulus. This technique would allow for the treatment of highly reactive gases such as titanium tetrachloride. However, since the gas in the outer shroud relies exclusively on the energy contained in the inner nozzle plasmagas to meet its thermal and chemical energy requirements, there is an upper limit to the quantity of the outer shroud gas that can be treated in this manner. A qualitative assessment of this limit for $TiCl_4$ is presented in Part I.

Transferred arcs are constricted by magnetic forces in the plasma column, resulting in a small column diameter with steep axial and radial temperature, velocity and current density profiles. The characteristics of these arcs have been thoroughly investigated experimentally at McGill University (Mehmetoglu and Gauvin, 1983; Choi and Gauvin, 1982; Tsantrizos and Gauvin, 1982). Extensive modeling work has been performed at the University of Minnesota under the leadership of Prof. E. Pfender (Hsu and Pfender, 1984; Hsu et al., 1983; Dinulescu and Pfender, 1980).

REFERENCES

Amelot, M.P., "Spray Drying With Plasma-Heated Water Vapour", M. Eng. Thesis, McGill University (1983).

American Metal Market, Oct. 21, 1983.

Baddour, R.F. and R.S. Timmins, "The Application of Plasma to Chemical Processing", M.I.T. Press (1967).

Barksdale, Jelks, "Titanium - Its Occurence, Chemistry and Technology", 2nd ed., The Ronald Press Company, New York, (1966).

Biceroglu, O., "Chlorination Kinetics of ZrO_2 in an Rf Plasma Tailflame", Ph. D. Thesis, McGill University (1978).

Bokhari, A. and M. Boulos, "Energy Balance for a DC Plasma Torch", Can. J. of Chem. Eng., 58, (4), 171 (1980).

Choi, H.K. and W.H. Gauvin, "Operating Characteristics and Energy Distribution in Transferred Plasma Arc Systems", Plasma Chemistry and Plasma Processing, Vol. 2, No. 4, pp. 361-387 (1982).

Choi, H.K., "Energy Distribution and Heat Transfer in an Argon Transferred-Arc Reactor", Ph.D. Thesis, McGill University (1981).

Dinulescu, H.A. and E. Pfender, "Analysis of the Anode Boundary Layer of a High Pressure-High Current Arc", J. Appl. Phys., Vol. 51, p. 3149 (1980).

Eckert, H.W., "The Induction Arc: A State of the Art Review", High Temp. Scie., 6, pp. 99-134 (1974).

Energy, Mines and Resources Canada, "Canadian Minerals Yearbook, 1982", Mineral Report No. 32, Minister of Supply and Services Canada (1984).

Farthing, T.W., "Applications of Titanium and Titanium Alloys", Titanium-Science and Technology, Proceedings of the 5th International Conference onTitanium, Sept. 10-14, 1984, Munich, FRG, pp. 39-54, (1985).

Froes, F.H., "Titanium Products and Applications", Journal of Metals, 39, 3,pp. 12-14, (1987).

Grosdidier de Matons, [illegible]., "Peat Classification in a Plasma-Heated Concurrent Reactor", M. Eng. Thesis, McGill University (1982).

Hamblyn, S.M.L., "A Review of Applications of Plasma Technology with Particular Reference to Ferro-Alloy Production", National Inst. for Metall., Rep. No. 1895 (1977).

Hard, R.A.,et al., US Patent 4,390,365, (1983).

Hellund, E.J., "The Plasma State", Reinhold (1961).

Howatson, A.M., "An Introduction to Gas Discharges", 2nd. ed., Permagon (1976).

Hsu, K.C. and E. Pfender, "Modeling of a Free-Burning, High-Intensity Arc at Elevated Pressures", Plasma Chemistry and Plasma Processing, Vol. 4, No. 3, pp. 219-34 (1984).

Hsu, K.C, K. Etemadi and E. Pfender, "Study of the Free-Burning High Intensity Argon Arc", J. Appl. Phys., Vol. 54, No. 3, pp. 1293-301 (1983).

Hunter, M.A., J. Amer. Chem. Soc., 32, 330 (1910).

Ikeshima, T., "Recent Developments in Titanium Sponge Production", Titanium-Science and Technology, Proceedings of the 5th International Conference on Titanium, Sept. 10-14, 1984, Munich, FRG, pp. 3-14 (1985).

Kane, R.D. and W.K. Boyd, "Use of Titanium and Zirconium in Chemical Environments", from "Industrial Applications of Titanium and Zirconium", ASTM Special Technical Publication 728, E.W. Kleefisch (ed.) (1981).

Katta, S. and W.H. Gauvin, "The Effect of Local Gas Velocity and Temperature on Local Heat Transfer to a Sphere in a High-Temperature Jet", Can. J. of Chem. Eng., 51, 307 (1973).

Kettani, M.A. and M.F. Hoyaux, "Plasma Engineering", Butterworth & Co. (1973).

Kroll, W.J., Trans. Electrochem. Soc., 78, 35 (1940).

Kubanek, G., "Heavy Oil Processing in Steam and Hydrogen Plasmas", M. Eng. Thesis, McGill University (1985).

Kubanek, G.R. and W.H. Gauvin, The Chemical Engineer, 332 (1968).

Lewis, J.A. and W.H. Gauvin, "Motion of Particles Entrained in a Plasma Jet", A.I.Ch.E. J., 19, (5), 982 (1973).

McQuillan, A.D. and M.K. McQuillan, "Titanium-Metallurgy of the Rower Metals-4", Butterworths Scientific Publications, London (1956).

Mehmetoglu, M.T., "Characteristics of a Transferred-Arc Plasma", Ph.D. Thesis, McGill Unversity (1980).

Mehmetoglu, M.T. and W.H., Gauvin, "Characteristics of a Transferred-Arc Plasma", A.I.Ch.E.J., Vol. 29, No. 2, pp. 207-15 (1983).

Miller, R.C. and R.J. Ayen, "Reactions of Titanium Tetrachloride in a Radio-Frequency Plasma Torch", I and EC Process Design and Development, 8, 371 (1969).

Munz, R.J., "The Decomposition of Molybdenum Disulphide in an Induction Plasma Tailflame", Ph.D. Thesis, McGill University (1974).

Randhawa, E.F., "Effect of Mass Transfer on Heat Transfer in High Temperature Surroundings", Master's Thesis, McGill University (1981).

Reed, T.B., "Induction Coupled Plasma Torch", J. Appl. Physics, 32, 821 (1961).

Sayegh, N.N., "Variable Property Flow and Heat Transfer to Single Spheres", Ph.D. Thesis, McGill University (1977).

Sheer, C., S. Korman, C.G. Stojanoff and P.S. Tschang, "Diagnostic Study of the Fluid Transpiration Arc", AFOSR, Final Rep., 70-0195 TR (1969).

Sheer, C., S. Korman, D.J. Angier and R.P. Cahn, "Arc Vaporization of Refractory Powders", Fine Particles, 2nd. Inter. Symp. of Electrochem. Scoc. Boston, 1973, pub. by E.Soc., ed. by W.E. Kuhn, pp. 133-152 (1974).

Somerville, J.M., "The Electric Arc", Methuen (1959).

Tsantrizos P. and W.H. Gauvin, "Operating Characteristics and Energy Distribution in a Nitrogen Transferred Arc Plasma", The Canadian Journal of Chemical Eng., Vol. 60, No. 6, pp. 822-30 (1982).

U.S. National Materials Advisory Board, "Plasma Processing of Materials", Report Number NMAB-415, Washington (1985).

PART I

STABILITY AND OPERATING CHARACTERISTICS OF A TITANIUM TETRACHLORIDE TRANSFERRED-ARC

ABSTRACT

A new technique for producing stable transferred arcs which utilizes plasmagas (plasma-forming gas) containing high concentrations of titanium tatrachloride has been developed. It involves replacing the commonly used thoriated tungsten cathode tip with a tantalum carbide tip.

It is shown that the instabilities observed by other investigators at $TiCl_4$ concentrations in the plasmagas above one percent are caused by chemical reactions between the tungsten and the chloride at the cathode surface. By replacing the tungsten with tantalum carbide such reactions are eliminated due to the exceptional stability of the carbide, even at the high temperatures characteristic of the cathode spot regions.

Stable transferred arcs were produced in a closed reactor using plasmagas containing various concentrations of $TiCl_4$ in argon, helium or hydrogen. $TiCl_4$ feed rates up to 25 g/min were tested. The total arc voltage for a 2.5-cm arc, utilizing 25 g/min $TiCl_4$ and 15NTP L/min argon as the plasmagas, and a TaC cathode, was measured at about 73 V. The arc column voltage gradient was calculated from the increase in total arc voltage due to a one-centimeter increase in arc length. Based on this approach, the column voltage gradient for very short arcs (1 to 3 cm) utilizing plasmagas rich in $TiCl_4$ is about 12 V/cm. Other operating characteristics of $TiCl_4$-rich arcs, including the energy

distribution and chemical reactions within the reactor are reported. Some operating data for arcs utilizing various plasmagas compositions (e.g. Ar, He, N_2, H_2 and NH_3) are also included for the purpose of comparison.

BACKGROUND INFORMATION

In the past three decades, a lot of efforts have been expended on the development of plasma applications for chemical and metallurgical processing. Broadly, such applications can be classified as follows:

1. Injection of thermal energy in high-temperature inorganic or organic reaction system (e.g. direct iron reduction, acetylene production, etc).

2. Recycling of iron, steel, strategic metal and super-alloy scrap.

3. Production of finely-divided (or aerosols) inorganic compounds.

4. Reduction, oxidation, thermal decomposition and other reactions intended to produce metallic materials or synthetic minerals.

For a review of these applications and research efforts one is referred to papers by Szekely (1983), Gauvin and Choi (1983), Sheer et al. (1982), Maske and Moore (1982), Aubreton and Fauchais (1978), Sayce (1977), Hamblyn (1977), Rykalin (1976) and Bonet (1976). A complete review of plasma applications was published recently by the U.S. National Materials Advisory Board (1985). Only research efforts relevant to the reduction of metal tetrahalides are reviewed in this thesis.

The plasma reduction of metal tetrahalides has been investigated lately by numerous research teams around the world. The two metals which have received most attention are zirconium and titanium. These two metals share some important characteristics that make them attractive candidates for plasma reduction. They are both commercially produced from their respective tetra-chlorides, their market volume is expected to increase rapidly over the next few years and new applications for their ceramics, alloys and powders, products easily manufactured in plasma reactors, are increasingly becoming the focus of modern material science.

The proposed plasma reduction processes for the production of silicon, zirconium and titanium are essentially the same. They all begin by feeding their respective tetrachlorides in an argon or hydrogen arc. Within the arc the molecule dissociates into atoms, ions and electrons. The metal, or its subchlorides, must then be collected on a target before it fully recombines with the chlorine. Hydrogen is commonly used to assist the removal of chlorine.

For the purpose of this study the reduction of metal tetrachlorides in a plasma reactor has been divided into two sections:

1. the dissociation of the $TiCl_4$ molecule, and

2. the collection of the reduced products.

The first section consists of injecting the chloride molecule into the hot region of the plasma where dissociation occurs, and is reviewed in the present Part. The collection of the products from the reduction of tetrachloride in plasma reactors is reviewed in Part III.

THERMODYNAMIC CONSIDERATIONS

There are many direct applications of the information provided by a thermodynamic analysis of any chemical reaction. These are particularly useful in plasma processes and include: (1) the prediction of processing temperatures required for maximum possible yield; (2) the determination of any physical or transport properties that may be required in an analysis; and (3) the concentrations and types of species produced by the reactions and available for recombination reactions in the quenching process.

At high temperatures, chemical reactions generally proceed very rapidly, and the time required to approach equilibrium may be very short even compared to the residence time in a plasma flow system. Thus, equilibrium compositions may very well be attained in the high-temperature region of a plasma reactor.

On the other hand, high-temperature chemistry can be quite complex, with unsuspected radicals, meta-stables, or other types of species participating in the reaction mechanisms. Nevertheless, equilibrium concentrations may be determined by the relative free energies of the possible system components. These free energies for high-temperature species are usually calculated from statistical mechanical relations. Thus energy levels as a function of temperature must be available from spectroscopic data for each of the various species under consideration. Accurate data of this type are available for most molecular and atomic species (JANAF Thermochemical Tables, 1960; Kubaschewski et al., 1956). Estimates may have to be made for certain unusual species.

Equilibrium concentrations for various mixtures of titanium chlorides have been calculated by many researchers during the last two decades. In 1969, Miller and Ayen described equilibrium calculations for three plasma systems:

1.	Ar-Ti-Cl	(72:1:4)
2.	Ar-Ti-Cl-Mg	(72:1:4:2)
3.	Ar-Ti-Cl-H	(72:1:4:4)

The numbers in parentheses indicate the overall system atom ratios. These systems were of interest to Miller and Ayen for the study of the decomposition of titanium tetrachloride in an induction plasma torch. Argon appears in large proportion as it was the working plasmagas. The temperature range extended to 14 000 K and the pressure was one atmosphere. The results of their calculations for the Ar-Ti-Cl system are shown in Figure 1.

Ten years later, Akashi and his coworkers (Akashi et al., 1977) made similar calculations for a Ti-Cl-H (1:4:9) system in the temperature range of 4 000-20 000 K and at atmospheric pressure. He was studying the possibility of formation of titanium metal from a mixture of titanium tetrachloride and hydrogen introduced into an argon plasma jet. Akashi's calculations ignore the effects of the argon partial pressure in his system.

In 1974, Yean and Riter studied a similar titanium tetrachloride-hydrogen system. They produced species concentration curves for a mixture of H_2 and $TiCl_4$ (Ti-Cl-H ratio 1:4:20) in the temperature range between 1 000 and 6 000 K and at a pressure of 0.01 atmosphere. They used their data to demonstrate the need for an extremely rapid preferential condensation of vapour phase titanium in the production of the metal from the plasma dissociation of $TiCl_4$. However they did not explain the effects that hydrogen has on the system.

The results from all three of the above studies show that titanium tetrachloride can be decomposed almost completely into titanium atoms, titanium ions, chlorine atoms and ions, and electrons at temperatures higher than 5 000 K. Typical temperatures in the hot region of an

FIGURE 1

EQUILIBRIUM GAS-PHASE COMPOSITION FOR THE SYSTEM Ar-Ti-Cl AT ATMOSPHERIC PRESSURE

Source: Miller and Ayen (1969)

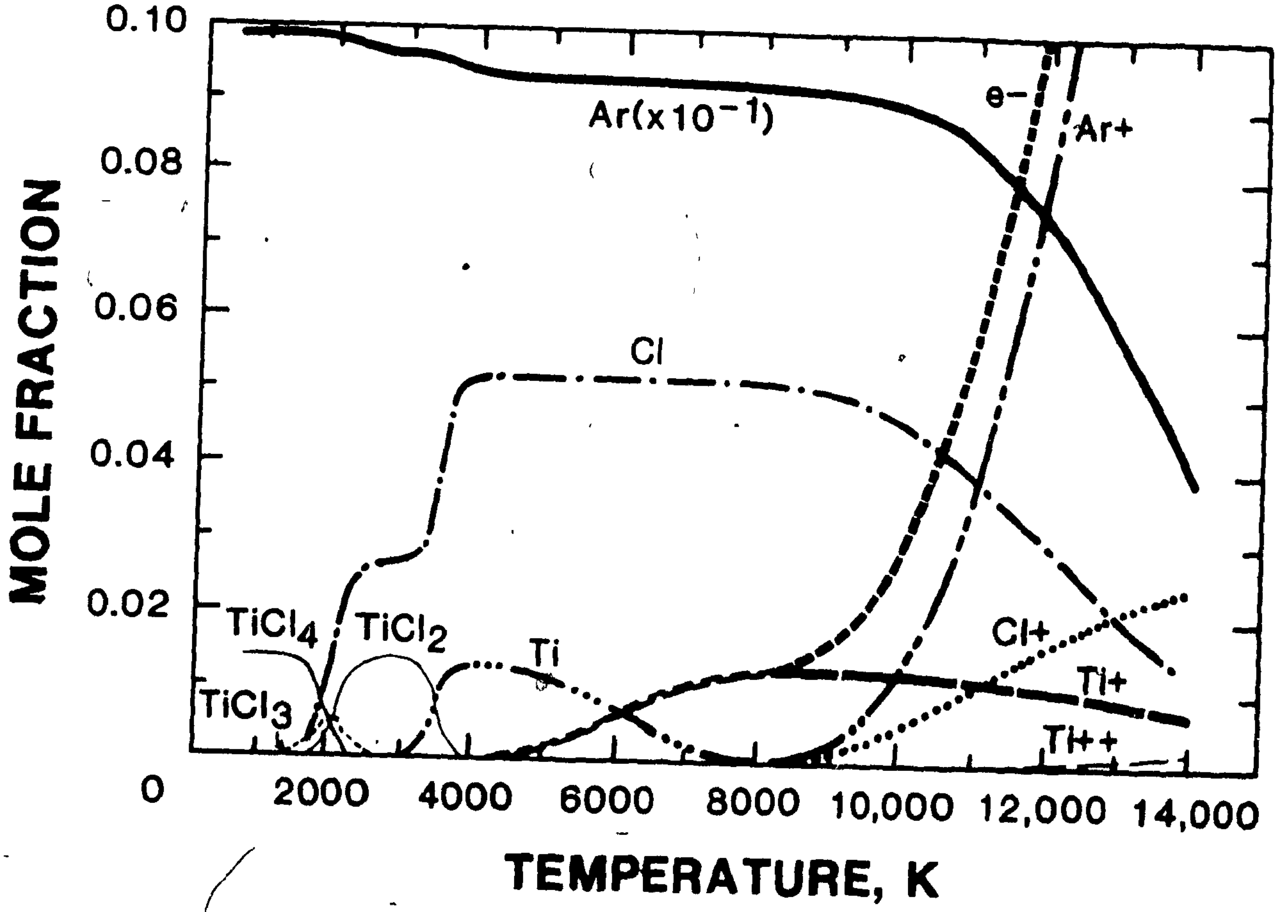
0.10
0.08
0.06
0.04
0.02
0
MOLE FRACTION
2000
4000
6000
8000
10,000
12,000
14,000
TEMPERATURE, K
Ar(x10−1)
e−
Ar+
Cl
TiCl4
TiCl3
TiCl2
Ti
Cl+
Ti+
Ti++

atmospheric pressure transferred arc are between 5 000 and 20 000 K, and species are at thermodynamic equilibrium concentrations. Therefore, one may assume that any $TiCl_4$ molecule entering the hot region of a transferred arc reactor will be completely dissociated. Unfortunately, no measured data on species concentrations for atmospheric pressure tetrachloride plasmas exist. Such measurements, which would also provide information about the $TiCl_4$ arc temperature and transport properties have been impossible thus far for two reasons:

1. The reduction of $TiCl_4$ produces titanium subchlorides such as $TiCl_3$ and $TiCl_2$. These chlorides condense at relatively high temperatures (1 100 K for $TiCl_3$ and 1 300 K for $TiCl_2$) quickly covering all reactor surfaces and preventing the use of conventional optical techniques for species concentration measurements.

2. Researchers have been unable to produce stable, highly-concentrated tetrachloride plasmas.

The latter of these reasons is addressed in this study.

ARC STABILITY CONSIDERATIONS

There is very little information in the literature about the operating characteristics of tetrachloride plasmas. However, from published results it is obvious that researchers have thus far been unable to produce stable tetrachloride plasmas at concentrations above one percent molar.

Miller (1968) studied the effects of introducing small quantities of titanium tetrachloride and hydrogen in a r.f. plasma torch operated with argon at one atmosphere pressure. Experimental coupling efficiencies obtained for a 4-MHz torch operated with pure argon indicated that about 63 percent of the generator plate power was transferred to the plasma. Efficiency appeared to be nearly independent of both the power level and the direction of the stabilizing flow (vortex or coaxial). Furthermore, hydrogen addition showed little effect on the coupling efficiency. This, however, was not the case for $TiCl_4$ addition. Even additions as small as 0.5 percent molar reduced the coupling efficiency to less than 50 percent. When the $TiCl_4$ concentration was about one percent the coupling efficiency was lowered to the point where the power available (8-10 kW) could not meet the power needs of the plasma which extinguished itself.

Miller noticed that the addition of $TiCl_4$ produced a very intense sky-blue radiation within the coil region and a long (12-30 cm) orange tail flame. He concluded that the $TiCl_4$-containing arc operated at significantly lower temperatures than the pure argon arc due to the lower ionization potential of the Ti atom (6.8 eV for Ti compared to 15.8 eV for Ar). He suggested that the drop in coupling efficiency could be minimized if the characteristics of the power supply could be better matched with the electrical requirements of the plasma. Another option would have been to increase the available power. Neither of these suggested solutions was actually attempted.

Others, such as Akashi et al. (1977) and Kikukawa et al. (1983) followed a different approach. They introduced the $TiCl_4$ in the tail flame of a d.c. torch using various mixtures of argon and hydrogen as the plasmagas. This method avoids the presence of the chloride in the current transferring region (the region between the cathode and the anode) of the arc but limits the amounts of $TiCl_4$ one can introduce in the reactor.

The energy required to fully dissociate a titanium tetrachloride molecule can be calculated from data available in the Handbook of Chemistry and Physics at about 1 717 kJ per mole. Furthermore, typical temperatures encountered in the tailflame of a d.c. torch operating in argon or hydrogen are around 10 000 K. After the introduction of $TiCl_4$ into the tailflame the mixture of tetrachloride and plasmagas must be at temperatures above 5 000 K to assure complete dissociation of the $TiCl_4$ molecule. Since the heat capacity of the argon, hydrogen and tetrachloride are about 21, 42 and 109 J/(mol.K) respectively (JANAF, 1965) one can estimate roughly that the maximum $TiCl_4$ feed rate is about 5 percent molar in argon and 9 percent in hydrogen. These are rough limits based on an energy balance which assume no heat losses and perfect mixing. Actual limits on $TiCl_4$ feed rate would be significantly lower.

There is little doubt that the fundamental weakness of all previous studies has been the inability to produce a highly concentrated chloride plasma. In all studies described above the maximum sustainable concentration of tetrachloride in the plasmagas has been around one percent molar. This concentration is too small to allow meaningful conclusions regarding the operating characteristics of tetrachloride plasmas or the technical feasibility of reducing metal chlorides in plasma reactors. A method of producing highly concentrated chloride arcs is essential to progress in this field.

An effort to produce highly concentrated or pure zirconium tetrachloride arcs was initiated at McGill University in the early 1980's. Using a transferred-arc reactor, various investigators attempted to inject large amounts of $ZrCl_4$ vapour into the arc (Kyriacou, 1982 and Spiliotopoulos, 1983). Unfortunately, in all cases the arc became unstable and operation was terminated. Furthermore, the $ZrCl_4$ feeding system used in these studies was incapable of producing constant feed rates. As a result it was not possible to assess the critical feed rate at which the arc would become unstable. It was concluded however that $ZrCl_4$ arcs required significantly higher power and suggested that the concentration limits were detemined by the power limits of the rectifier (about 50 kW for both studies).

The study described in this Part was aimed at:

1. Understanding the causes for instability in highly-concentrated titanium tetrachloride transferred arcs.
2. Producing stable, highly-concentrated tetrchloride arcs and studying their operating characteristics

EXPERIMENTAL

APPARATUS

The apparatus that was used in the experimental work consisted of the following main components:

i. The Power Supply,

ii. The Transferred-Arc Reactor,

iii. The Plasmagas Feeding System, and

iv. The Exhaust Gas Treatment System.

A schematic drawing of the overall set-up is shown in Figure 2. Descriptions of each of the main components follows.

i. Power Supply

The power was supplied to the arc by a Miller model SRS-1500F7 silicon diode rectifier capable of providing a maximum power of 70 kW. It had a drooping volt-ampere curve and could be operated in the open circuit voltage range of 100-400 volts. In this study, the 400-volt

FIGURE 2

SCHEMATIC DRAWING OF APPARATUS

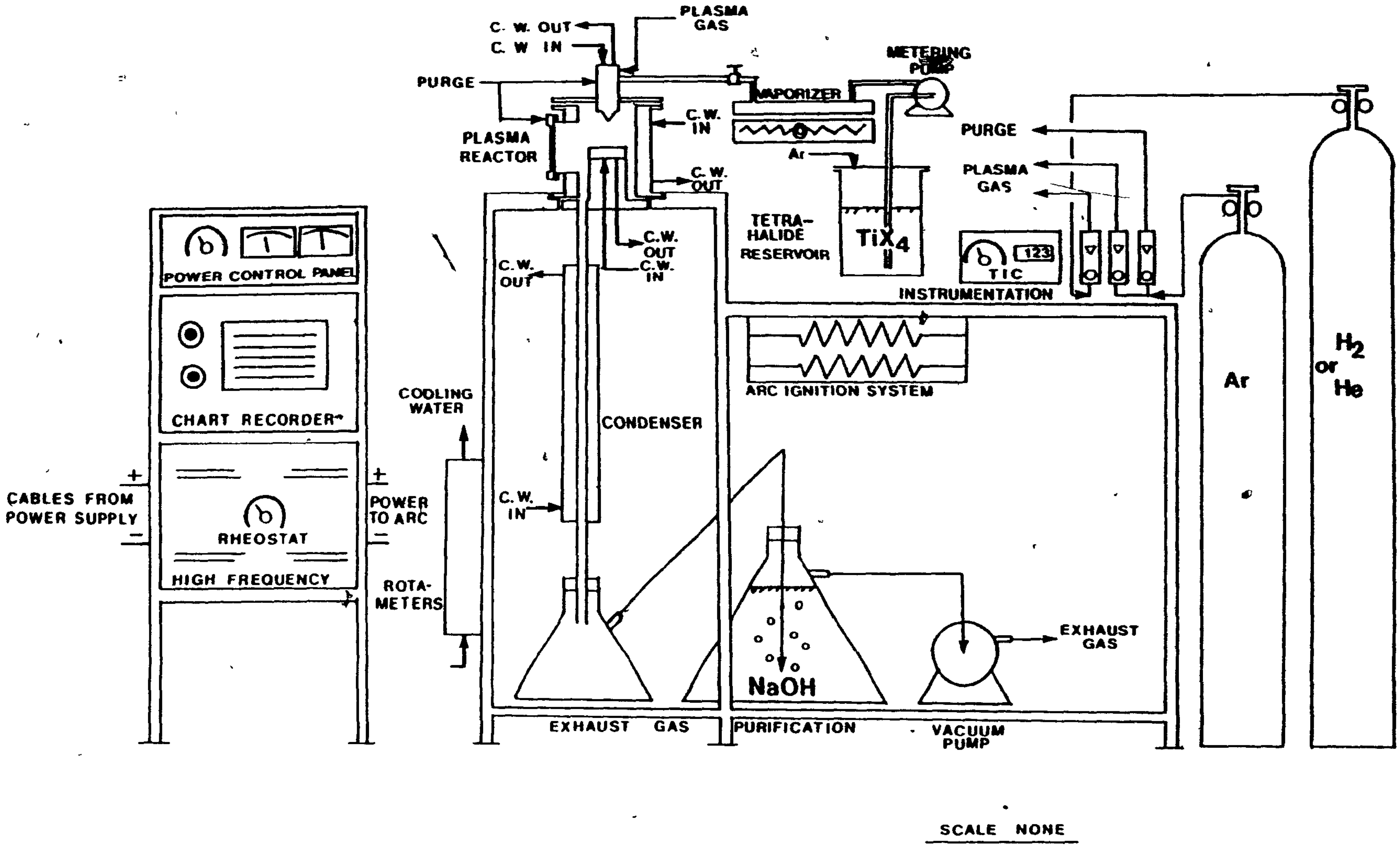
PLASMA GAS
C. W. OUT
C. W IN
PURGE
METERING PUMP
VAPORIZER
C.W. IN
Ar
PLASMA REACTOR
C.W. OUT
PURGE
PLASMA GAS
TETRA-HALIDE RESERVOIR
TiX_4
123
TIC
INSTRUMENTATION
C.W. OUT
C.W. IN
C.W. OUT
POWER CONTROL PANEL
CHART RECORDER
ARC IGNITION SYSTEM
COOLING WATER
CONDENSER
Ar
H_2 or He
CABLES FROM POWER SUPPLY
+
−
RHEOSTAT
HIGH FREQUENCY
+
POWER TO ARC
−
C.W. IN
ROTA-METERS
NaOH
EXHAUST GAS
EXHAUST GAS
PURIFICATION
VACUUM PUMP
SCALE NONE

open circuit was used. The power output from the rectifier could be adjusted through a range of arc currents, up to 1500 amperes, by a rheostat located on the control panel of the power supply.

A Miller, model HF-15-1, high-frequency arc starter and a 2.2-Ohm Ohmite resistor were used to initiate the breakdown of the arc gap. The arc was first ignited between the cathode tip and the nozzle (see Figure 4), which in this case served as an auxiliary anode, and then transferred to the primary anode. The nozzle was grounded through the 2.2-Ohm resistor which provided the resistance necessary to assure the arc's transfer. Once the arc had been transferred to the primary anode, a switch was used to disconect the nozzle from the ground. Once disconected, the nozzle floated at a voltage between that of the cathode and of the anode.

ii. The Transferred-Arc Reactor

The transferred-arc reactor that was used in this study consisted of three main components:

(a) the anode assembly,

(b) the cathode and nozzle assemblies, and

(c) the main reactor body.

Each of these components was completely separate from the others. Thus extensive modification of any one component was possible without requiring alterations to the others. The three components were attached together using high pressure quick release clamps.

(a) The anode assembly shown schematically in Figure 3, consisted of the anode base, the cooling system, the anode plate holder,and the anode plate. The anode base was used to adjust the protrusion of the anode by fitting cylindical rings of known thickness on top of each other. The gas exhaust system and electric lead to the power supply were attached to the anode base. The cooling system was fitted on top of the anode base and was designed to provide maximum cooling at the anode spot region (center of the anode plate) while maintaining a high cooling water velocity throughout the anode surface. The anode plate holder was fitted on top of the cooling system and a flat, circular copper plate (anode plate) was attached to it using six equally spaced screws. This allowed for frequent replacement of the anode plate which could be easily cut from a commercially available plate. For the purpose of identifying the effect the anode material had on arc operation, the copper plate was replaced by a molybdenum plate in some experiments.

(b) The cathode and nozzle assemblies, shown schematically in Figure 4, consisted of the nozzle base, the nozzle assembly, and the cathode

(c) the main reactor body.

Each of these components was completely separate from the others. Thus extensive modification of any one component was possible without requiring alterations to the others. The three components were attached together using high presure quick release clamps.

(a) The anode assembly shown schematically in Figure 3, consisted of the anode base, the cooling system, the anode plate holder,and the anode plate. The anode base was used to adjust the protrusion of the anode by fitting cylindical rings of known thickness on top of each other. The gas exhaust system and electric lead to the power supply were attached to the anode base. The cooling system was fitted on top of the anode base and was designed to provide maximum cooling at the anode spot region (center of the anode plate) while maintaining a high cooling water velocity throughout the anode surface. The anode plate holder was fitted on top of the cooling system and a flat, circular copper plate (anode plate) was attached to it using six equally spaced screws. This allowed for frequent replacement of the anode plate which could be easily cut from a commercially available plate. For the purpose of identifying the effect the anode material had on arc operation, the copper plate was replaced by a molybdenum plate in some experiments.

(b) The cathode and nozzle assemblies, shown schematically in Figure 4, consisted of the nozzle base, the nozzle assembly, and the cathode

FIGURE 3

SCHEMATIC DRAWING OF ANODE ASSEMBLY

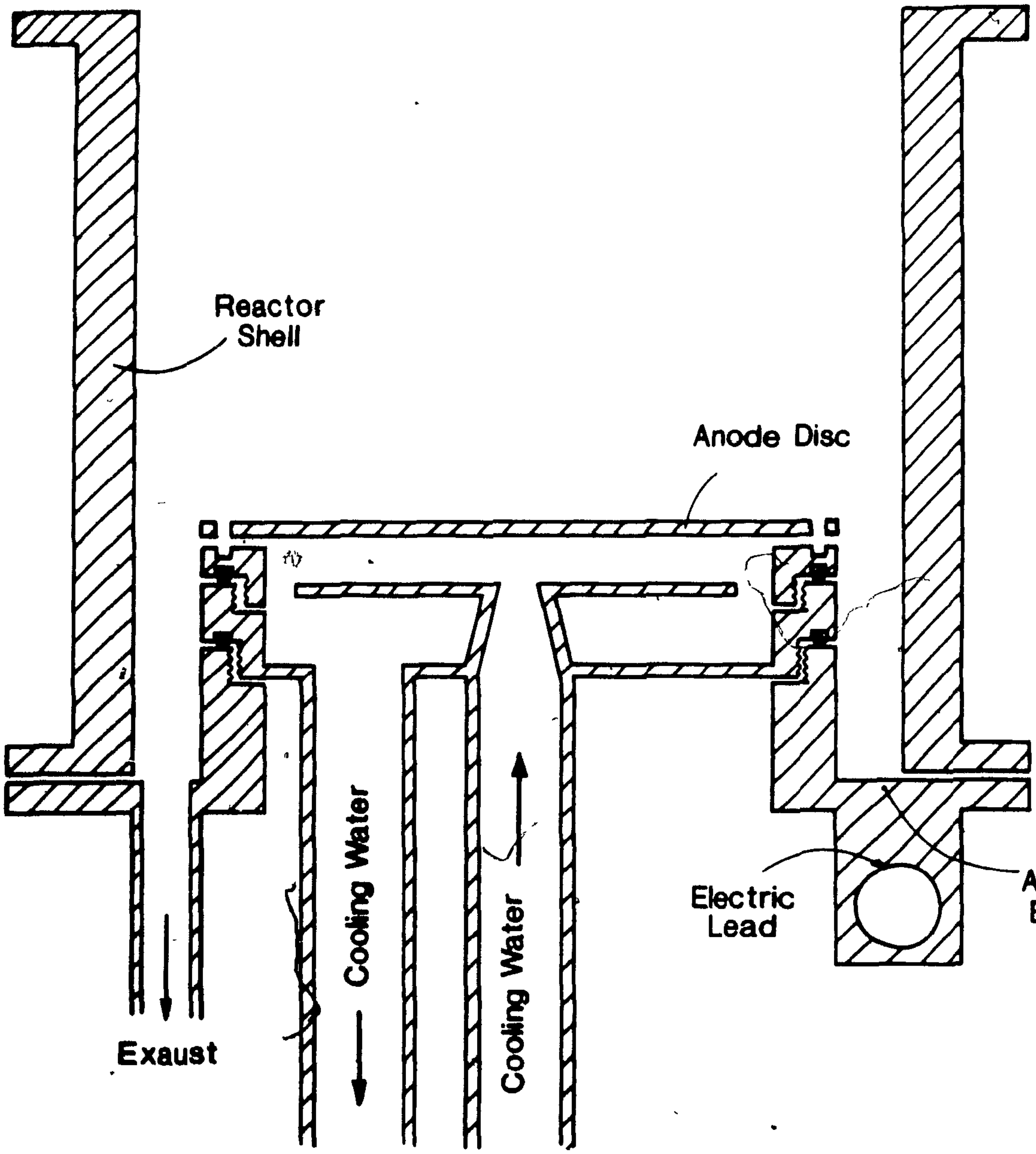
Reactor Shell
Anode Disc
Cooling Water
Cooling Water
Exaust
Electric Lead
Anode Base

FIGURE 4

SCHEMATIC DRAWING OF CATHODE AND NOZZLE ASSEMBLIES

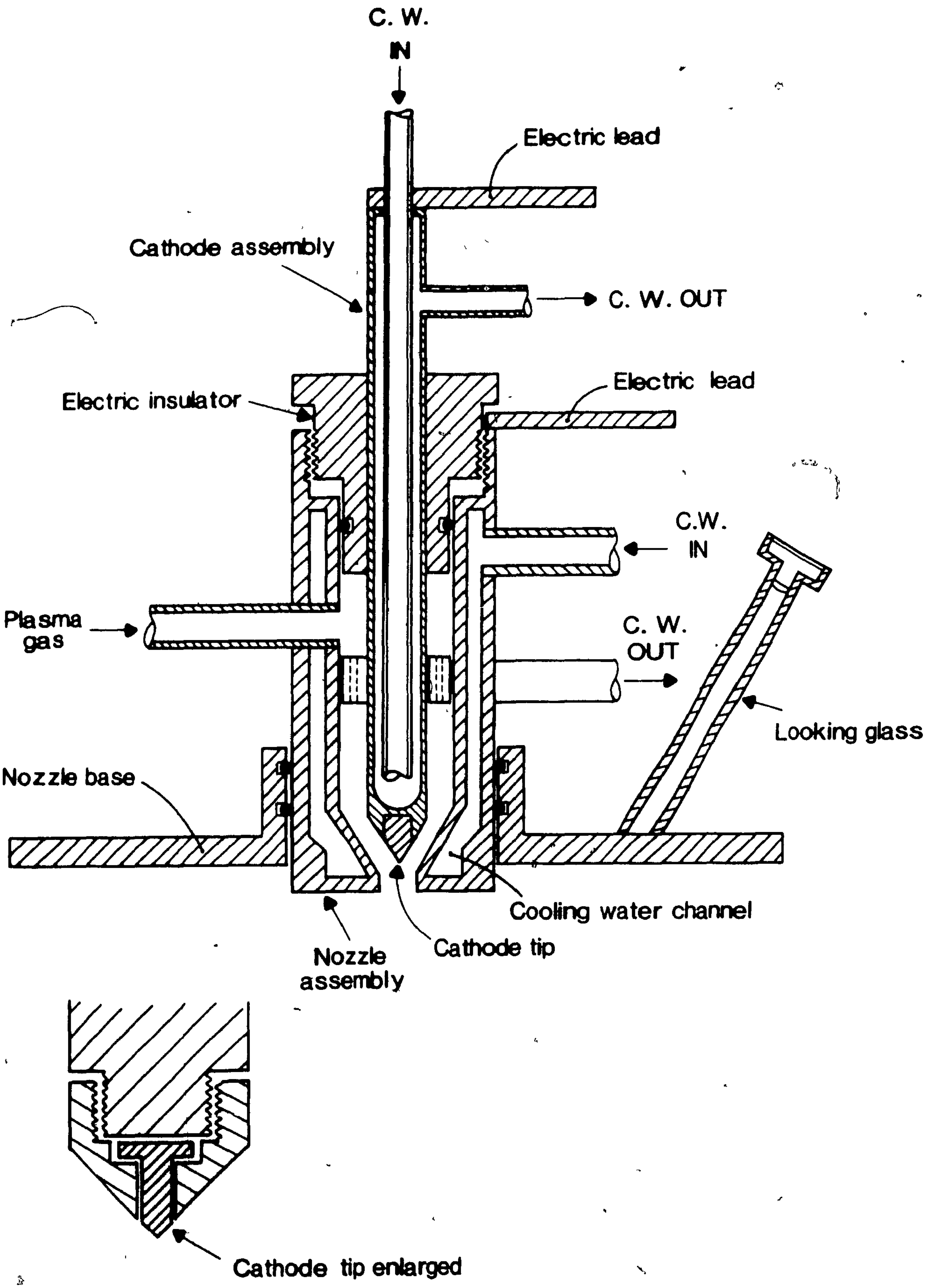
C. W.
IN
Electric lead
Cathode assembly
C. W. OUT
Electric insulator
Electric lead
C.W.
IN
Plasma
gas
C. W.
OUT
Looking glass
Nozzle base
Cooling water channel
Cathode tip
Nozzle
assembly
Cathode tip enlarged

assembly. The nozzle base was used to adjust the protrusion of the nozzle and to seal-off the top of the reactor. It was floating at the same electrical potential as the nozzle. This avoided accidental "sparking" between the nozzle and the base. A window was installed on the nozzle base to allow direct viewing of the anode's surface during operation. The water-cooled nozzle assembly surrounded the cathode and served as an auxiliary anode during arc ignition. The main plasmagas flowed in the gap between the nozzle and the cathode assemblies. Two "O" rings between the nozzle assembly and its base allowed one to adjust the height of the cathode without leakage between the reactor's inside and outside environments. The bottom plate of the nozzle assembly was fitted with a molybdenum ring which allowed close control of the nozzle's diameter and minimized damage during arc ignition.

The heart of the cathode assembly is a water-cooled conical cathode tip. The tip of the cone was cut flat to a diameter of 0.2 cm in an effort to increase the area of the cathode spot region and thus minimize cathode erosion. The cathode tip was attached to the cathode assembly through the use of a fitting ring (see insert in Figure 4). The fitting ring would screw on the assembly and press the tip firmly against it. This arrangement allowed both the easy replacement of the cathode tip and the possibility of using a variety of cathode tip materials. The shape of the cone could also be easily varied based on this arrangement. The cathode tip's position in relation to the bottom surface of the nozzle could be adjusted using the electrically insulating screw on the top of the cathode assembly.

(c) The main reactor body was important in sealing the system and in providing measuring and observation ports. The reactor body used in this study is shown in Figure 5. It consisted of a water-cooled cylinder 12 cm in diameter and 12 cm in height open at both ends to accommodate the cathode and anode assemblies. It included six measuring ports and one viewing window. The measuring ports were spaced one centimeter apart between two and seven centimeters from the top of the reactor and were one centimeter in diameter each. They were used to measure pressure and temperatures inside the reactor.

The viewing window was rectangular, 5.0 cm in height and 1.5 cm in width. It was kept clean using two mechanisms:

1. A molybdenum screen that closed the window from the arc and opened it only temporarily for an observation, and

2. injection of argon between the screen and the window to maintain a slightly positive pressure behind the metal screen. This both prevented reactor gases from coming in contact with the window and cooled the metal screen.

A similar set of cleaning mechanisms were used on the window attached to the nozzle base (shown in Figure 4).

FIGURE 5

SCHEMATIC DRAWING OF MAIN REACTOR BODY

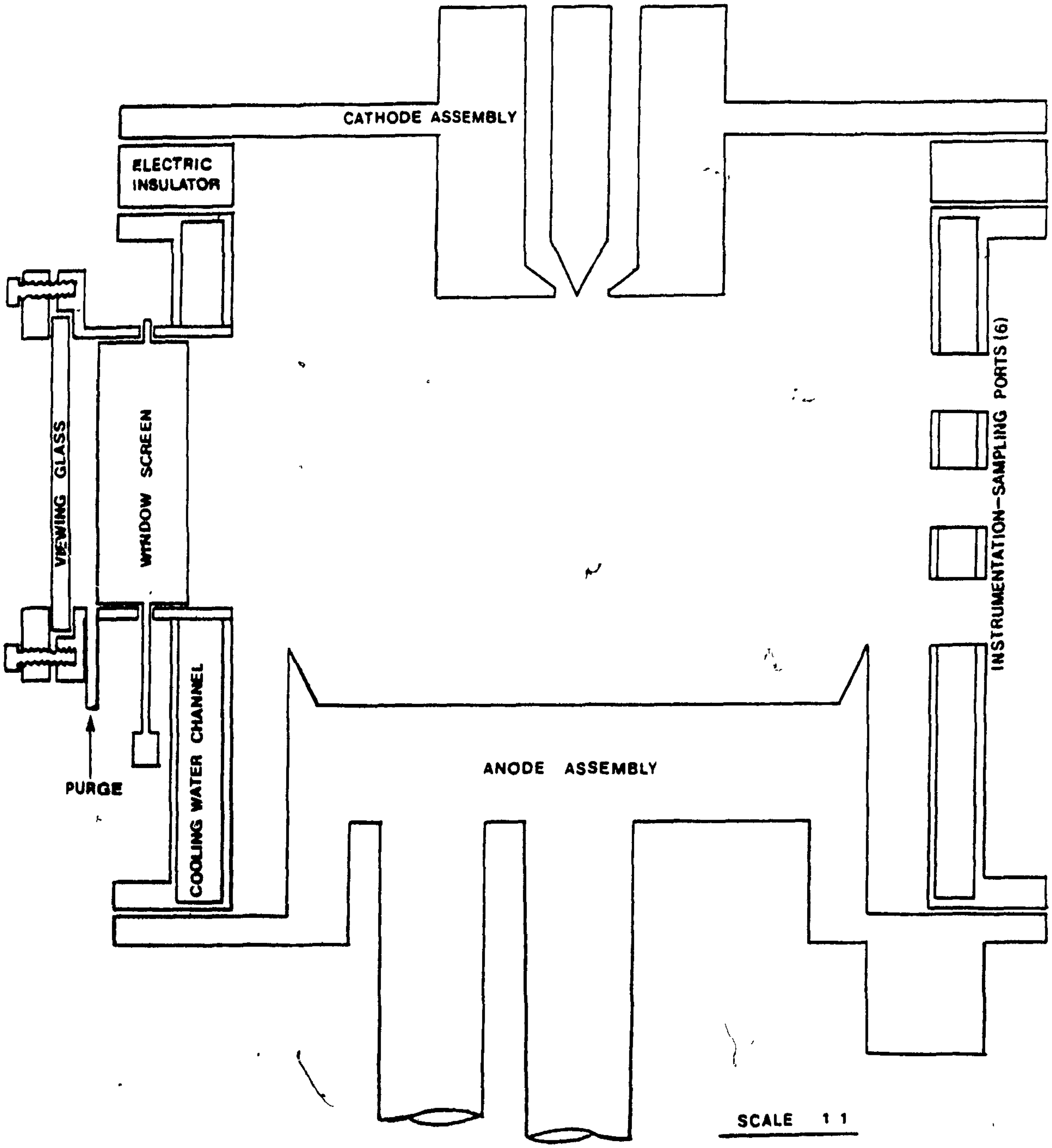
CATHODE ASSEMBLY
ELECTRIC INSULATOR
VIEWING GLASS
WINDOW SCREEN
PURGE
COOLING WATER CHANNEL
INSTRUMENTATION–SAMPLING PORTS (6)
ANODE ASSEMBLY
SCALE 1 1

iii. The Plasmagas Feeding System

The capacity to feed a variety of gases into the transferred arc system was required for this study. The gas feeding system used provided volumetrically-controlled flows of four gases (one purge gas, two plasma-forming gases (plasmagas) and the titanium tetrachloride) into the reactor.

The purge gas was argon. Its flow rate was controlled through a gas rotameter (see Figure 2) with a capacity of 30 L/min. This gas was used to purge the apparatus from oxygen and nitrogen thus preventing contamination of the reactants, and to maintain the viewing window and instrumentation ports clean from condensing chlorides. During arc operation, the total purge gasflowrate to the reactor ports and windows was 3 L/min.

Two plasmagases, not including the titanium tetrachloride, could be fed to the plasma reactor simultaneously. The flow rates of both gases were controlled by two independent gas rotameters. The availability of two plasmagas feed lines was essential to this study. Some experiments required the presence of both an inert gas and a reducing gas (e.g. hydrogen) in the reactor, while others required an easily-ionized gas (e.g. argon) for arc ignition and a more energetic gas (e.g. helium) during arc operation.

The main plasmagas could be preheated to 400° C using an electrically-heated copper tube. The tube was filled with copper turnings (a material like steel wool) in order to increase the heat transfer area and the gas velocity. The preheater also purified the plasmagas through the oxidation of copper. The copper turnings were replaced periodically.

The titanium tetrachloride feeding system consisted of a 3-L tetrachloride reservoir, a Masterflex tubing pump using a 14-size Viton tube capable of delivering exact amounts of liquid at flowrates up to 21 mL/min, and an enclosed hot plate. The tetrachloride was pumped cold from the reservoir to the hot plate through the pump at the desired feed rate. It was vapourized instantly on the hot plate's surface thus allowing exact control of the gas feed rate to the reactor. A small amount (about 1 L/min) of plasmagas was also fed to the hot plate to assure that all tetrachloride vapour was quickly delivered to the reactor. The addition of the plasmagas increased the total volumetric flowrate through the inclosed hot plate vapourizer, thus reducing the $TiCl_4$ residence time in the vapourizer. All plasmagas feed lines to the reactor were heated to avoid condensation.

iv. The Exhaust Gas Treatment System

The gases leaving the plasma reactor include a variety of subchlorides, oxychlorides, Cl_2 and HCl (whenever H_2 was used in the plasmagas). These mildly toxic and corrosive compounds had to be removed prior to venting the gas to the atmosphere. The exhaust gas treatment system included a condenser and two gas scrubbing reservoirs in series. The condenser was connected directly to the exhaust port of the anode base and was used to cool the exhaust gas and condense the sub-chlorides and oxychlorides. The Cl_2 (or HCl) was removed in the gas scrubbers using a 10 percent molar sodium hydroxide solution.

EXPERIMENTAL PROCEDURE

Prior to all the experiments conducted in this study, the reactor system was thoroughly cleaned and the electrode spacing was adjusted to the desired value. The reactor was then sealed gas-tight and was purged for 15 minutes with argon. The arc was ignited first between the cathode and the nozzle, which also served as an auxiliary anode for this purpose, and then transferred to the primary anode. Pure argon was used as the plasmagas during arc ignition. Following ignition, the nozzle was disconnected from the ground (positive lead of d.c. current), the current was adjusted to 200 A and the main plasmagas composition was introduced at the desired flowrate. Finally, the $TiCl_4$ was fed into the vapourizer and consequently into the plasmagas at the desired feedrate.

The total arc voltage and current were measured continuously through the use of a two-channel SERVOGOR 460 recorder. Photographs of the arc were taken through the reactor window by briefly opening the molybdenum screen and permitting temporary viewing access to the arc column. The photographs were taken with a 35mm SLR Nikon camera, using a 135mm-lens at shutter speeds of 1/2000 of a second and lens apertures of f-16 to f-32. A 2x gray lens filter and a 64 ASA film provided acceptable quality photographs.

The operating variables, including the arc current, the arc length, and the plasmagas(es) and $TiCl_4$ feedrates were held constant throughout the duration of an experiment. Thus, each data point shown in this study represents a complete experiment. To some degree, this was necessitated by the rapid deterioration of the water-cooled anode plate. The anode plate material was consumed through its reaction with chlorine from the dissociated $TiCl_4$ molecules. The chlorides formed on the anode surface, having relatively low boiling points, would vapourize, resulting in the perforation of the anode disc and the interruption of the experiment. To avoid such problems the maximum duration of each experiment was limited to about 8 minutes. It was felt that such short run durations did not assure that steady state could be reached for more than one set of operating conditions. A new anode plate was used for each experiment.

At the end of each run the $TiCl_4$ feed was terminated first and the reactor was purged with argon for 5 minutes. During this time the arc was maintained at relatively low currents (about 100 A) using argon as the plasmagas. Then, the arc was extinguished and the reactor was purged with argon for another 20 minutes. Finally, the reactor and the $TiCl_4$ feed system were opened, cleaned and prepared for the next experiment.

DISCUSSION AND RESULTS

The factors influencing the stability and operating characteristics of highly-concentrated titanium tetrachloride transferred arcs are described in this section.

Arc Stability Characteristics

The factors that determine the stability of a transferred arc are not completely understood. What is known, however, is that arc instability is due to the inability of electrons to pass from the cathode to the anode in a continuous fashion. This may be caused by phenomena occurring within the arc column, at the surface of the electrodes, or at the power supply system.

1. Power Supply Stability

The power supply system used in this study, when operated at 400 volts open circuit voltage, could easily provide currents of 200 to 300 amperes at arc voltages up to 200 volts. Power demands higher than that could not be met and resulted in the extinction of the arc. Having set these upper limits on the available current and voltage for the titanium tetrachloride arc, the arc's stability was studied based on two factors:

1. the power demands of the arc column, and

2. electrode phenomena.

Another potential cause of electrical instability may be due to the power supply load line's inability to intercept the arc characteristic voltage-current line. This situation, which is explained in detail by Hoyaux (1968), is primarily observed in arcs with falling characteristics (i.e. voltage drops with increase in current). Since high current, atmospheric pressure arcs tend to exibit a rising or flat characteristic, this potential source of instability was not examined any further.

ii. Arc Column Characteristics

The power required to sustain a stable arc depends to a great extent on the composition of the plasmagas. Starting with an energy balance at the arc center, Lowke (1979) derived the following equation for calculating the total arc voltage for a short argon plasma column:

$$V = 0.52 \left(\frac{h \cdot z}{\sigma}\right)^{\frac{1}{2}} (\mu \cdot j_o \cdot \rho)^{1/4} \quad I^{1/4} \tag{1}$$

where h is the enthalpy of the gas in J/g, z is the arc length in cm, σ is the electrical conductivity in (Ohm cm)$^{-1}$, μ is the permeability and is equal to 0.126 dyne/A^2, j_o is the current density in A/cm^2, ρ is the gas density in g/cm^3 and I is the arc current in A. Lowke's equation is somewhat curious in that it is neither dimensionally sound nor does it include terms relevant to the electrode fall regions. Nonetheless, it does provide important qualitative information regarding the major factors influencing the voltage of the arc column.

For a first approximation of the arc's energy requirements one may claim that fluctuations in all variables to the 1/4 power have little effect on the voltage and can thus be assumed constant. Ramakrishnan and Nuon (1980), for example, calculated the arc column voltage of a 200-A argon arc for current densities between 2×10^3 and 32×10^3 A/cm^2. The results showed arc column voltage variations of about 2 percent.

Similar results were obtained experimentally by Choi and Gauvin (1982) and Tsantrizos and Gauvin (1982) for argon and nitrogen arcs respectively due to current variations between 100 and 400 A.

Consequently, the Lowke equation can be simplified to the form:

$$V = C \left(\frac{h \cdot z}{\sigma}\right)^{\frac{1}{2}} \qquad (2)$$

with little error introduced. From this equation one may conclude that for a given arc length and arc current, the power requirements of a stable transferred arc system depend primarily on the ratio of the plasmagas' enthalpy and electrical conductivity.

The enthalpy of a plasma includes the kinetic energy of the particles, consisting of translational and excitational energy, and its chemical energy, consisting of dissociation and ionization energy. On the other hand, the electrical conductivity of a plasma is primarily influenced by the plasmagas' ionization potential. This is quite obvious since a plasma must contain sufficient ionized species to conduct electricity and its degree of ionization is a function of temperature and ionization potential.

By calculating the ratio between enthalpy and electrical conductivity, one could therefore assess the relative value of the arc column voltage for various plasmagases. Thus, argon, nitrogen and hydrogen which have comparable ionization potentials (15.8, 14.5 and 13.6 eV respectively) have about the same electrical conductivity (about 30 $(\text{Ohm cm})^{-1}$ at 10 000 K) and their respective arc column voltage is proportional to the square root of their enthalpy. Argon, with no dissociation energy has the lowest enthalpy and arc column voltage, whereas hydrogen with the highest dissociation energy exhibits the highest voltage. Ramakrishnan and Nuon (1980) give the arc column voltage gradient for argon, nitrogen and hydrogen as 6, 9 and 10 V/cm respectively. One should note that in the conventional units for enthalpy (i.e. J/mol) nitrogen's dissociation energy is higher than hydrogen ($95\text{x}10^3$ and $44\text{x}10^3$) respectively. However the Lowke equation uses J/g for enthalpy units, resulting in a higher value for hydrogen than nitrogen due to the former's lower molecular mass.

7

Helium, just as argon, is monoatomic and therefore has no dissociation energy. However, its higher voltage gradient (about 30 percent higher than argon) can be explained partly by its higher ionization potential (24.5 eV) which results in a low electrical conductivity (about 5 $(\text{Ohm cm})^{-1}$ at 10 000 K).

A preliminary investigation was conducted in an effort to measure experimentally the arc column voltage gradients of various plasmagas compositions in the present transferred arc reactor. Pure argon, helium nitrogen, hydrogen and ammonia were tested. All experiments used a plasmagas flow rate of 15 L/min and an arc current of 200 A. The arc column voltage gradients were calculated based on the difference in total arc voltage between a 2-cm and a 3-cm arc. The measured arc column voltage gradients for Ar, He, N_2, H_2 and NH_3 were 5, 8, 12, 14 and 15 respectively.

The effect of mixing titanium tetrachloride into the plasmas is twofold. Titanium tetrachloride is polyatomic and must therefore be completely dissociated in the arc. This increases the plasma's enthalpy and therefore the arc column's voltage. One should note however, that the dissociation energy of $TiCl_4$ is relatively small (about 9 kJ/g) compared to that of gases such as hydrogen and nitrogen (218 kJ/g and 34 kJ/g respectively).

Furthermore, both titanium and to a lesser extent chlorine have lower ionization potentials than argon (6.8 eV for Ti and 13.0 eV for Cl compared with 15.8 eV for Ar). Therefore, their introduction into the arc should result in an increase of the plasma's electric conductivity thus minimizing the increase in the arc column voltage gradient caused by the enthalpy factor. This effect can be seen, for example, in the data provided by Ramakrishnan and Nuon (1980) on the properties of arcs in nitrogen and nitrogen-copper vapour mixtures. At 200 A arc current the arc column voltage gradient for pure nitrogen was about 9 V/cm whereas for 10 percent Cu vapour in N_2 the voltage gradient fell to 8 V/cm. For equi-molar feed ratio of Cu vapour and N_2 the voltage gradient was only 5 V/cm. Copper, like titanium, has a low ionization potential (7.7 eV) and is able to increase the nitrogen's electrical conductivity.

Based on this analysis it seems unlikely that instability in the operation of titanium tetrachloride arcs is caused by excessive energy demands within the arc column. Experimental data on the present system verified this hypothesis. Figure 6 shows the total arc voltage for various concentrations of $TiCl_4$ in 1.3-cm and 2.3-cm argon arcs. From this Figure, it can be seen that although the total arc voltage increases quite rapidly with concentration, the voltage gradient within the arc column increases far slower. For example, the total voltage for a pure 1.3-cm argon arc is 24 V and increases to 29 V for a 2.3-cm arc. Therefore the measured voltage gradient in the arc column is about 5 V/cm. By comparison, the total arc voltage for the plasmagas containing 25 g/min $TiCl_4$ in 10 L/min argon (about 18 g/min Ar) is 57 V for the 1.3-cm arc and increases to 69 V for the 2.3-cm arc for a voltage gradient in the arc column of 12 V/cm. Thus, the addition of 25 g/min of $TiCl_4$ increased the arc column voltage gradient by only 7 V/cm.

The total arc voltage includes the arc column voltage and the two electrode fall voltages of the transferred arc system. Since the total voltage for the 1.3-cm arc increased by 33 V when the $TiCl_4$ was introduced into the argon arc (from 24 V for pure Ar to 57 V for 25 g/min $TiCl_4$ in Ar) and the arc column voltage increased by only 7 V/cm,

FIGURE 6

VARIATIONS IN TOTAL ARC VOLTAGE DUE TO THE INTRODUCTION OF TITANIUM TETRACHLORIDE INTO AN ARGON ARC

Fixed Operating Parameters

Arc Current = 200 A

Argon Flowrate = 10 L/min

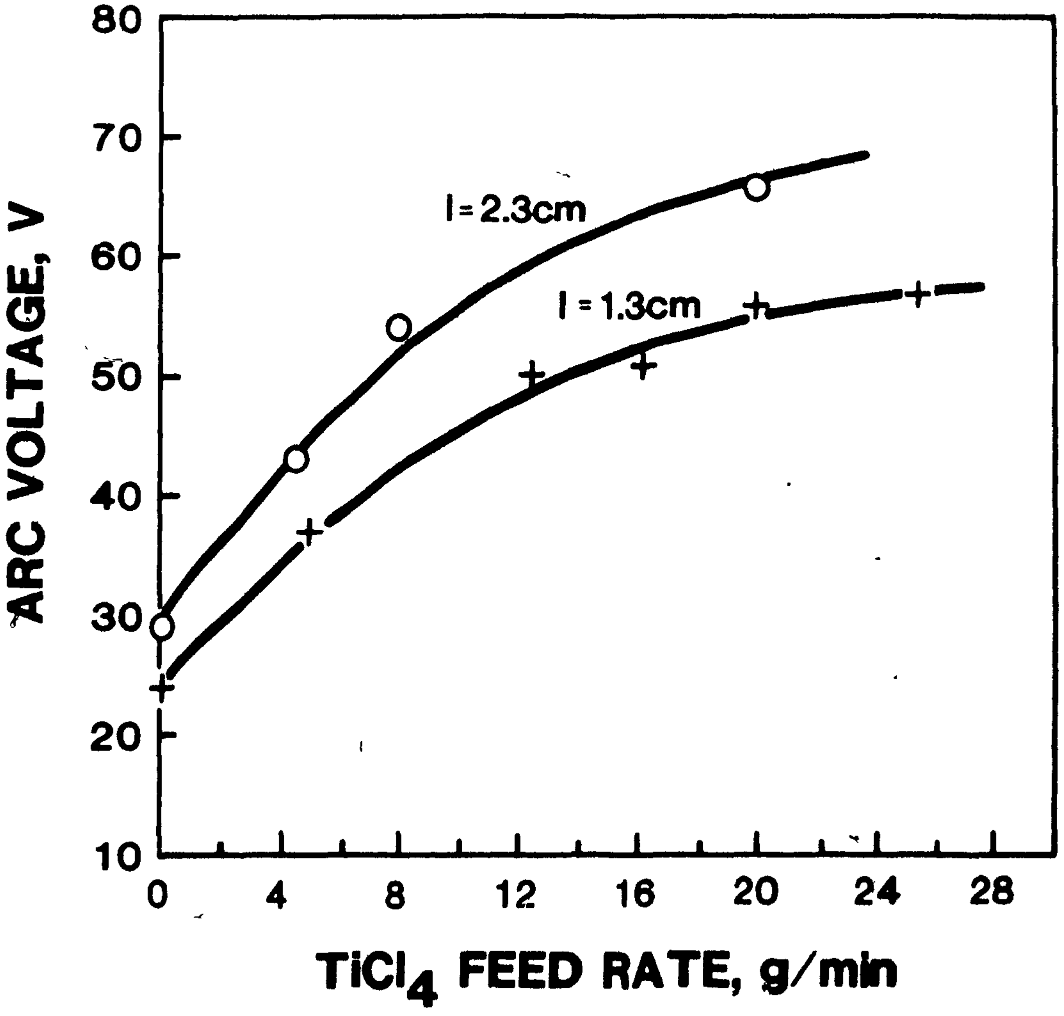

80
70
60
50
40
30
20
10
0
4
8
12
16
20
24
28
ARC VOLTAGE, V
$TiCl_4$ FEED RATE, g/min
l = 2.3cm
l = 1.3cm

one may conclude that the majority of the total arc voltage increase for the $TiCl_4$ containing arcs (around 24 V at 25 g/min $TiCl_4$ feedrate) is due to phenomena occurring at the electrodes.

The effects of $TiCl_4$ feed rate on arc voltage for various plasmagas compositions are shown in Figure 7. At high $TiCl_4$ concentration there was little variation introduced in the arc's total voltage when argon was replaced by helium. The voltage for pure helium was significantly higher than pure argon (34 V for He and 24 V for Ar). However, at $TiCl_4$ feed rates higher than 5 g/min the voltage difference between the two gases had mostly disappeared. The reason for this phenomenon may be due to the characteristics of the two inert gases. As explained earlier, argon and helium have about the same enthalpy but very different ionization potentials. When $TiCl_4$ is introduced into the plasmagas it provides a source of easily ionizable species, primarily Ti. The concentration of electrons, dissociated from the Ti^+ ions, controls the electrical conductivity of the plasma thus eliminating the significance of helium's higher ionization potential.

The experimental data presented in Figures 6 and 7 show the total arc voltage for a transferred arc between a thoriated tungsten cathode and a copper water-cooled anode after two minutes of arc operation. In fact, the voltage increased constantly with time until the arc would become completely unstable and extinguish itself. Variations of arc voltage with operating time for arcs utilizing $TiCl_4$-rich argon, helium

FIGURE 7

VARIATIONS IN TOTAL ARC VOLTAGE DUE TO THE INTRODUCTION OF TITANIUM TETRACHLORIDE INTO ARCS UTILIZING VARIOUS PLASMAGAS COMPOSITIONS

Fixed Operating Parameters

Arc Current = 200 A

Main-Plasmagas Flowrate = 10 L/min

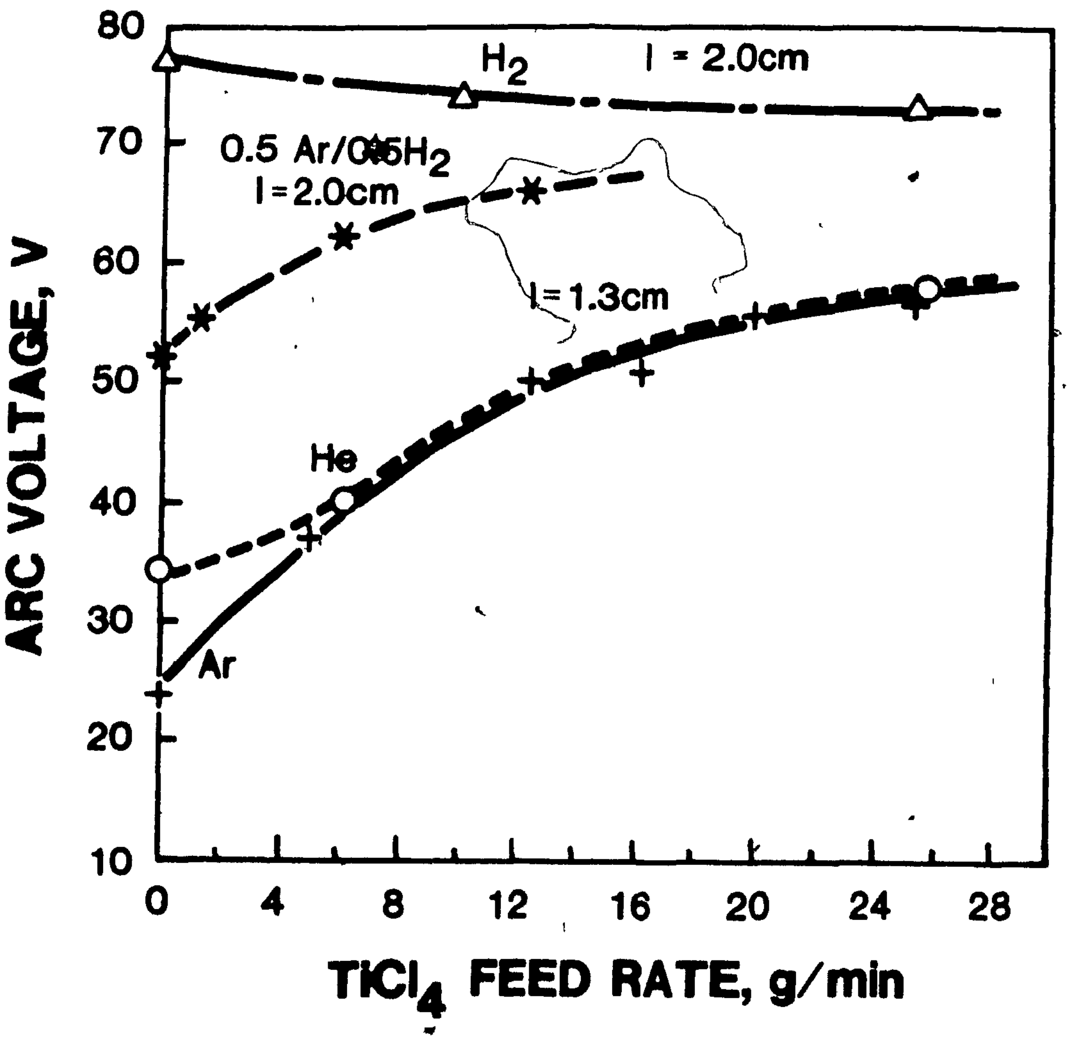
ARC VOLTAGE, V
80
70
60
50
40
30
20
10
0
4
8
12
16
20
24
28
TiCl4 FEED RATE, g/min
H2
l = 2.0cm
0.5 Ar/0.5H2
l=2.0cm
l=1.3cm
He
Ar

or hydrogen plasmagas are shown in Figure 8. In this Figure, the error bars are a measure of the voltage noise. The two-minute voltage was assumed to mark the interface between two sources of voltage increase. During the first minute or two, depending on the $TiCl_4$ feed rate, the voltage increased primarily due to increases in $TiCl_4$ concentration in the plasmagas feed. It would take about that ong for the $TiCl_4$ feed system to reach equilibrium operation. After this start-up time, the composition of the plasmagas remained constant and any further increases in voltage is explained best by phenomena occurring at the electrodes.

Titanium tetrachloride vapour was also adde to plasmagas containing pure hydrogen or equi-molar mixtures of hydrogen and argon, as shown in Figure 7. The case of pure hydrogen is of particular interest since the addition of $TiCl_4$ resulted in a small reduction in the total arc voltage after two minutes of operation. As shown in Figure 8, within 30 seconds from the time the $TiCl_4$ was first fed to the $TiCl_4$ vapourizer, the arc voltage was reduced to 64 V from its initial value of 77 V for pure H_2. After that the voltage started increasing again and eventually reached values higher than 85 V. The initial reduction in the voltage, although relatively small considering that the voltage noise for both pure H_2 and $TiCl_4$ rich plasmagas was between 2 and 16 V, may suggest that the energy requirements for the $TiCl_4$ arc column are lower than those for H_2, owing to a lower energy of ionization. It is likely that the initial voltage drop is due to changes occuring within the arc column, whereas subsequent increases are

FIGURE 8

VOLTAGE VARIATIONS WITH TIME FOR $TiCl_4$-RICH ARCS USING A THORIATED TUNGSTEN CATHODE

Operating Parameters

	Line A	Line B	Line C
Main Plasmagas	He	Ar	H_2
Main PLasmagas FLowrate, L/min	10	10	10
$TiCl_4$ Feedrate, g/min	6	25	25
Arc Current, A	200	200	200
Arc Length, cm	1.3	1.3	2.0

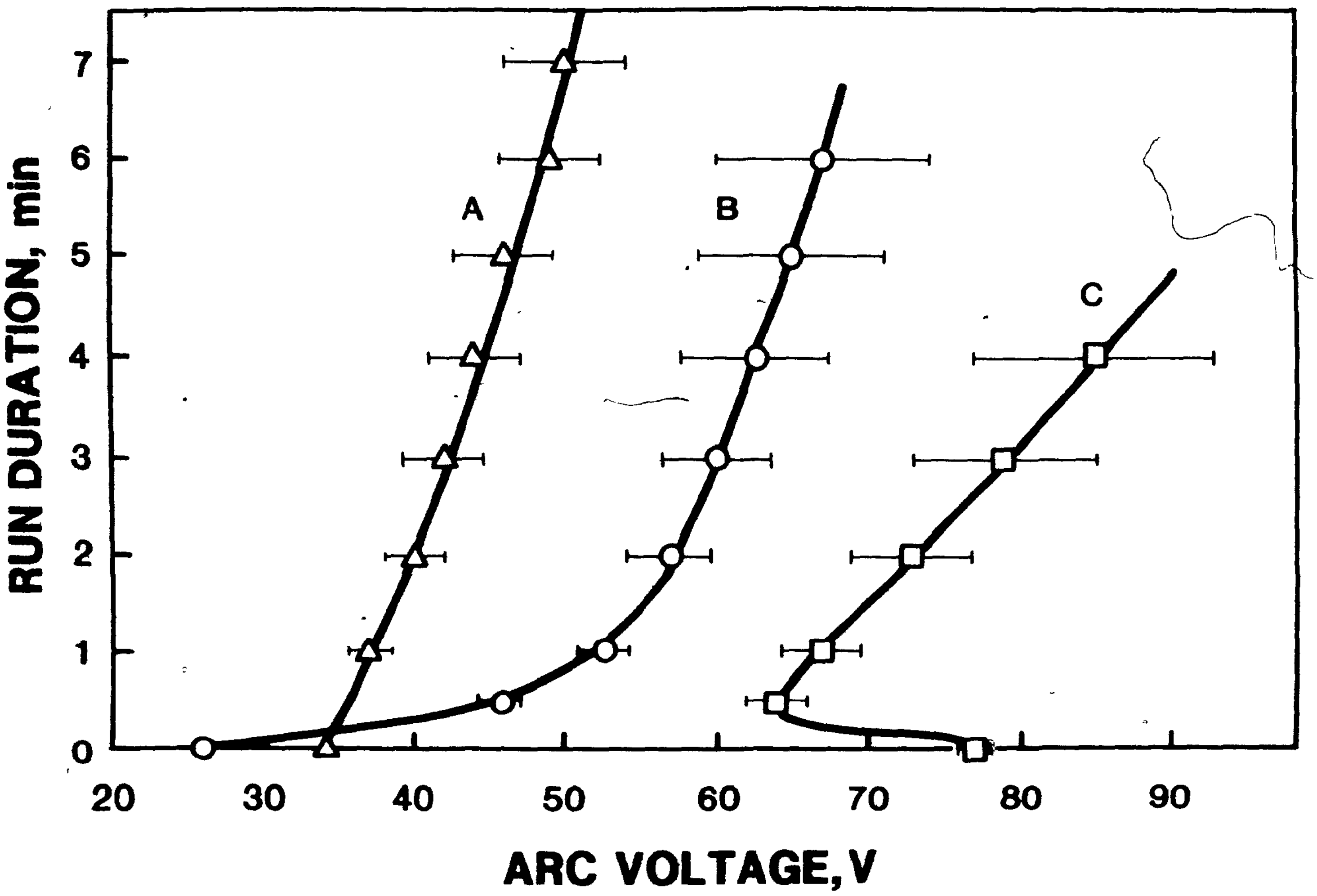
RUN DURATION, min
0
1
2
3
4
5
6
7
20
30
40
50
60
70
80
90
ARC VOLTAGE, V
A
B
C

the result of electrode deterioration. These results are consistent with data provided earlier for the arc column voltage gradient of pure hydrogen (14 V/cm) and $TiCl_4$ rich plasmagas (12 V/cm). They may also explain the small reduction in the total arc voltage resulting from the introduction of $TiCl_4$ into an H_2 arc as shown in Figure 7.

iii. Electrode Phenomena

The transferred arc system used in this study utilized an electron emitting surface (cathode), an electrically conductive medium (arc column) and an electron receiving surface (anode). The total arc voltage was the sum of the voltage drops occurring in the cathode attachment region (cathode fall), in the arc column and in the anode attachment region (anode fall). Of these three regions, the cathode fall is the most crucial in determining the operating stability of the plasma and contributes significantly to the total power requirments. Consequently, it is within this region that the source of instability of the $TiCl_4$ rich plasmas was investigated.

It was observed that whenever $TiCl_4$ was introduced into the plasmagas, the cathode deteriorated rapidly, and both the total arc voltage and the voltage noise increased with operating time and $TiCl_4$ concentration. All of these observations can be explained by phenomena occurring at the cathode surface.

Cathode deterioration can be either due to thermal erosion or chemical corrosion. Thermal erosion is caused by high temperatures typical of the transferred arc's cathode spot (arc attachment area). The temperature of the cathode spot can be calculated using the Richardson-Dushman equation:

$$j_o = A \cdot T^2 \exp(-\phi/kT) \qquad (3)$$

where **j_o** is the current density, **ϕ** is the cathode material's thermionic work function in eV, and **A** is a theoretical constant (1.20 $A/(mm^2 \cdot K^2)$) whose experimental value is sensitive to surface conditions, particularly to surface films, **k** is Boltzmann's constant and **T** is the temperature at the cathode surface, in K.

The cathode spot temperature for plasmas utilizing inert plasmagas is near or above the melting temperature of the cathode material. For thoriated tungsten the cathode spot temperature may be between 3 000 and 5 000 K resulting in minimum thermal erosion. However, should for some reason the thoria, which plays a crucial role in reducing the thermionic work function and operating temperature, be depleted, thermal erosion would increase rapidly.

Exceptionally high cathode deterioration rates, such as those observed in this study, usually imply the presence of a chemical reaction on the cathode's surface. Considering the high cathode spot temperatures one may expect that providing favourable thermodynamic conditions, reactions at the cathode's surface would occur very rapidly. Furthermore, some of the products, such as oxides and chlorides, would have boiling temperatures lower than the cathode spot temperature and would instantly vapourize upon formation while others, such as metals, carbides and nitrides, would have high boiling points and could remain on the cathode's surface.

Consequently, cathode deterioration may occur based on one or all of the following mechanisms:

1. chemical reactions between the plasmagas and the emitter (commonly ThO_2) can increase the cathode's work function resulting in increased thermal erosion,

2. chemical reactions between the plasmagas and the base metal (commonly tungsten) resulting in the formation of products with low boiling points and an unstable, retreating cathode surface, and

3. chemical reactions between the plasmagas and the cathode material resulting in the formation of high boiling point products (such as titanium metal) which condense on the cathode's surface preventing electron emission and effectivly suffocating the arc.

Any of these mechanisms would result in excessive cathode deterioration, unstable arc operation and increased cathode fall voltage.

Experimental results of the degree of cathode deterioration, measured in terms of mass loss of the cathode material, are shown in Table I. All arcs operated at an arc current of 200 A. Pure argon or helium arcs showed no measurable cathode deterioration whereas pure hydrogen arcs exibited relatively small yet measurable mass loss (about 0.1 mg/min). However, as soon as $TiCl_4$ was injected into the arc the cathode deterioration became extensive with measured losses as high as 0.21 g/min for highly concentrated $TiCl_4$ arcs. These high deterioration rates suggest that the cathode material is reacting with $TiCl_4$ based on one or more of the mechanisms outlined above.

It should be noted that the cathode deterioration rates shown in Table I represent values calculated by dividing the total weight loss of the cathode by the operating time of the $TiCl_4$ arc, usually about 18 minutes. There is no basis for the implied assumption that the deterioration rate is constant throughout the run. Hence, the values in Table I should be used only to demonstrate the fact that rapid cathode deterioration results from the presence of $TiCl_4$ in the plasmagas and that the degree of deterioration is a strong function of the $TiCl_4$ concentration.

TABLE I. THORIATED TUNGSTEN CATHODE DETERIORATION DATA

PLASMAGAS (L/min)	ARC LENGTH (cm)	$TiCl_4$ FEED (g/min)	ARC VOLTAGE (V)	CATH. DETERIOR. (mg/min)
10-Ar	2.0	0	26	0.0
10-He	1.3	0	34	0.0
10-H2	2.0	0	77	0.1
10-H2	2.0	20	72	120
5-Ar + 5-H2	2.0	1	55	3.5
15-Ar + 15-H2	2.0	5	67	13
5-Ar + 5-H2	2.0	5	62	170
10-Ar	1.3	12.5	54	210

Furthermore, data presented in Figure 8 show that the voltage noise,represented in Figure 8 by the error bars, is constantly increasing during the duration of each run. This suggests that the reaction mechanism has a cummulative effect on the cathode surface. Assuming that the reaction rates are very fast, a safe assumption considering the high cathode spot temperature, the first two mechanisms are not likely to produce a cumulative effect. Since all products formed in these mechanisms vapourize and leave the cathode surface, the surface would remain clean and reach a steady-state composition despite its rapid deterioration. In essence the transferred arc system would function much in the same way as those systems which utilize a consumable cathode.

Suspecting the third mechanism, the surface of a cathode tip was examined before and after a run. Using an Electron Scanning Microscope (JOEL JSM-35CF), photographs of the surface were taken of a new cathode, of one that had been used in an argon arc and of one that had been used in a $TiCl_4$ rich argon arc. The microscope used images from a Secondary Electron Detector for these photographs. The results are shown in Figure 9. While the surface destruction of the pure argon-operated cathode was minimum, the $TiCl_4$-rich (25 g/min in 10 L/min Ar) plasmagas had caused extensive corrosion. After operating the $TiCl_4$ arc for only 8 minutes, chemical corrosion had consumed the cathode material up to 3 mm in depth. On one side of the cathode's surface a small (about 1 mm) protrusion appeared (the black area in Figure 9-d). This protrusion was

FIGURE 9

PHOTOGRAPHS OF THE CATHODE'S SURFACE

9-a. new unused cathode

9-b. cathode after 10-minute operation using pure argon plasmagas

9-c. cathode after 8-minute operation using $TiCl_4$-rich plasmagas

9-d. titanium concentration map

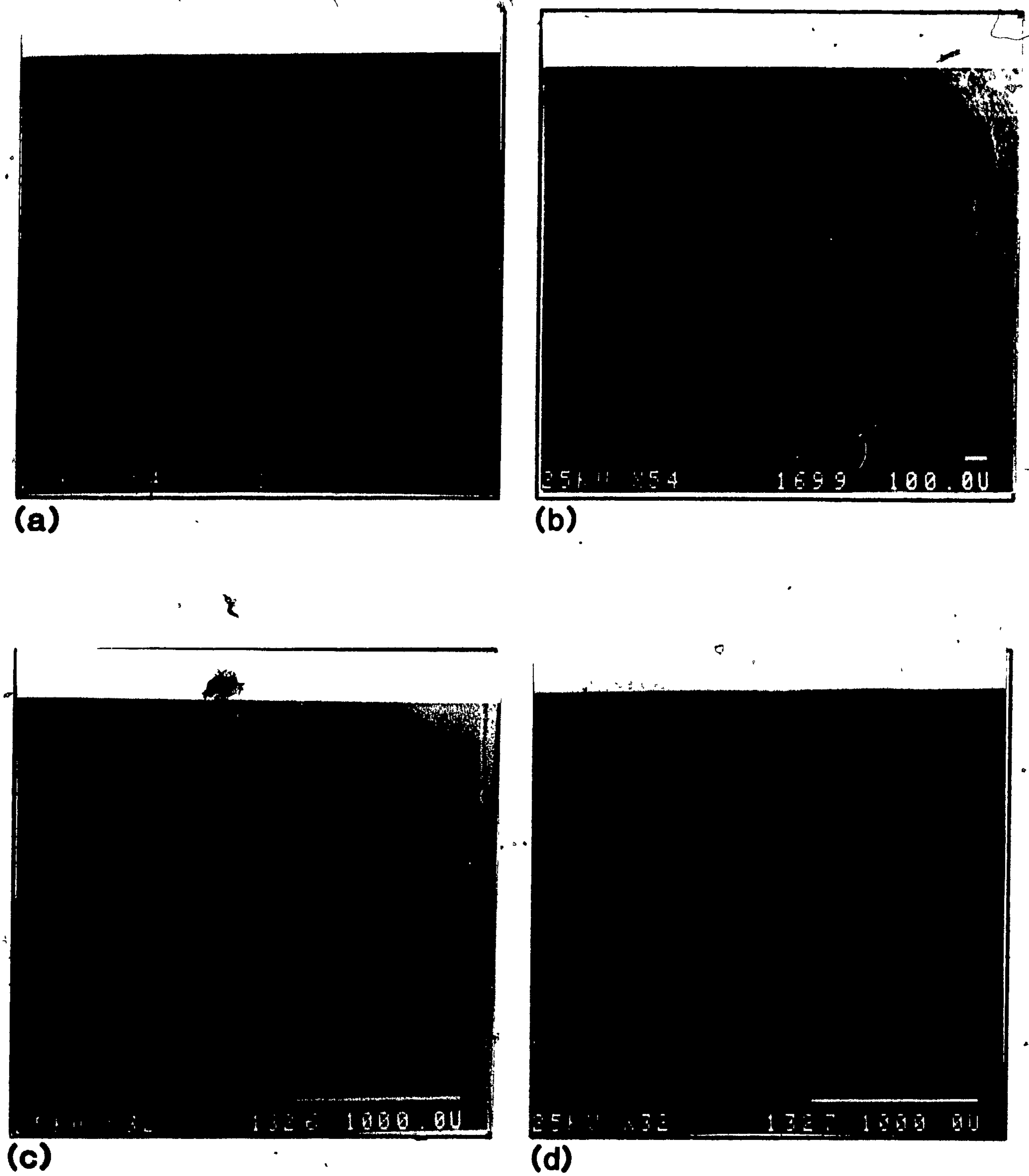
25KV X54 1699 100.0U
1326 1000.0U
25KV X32 1327 1000.0U
(a)
(b)
(c)
(d)

present on the cathode surface after each $TiCl_4$ run and is believed to designate the location of the cathode spot at the termination of the run.

The composition of the cathode surface was examined using an Energy Dispersive X-Ray Mapping method. The resulting titanium concentration map is also shown in Figure 9. It was discovered that the entire surface outside the protrusion was covered with titanium metal. The protrusion itself consisted of tungsten. There was no evidence of chlorine or thoria anywhere on the surface. In the map shown in Figure 9-d, the light areas indicate the presence of titanium, whereas only tungsten was found in the darker areas.

The photographic and chemical analyses of the cathode surface, when combined with results presented earlier on arc voltage, voltage noise and cathode deterioration, suggest an answer to the mechanism responsible for arc instability in $TiCl_4$-rich plasmas. Tungsten and thoria react with $TiCl_4$ to form tungsten chlorides, thorium chlorides and oxychlorides and titanium. The chlorides and oxychlorides vapourize from the cathode instantly, whereas the titanium metal condenses on the surface forming a blanket able to suppress electron emission. In the hottest region of the cathode, namely the cathode spot, the titanium vapourizes and molten tungsten maintains electron emission. Eventually, the blanket of condensing titanium becomes thick enough to suffocate the cathode spot and extinguish the arc.

From the above analysis it became clear that it would not be possible to produce a stable $TiCl_4$ arc using thoriated tungsten as the cathode material and a search was initiated for a replacement. The properties considered important in the selection of a cathode material were its thermionic work function, its reactivity with $TiCl_4$ at high temperatures and its melting and boiling points. A number of materials were evaluated based on these properties. The result of the evaluation are shown in Table II.

The chemical reactivity was assesed using the F.A.C.T. Equilibrium program in the McGill computer library. This program is designed to calculate the equilibrium concentration of all possible products containing the chemical species of the reactants based on minimizing the system's total free energy of formation. The reactivity coefficient **α** shown in Table II represents the fraction of the original cathode material reacting with $TiCl_4$ to form chlorides or oxychlorides at equilibrium. It is calculated based on the equation:

$$R + TiCl_4 \rightarrow \alpha RCl_x + TiCl_y + (1-\alpha)R \qquad (4)$$

The above equation does not represent events occurring on the cathode surface. It simply provides a method of evaluating the relative reactivity of different materials to $TiCl_4$. However, even a small coefficient can have catastrophic consequences since the reactions

TABLE II. CHEMICAL REACTIVITY OF MATERIALS TO TITANIUM TETRACHLORIDE

MATERIAL	REACTIVITY, α		M.P.	B.P.	ϕ
	2 000 K	4 000 K	(K)	(K)	(eV)
W	0.175	0.640	3 680	5 930	4.5
Ta	0.189	0.002	3 270	5 700	4.3
Nb	0.180	0.070	2 740	5 015	4.0
Mo	0.000	0.150	2 890	4 885	4.2
ThO_2	0.154	0.790	3 490	4 670	3.3
ZrO_2	1.000	1.000	2 970	5 270	3.6
WC	0.005	0.547	3 140	6 270	4.5
TaC	0.000	0.000	4 150	5 770	3.8
NbC	0.069	0.022	3 770	-	4.2
Mo_2C	0.000	0.080	2 960	-	4.6
TiC	0.074	1.000	3 410	5 090	4.3
ZrC	0.994	1.000	3 810	5 370	3.6

proceed very rapidly at high temperatures and there is a constant supply of fresh $TiCl_4$ at the cathode. For this reason, TaC was chosen as the preferred cathode material. Along with its complete resistance to $TiCl_4$, tantalum carbide offers a relatively low thermionic work function and its melting and boiling points compare well with those of tungsten.

Thoria plays a crucial role in lowering the work function of conventional cathodes. Not only it has a low work function of its own, but in small concentrations it can lower the work function of the cathode even below the value of either component. Matskevich (1968), for example, measured the work function of thoriated tungsten at 3.15 eV compared to measured work functions of 4.55 eV for tungsten and 3.3 eV for thoria. Not knowing the effect of thoria on tantalum carbide cathodes it was decided that both thoriated (1 % ThO_2) and pure TaC cathode should be tested.

The results of using the thoriated TaC cathode on arc voltage as a function of time are shown in Figure 10. Indeed the new cathode material was highly successful in stabilizing both the arc voltage and the voltage noise. The remaining voltage noise, indicated in Figure 10 by the error bars, is probably caused by fluctuations in the $TiCl_4$ feed. The $TiCl_4$ feed system consisted of pumping the reactant in its liquid form onto a hot plate where it instantly vapourized. The peristaltic nature of the pump would therefore introduce unavoidable fluctuations in the plasmagas composition. Not suprisingly, such

FIGURE 10

ARC VOLTAGE VARIATIONS WITH TIME FOR $TiCl_4$-RICH ARCS WHICH UTILIZE A THORIATED TANTALUM CARBIDE CATHODE

Operating Parameters

	Line A	Line B
Main Plasmagas	Ar	Ar
Main Plasmagas Flowrate, L/min	15	15
$TiCl_4$ Feedrate, g/min	7	25
Arc Current, A	200	200
Arc Length, cm	2.5	2.5

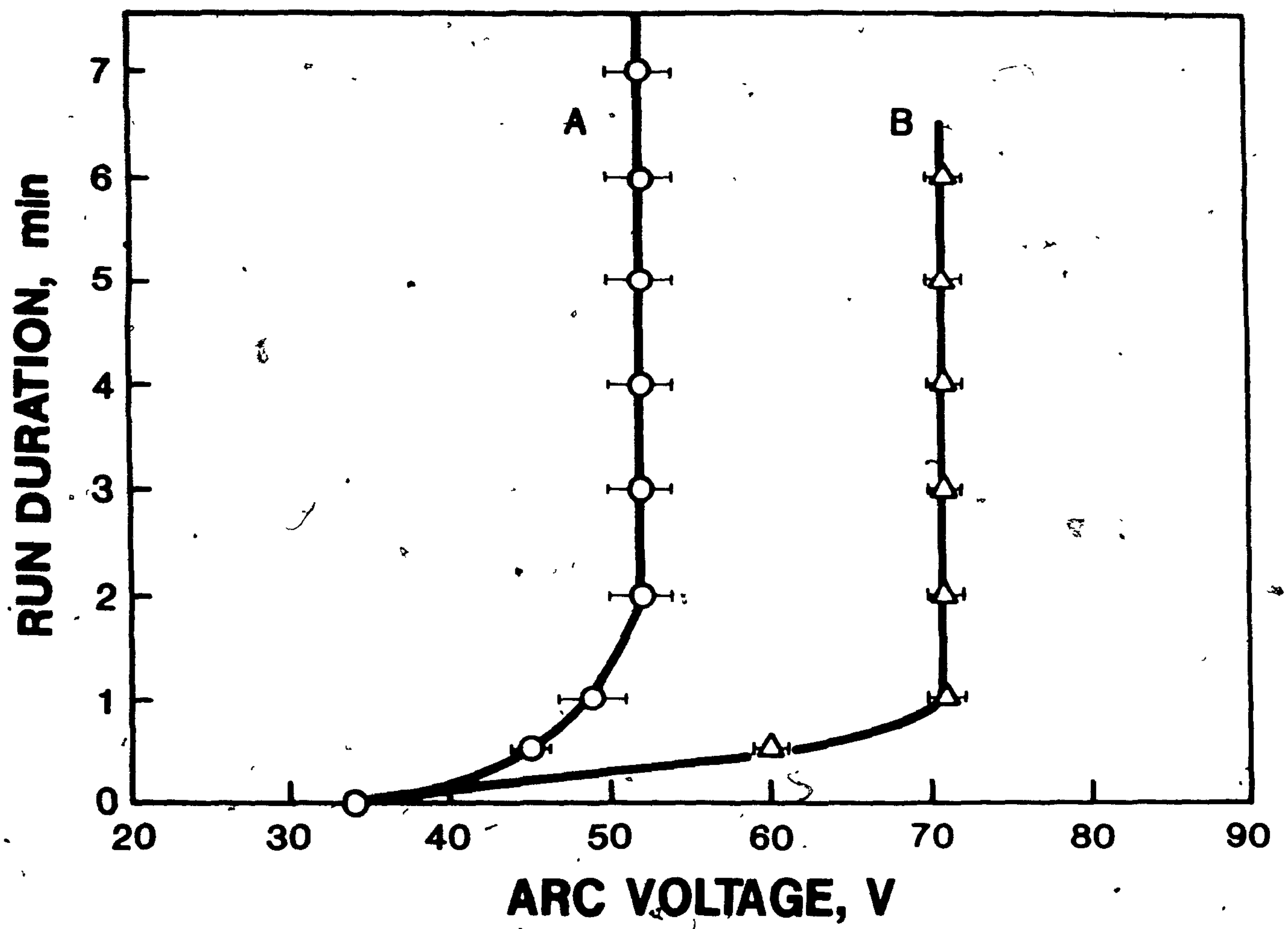
A
B
RUN DURATION, min
0
1
2
3
4
5
6
7
20
30
40
50
60
70
80
90
ARC VOLTAGE, V

fluctuations were minimized at higher $TiCl_4$ feed rates when the frequency of the peristalses increased. It is for this reason that the voltage noise shown in Figure 10 decreases at higher $TiCl_4$ feed rates.

There was little difference between the operation of thoriated and of pure TaC cathodes operating in $TiCl_4$ rich plasmagas. This may be explained by the fact that thoria is rapidly consumed at the cathode surface through its reaction with $TiCl_4$ and is thus unable to contribute to electron emission. There was, however, a more noticable difference when the two tips were operated in pure argon plasmagas. For a 2.5-cm long arc operating at 200 A current and 15 L/min argon gas flowrate, the thoriated TaC cathode produced an arc voltage of 32-35 V. Under the same conditions the pure TaC cathode produced an arc voltage of about 38 V. Furthermore, the cathode spot area of the pure TaC tip appeared fused, indicating operating temperatures above the melting point of TaC (4 150 K). No fused spot appeared in the thoriated TaC cathode.

The deterioration rates for both thoriated and pure tantalum carbide cathodes operating either in pure argon or in $TiCl_4$-rich plasmagas are shown in Table III. The deterioration of the TaC cathodes was generally higher than that of tungsten in inert atmospheres. However, in the presence of $TiCl_4$ the deterioration of TaC was much lower than that observed with tungsten. Furthermore, the deterioration rate of TaC in the presence of $TiCl_4$ was not significantly different than its rate in inert atmospheres, suggesting the absence of chemical

TABLE III. TANTALUM CARBIDE CATHODE DETERIORATION DATA

PLASMAGAS (L/min)	ARC LENGTH (cm)	$TiCL_4$ FEED (g/min)	ARC VOLTAGE (V)	THORIA (%)	CATH. DETERIOR. (mg/min)
15-Ar	2.5	0	34	1	0.8
15-Ar	2.5	16	69	1	8
15-Ar	2.5	25	71	1	2
15-Ar	2.5	0	38	0	8
3-Ar	2.5	25	77	0	6

corrosion.

The cathode deterioration rates, shown in Table III, for thoriated TaC cathodes operating with pure argon plasmagas were lower than those for pure TaC cathodes (0.8 mg/min compared to 8 mg/min). However, these numbers may include large errors due to the poor structural properties of the available TaC and thoriated TaC cathode ~~tips.~~ The density of the available rods, from which cathode tips were made, was only about 75 percent of the material's theoretical density. At this low density, the tips fracture quite easily and it is imposible to distinguish between deterioration resulting from plasma phenomena and mass loss due to simple attrition or fracture. Denser TaC cathode tips are required if such tips are to be used extensively with halide plasmagas.

Operating Characteristics of Titanium Tetrachloride Arcs

Some important operating characteristics of transferred titanium tetrachloride arcs are described in this section. All data presented here are for atmospheric pressure arcs operating at an arc current of 200 A. Only relatively short arc lengths (less than 3 cm) were used in this study.

1. General Observations

The introduction of $TiCl_4$ significantly changed the appearance of the transferred arc. In fact, the appearance of the $TiCl_4$ containing arc was completely different from that of any arc utilizing a pure plasmagas. The arc columns of pure plasmas (i.e. plasmagas consisting of a single element, atomic or molecular), appear visually homogeneous, their color being determined by the spectrum of the plasmagas. Thus the luminous part of the argon arc column appears white in its entirety, just as the luminous part of the hydrogen arc column appears red in its entirety. However, the introduction of $TiCl_4$ into the plasmagas results in an non-homogeneous arc column. While the central region of the arc column maintained its pre-$TiCl_4$-injection appearance, a luminous light blue sheath formed on the outside. As the concentration of $TiCl_4$ increased, the central region shrunk, allowing the sheath region to expand towards the core. Arc column photographs of various plasmas are shown in Figure 11.

The most likely reason for the appearance of the sheath in $TiCl_4$-containing arcs is the strong temperature and concentration gradients within the arc column. Despite their homogeneous appearance arc columns are not at a uniform temperature, their central region being significantly hotter than the periphery. Strong radial gradients of velocity and species concentration also exist. For example, Mehmetoglu and Gauvin (1983) measured the temperature at various locations within

FIGURE 11

PHOTOGRAPHS OF TRANSFERRED ARC

11-a. equi-molar Ar-H_2 mixture

11-b. 5 g/min $TiCl_4$ in Ar-H_2 equi-molar mixture

Operating Parameters

Arc Length = 2.5 cm

Arc Current = 200 A

Plasmagas Flowrate = 30 L/min

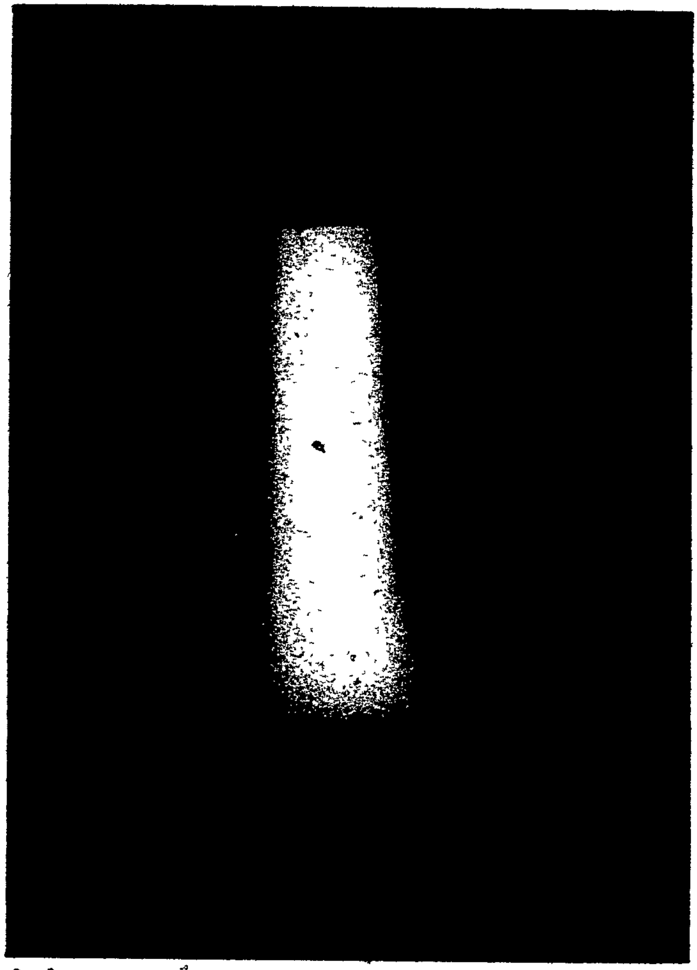

(a)

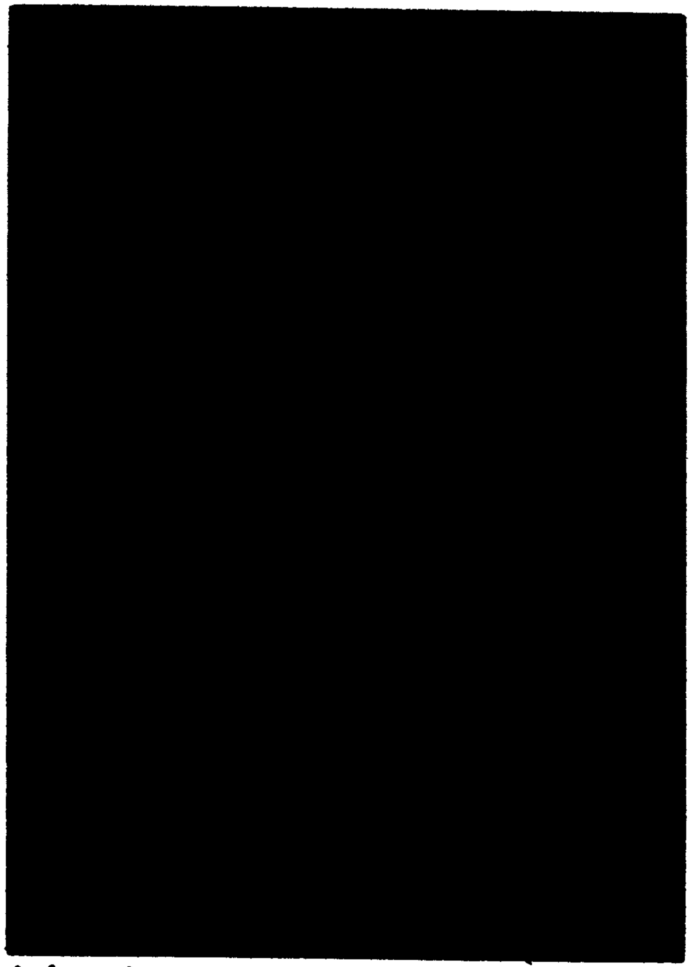

(b)

an argon arc column. They reported temperatures around 18 000 K near the cathode tip, 13 000 K in the center of the arc column and 3 cm below the cathode, and only 9 000 K at the periphery of the luminous region.

While the work of Mehmetoglu and Gauvin did not deal with diffusion phenomena in transferred arcs, the theories of thermal diffusion in arcs containing mixed plasmagases are described by Vacquie (1984). Based on such theories, plasmagas mixtures containing an atomic gas A (e.g. Ar) and a molecular gas B (e.g. $TiCl_4$) result in arcs which operate with an increase in the concentration of A in the center of the column, and an increase in the concentration of B in the colder peripheral region. Furthermore, plasmas containing atoms with different ionization potential (e.g. Ti, Cl, and Ar have ionization potentials of 6.8, 13.0, and 15.8 eV, respectively) operate with an increase of the species with the highest ionization potential in the central region of the column.

When $TiCl_4$ is introduced into the plasmagas, the overall temperature of the arc column begins to drop due to the lower ionization potential of the Ti atom. At the same time, thermal diffusion results in high concentrations of Ti^+ ions, and non-dissociated titanium subchlorides in the peripheral region of the arc column. However, while the concentration of $TiCl_4$ is still low, the current cannot be carried by the electrons contributed by the Ti alone. Therefore, the arc column temperature must remain high enough to assure that at least some of the main plasmagas becomes ionized. Consequently, the central region of the arc column, which is highly concentrated with the ionized and atomic constituents of the main plasmagas (e.g. Ar), appears the same as it did prior to the injection of $TiCl_4$. On the other hand, the periphery becomes too cold to ionize the main plasmagas and contains only the charged species contributed by the Ti atoms. It is these concentration and temperature gradients that result in the formation of the sheath in $TiCl_4$ containing arcs.

As the $TiCl_4$ concentration in the plasmagas increases, more and more easily ionizable Ti atoms become available, the electrical conductivity continues to increase, and the overall temperature of the arc column continues to drop. Hence the central luminous region shrinks as increasingly smaller volume of the column is hot enough to ionize the main plasmagas. Finally, when the Ti concentration is high enough to provide all the current carriers needed, the central region disappears and the arc column becomes once again homogeneous in appearance, characterized throughout by a light blue colour.

Based on this analysis, the formation of a sheath should not be a unique characteristic of $TiCl_4$ containing arcs but rather should occur whenever the plasmagas contains constituents with significantly different ionization potential. This was verified experimentally through the operation of transferred arcs containing various mixtures of argon and helium (ionization potential of He = 24.5 eV) in the plasmagas.

When small amounts of Ar are introduced into an He arc a sheath is formed much in the same manner observed through the introduction of small amounts of $TiCl_4$. Helium plasmas, characterized by a bright peach color, are much hotter than Ar plasmas due to helium's high ionization potential. Thus, the introduction of Ar results in a drop in the arc column temperature seen by the formation of the white sheath, characteristic of Ar ionization, in the column's periphery. When the molar concentration of argon in the plasmagas reaches 15 percent, only a very thin peach-coloured core region, extending from the anode to the cathode, still appears. When the Ar concentration exceeds 15 percent molar the peach luminous region retreats to the vicinity of the cathode spot and is barely noticeable at Ar concentrations higher than 50 percent molar.

Assuming the above analysis to be correct, it may be possible to make some qualitative speculations about the temperature of $TiCl_4$-containing arcs. From the work of Mehmetoglu and Gauvin we know that the lowest temperature at which an argon arc is still luminous is about 9 000 K. Thus, in a plasma utilizing Ar as the main plasmagas, the contour dividing the central region from the sheath is probably at around 9 000 K. Everything within the central region would be at a higher temperature, just as everything within the sheath would be at a temperature lower than 9 000 K. The ionization of chlorine from the $TiCl_4$ molecule or the introduction of hydrogen in the main plasmagas are likely to have only a relatively small effect since the ionization potential of Cl and H are roughly the same as that of Ar. Unfortunately, such speculations cannot be verified since no direct temperature measurements were made in this study.

ii. Power Requirements of Transferred Titanium Tetrachloride Arcs

The power required to operate a transferred titanium tetrachloride arc is directly proportional to the total arc voltage of $TiCl_4$ plasmas. Some arc voltage data for arcs utilizing $TiCl_4$-rich plasmagas have been given previously in the Arc Column Characteristics section. Additional information for stable $TiCl_4$ arcs (i.e. arcs using TaC cathode tips) are provided here.

The change in total arc voltage due to the introduction of $TiCl_4$ in the plasmagas is shown in Figure 12. For a 2.5-cm long transferred arc utilizing 15 L/min of pure argon as the plasmagas, a thoriated tantalum carbide cathode and a water-cooled molybdenum anode, the measured arc voltage was 34 V. As $TiCl_4$ is introduced to the plasmagas the voltage increases quickly. At a $TiCl_4$ feed rate of 16 g/min the voltage reaches a value of about 68 V. A $TiCl_4$ feed rate of 16 g/min in 15 L/min of Ar corresponds to a molar $TiCl_4$ concentration of about 12.5 percent.

Further increases in $TiCl_4$ feed rate caused little changes in the arc's voltage. Thus, it appears that the power requirements of argon

FIGURE 12

TOTAL VOLTAGE OF TRANSFERRED ARCS USING $TiCl_4$-RICH PLASMAGAS AND A THORIATED TANTALUM CARBIDE CATHODE

Operating Parameters

Arc Length = 2.5 cm

Arc Current = 200 A

Argon Plasmagas Flowrate = 15 L/min

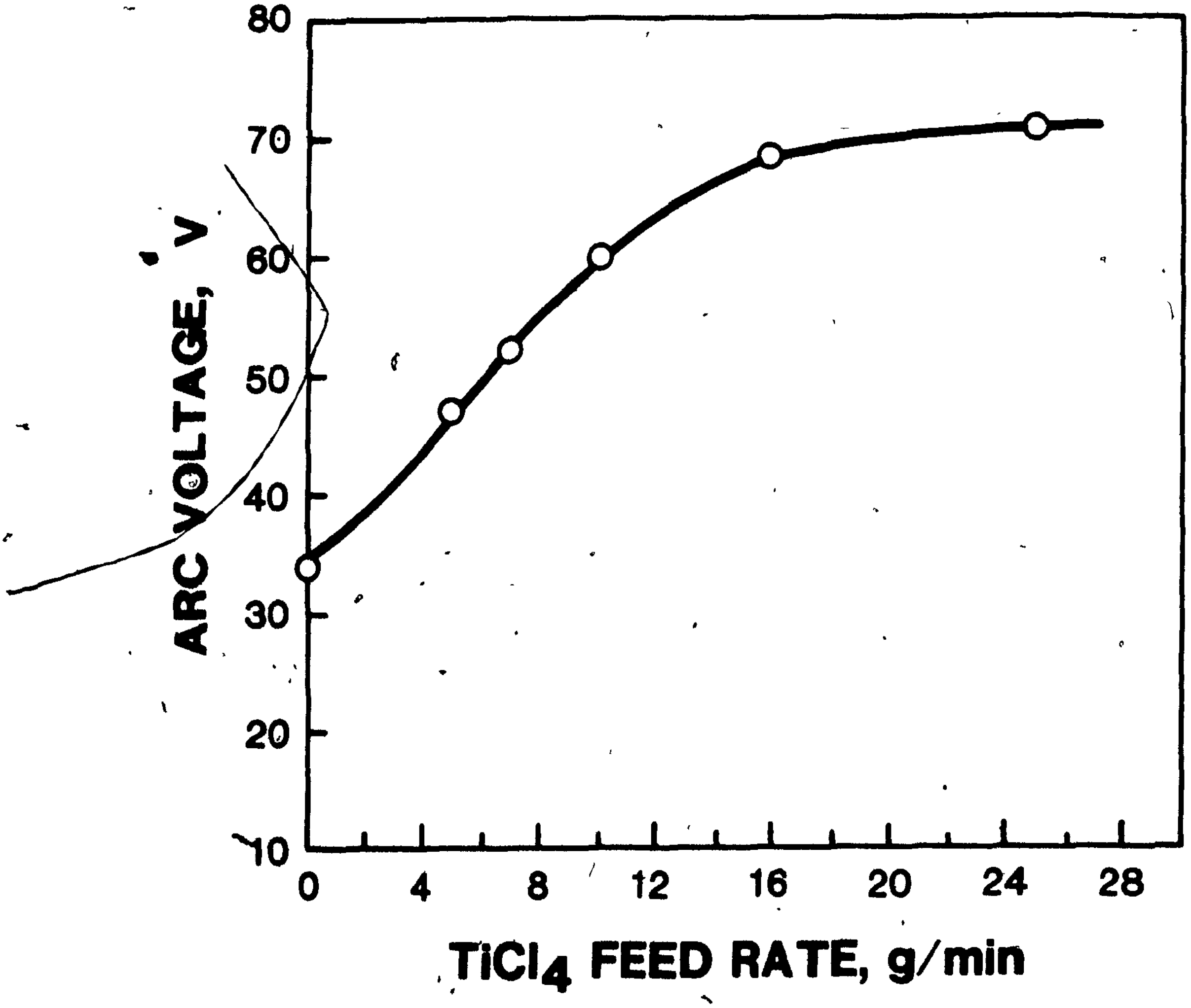
80
70
60
50
40
30
20
10
ARC VOLTAGE, V
0
4
8
12
16
20
24
28
TiCl4 FEED RATE, g/min

plasmas containing more than 12.5 percent molar $TiCl_4$ are characterized more by the properties of $TiCl_4$ than those of Ar. Unfortunately, the experimental apparatus used in this study did not allow for $TiCl_4$ feed rates much higher than 25 g/min. Therefore, it was not possible to test the above hypothesis by further increasing the $TiCl_4$ feed rate. Instead, it was decided that the effect of increasing the plasmagas chloride concentration above 12 percent could be evaluated by keeping the $TiCl_4$ feed rate constant at its maximum permisible value and reducing the argon flowrate. The results of these experiments are shown in Figure 13.

Using a 2.5-cm long arc, a TaC cathode and a Mo water-cooled anode, the total arc voltage was measured for plasmagas compositions containing 25 g/min of $TiCl_4$ and decreasing flowrates of argon. At the maximum Ar flowrate (23 L/min) for line B the $TiCl_4$ concentration was just under 12 percent molar. At the minimum Ar flowrate (3 L/min) the $TiCl_4$ plasmagas concentration was about 50 percent molar. Further decreases in the argon flowrate were not attempted because the transferred arc system used in this study was unable to maintain stable operation at total plasmagas flowrates lower than 5 L/min. This instability at very low plasmagas flow rates was also observed in pure Ar plasmas using thoriated tungsten cathodes. Experimentally measured variations in total arc voltage due to changes in plasmagas flowrate for pure argon arcs are also presented in Figure 13 (Line A) for the purpose of comparison.

FIGURE 13

TOTAL VOLTAGE OF $TiCl_4$-RICH ARCS USING A TANTALUM CARBIDE CATHODE

Operating Parameters

	Line A	Line B
Main Plasmagas	Ar	Ar
$TiCl_4$ Feedrate, g/min	0	25
Arc Current, A	200	200
Arc Length, cm	2.5	2.5

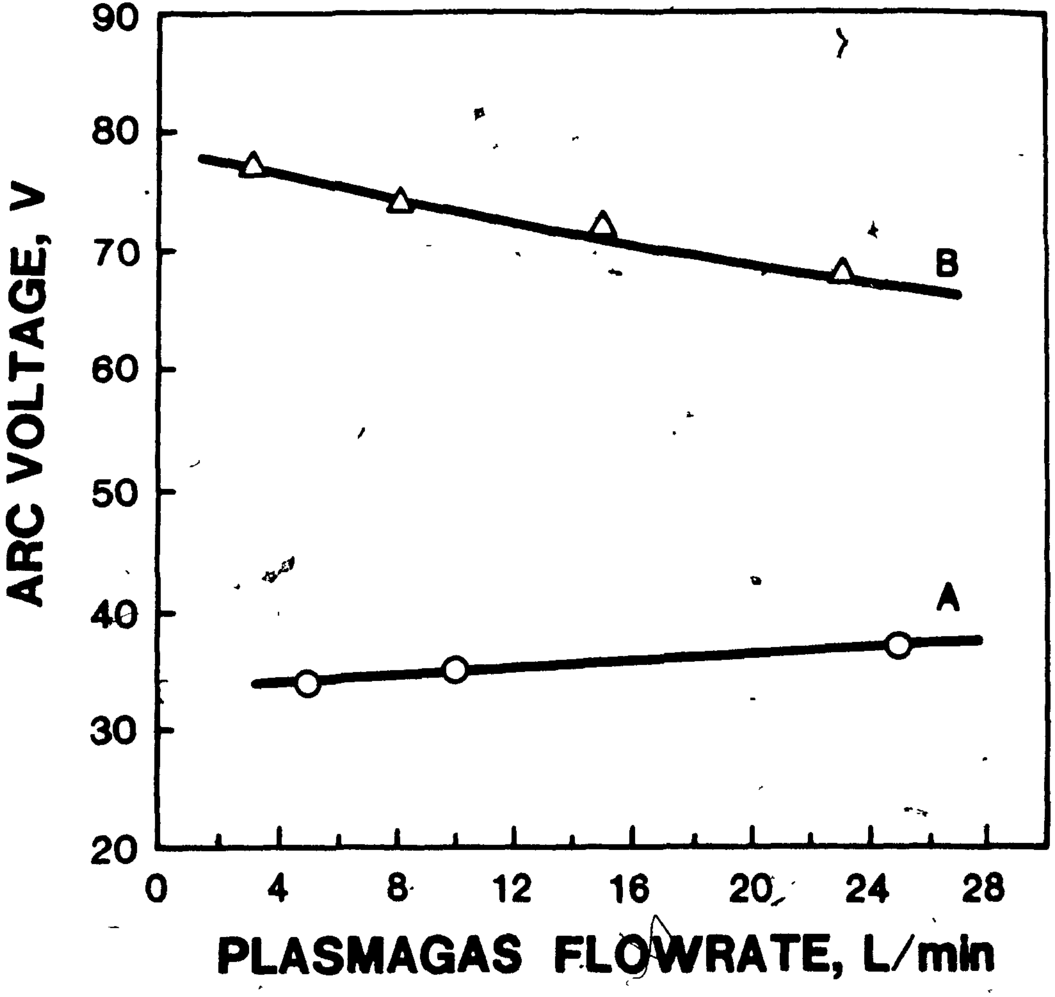
90
80
70
60
50
40
30
20
ARC VOLTAGE, V
0
4
8
12
16
20
24
28
PLASMAGAS FLOWRATE, L/min
B
A

From the results shown in Figure 12, one may conclude that the total arc voltage of highly concentrated $TiCl_4$ plasmas increases only slightly at $TiCl_4$ plasmagas concentrations above 12 percent. A plasmagas containing 23 L/min Ar and 25 g/min $TiCl_4$ ($TiCl_4$ concentration = 12 % molar) operated at an arc voltage of 68 V. When the argon flowrate was reduced to 3 L/min ($TiCl_4$ concentration = 50 % molar) the voltage increased only to 77 V. This increase in voltage is small when compared to voltage increases observed at lower $TiCl_4$ concentrations (see Figure 12), and may be attributed to either an increase in the arc's enthalpy or to electrode phenomena. It was not possible from the results of this study to separate voltage increases caused by electrode phenomena from those caused by changes in the arc column composition and total plasmagas flowrate.

The reasons for the apparent ability of $TiCl_4$ to dominate the characteristics of the arc, even at relatively low molar concentrations, were not investigated. However, the observation that variations in the total arc voltage are not proportional to the concentration in the plasmagas mixture is not unusual. For example, the total voltage of a 2-cm pure helium transferred arc operating at a current of 200 A and atmospheric pressure, between a copper water-cooled anode and a thoriated tungsten cathode, is about 40 V. Under the same conditions a pure argon arc's total voltage is about 25 V. However, an arc utilizing an equi-molar plasmagas composition of Ar and He, and the same total gas flowrate, has a voltage of 27 V, only 2 V higher than that of pure Ar. A plasma containing 10 percent molar argon in helium has a voltage approximately half way between that of pure Ar and pure He.

From the results shown earlier (Figure 6) the arc column voltage gradient for arcs utilizing pure argon and $TiCl_4$-rich (25 g/min in 10 L/min Ar) plasmagas are 5 V/cm and 12 V/cm, respectively. Using these results, and assuming that the voltage gradient in the arc column is constant throughout the length of the arc, one may calculate the column voltage for a 2.5-cm arc at about 13 V for pure Ar and 30 V for the $TiCl_4$-rich arc. From results shown in Figure 13 the total arc voltage of pure Ar plasmas (10 L/min flowrate) is 35 V compared to 73 V for $TiCl_4$-rich plasmas (10 L/min Ar + 25 g/min $TiCl_4$). By subtracting the column voltage from the total arc voltage, the electrode fall voltage can be calculated at 22 V for pure Ar and 43 V for $TiCl_4$-rich plasmas. These electrode fall voltages apply only to the above mentioned arcs operating between a tantalum carbide cathode and a water-cooled molybdenum anode.

Since the anode fall voltage has been shown to be very small (Dinulescu and Pfender, 1980) it is likely that these calculated electrode fall voltages represent the cathode fall. Caution must be exercised in using these results since the data shown in Figure 6 were obtained using a thoriated tungsten cathode, whereas the results shown in Figure 13 were obtained using a TaC cathode. Small amounts of tungsten chlorides and thoria oxychlorides could have entered the plasma in experiments using ThO_2-W cathodes and may have affected the arc column voltage gradient.

For the purpose of comparison, the cathode fall potential was estimated for a variety of plasmagas compositions. Using the present experimental set-up, the total arc voltage for 2-cm and 3-cm transferred arcs were measured utilizing 15 L/min of Ar, He, N_2, H_2 or NH_3 as the plasmagas. All arcs were operated at an arc current of 200 A between a thoriated tungsten cathode and a molybdenum water-cooled anode. Using the results from these experiments and the calculation methodology outlined in the above paragraphs the cathode fall voltage for Ar, He, N_2, H_2, and NH_3 were estimated at 18 V, 24 V, 27 V, 49 V, and 29 V respectively. Hydrogen, which exhibited the highest cathode fall voltage, was also the plasmagas to show the highest cathode erosion.

The cathode fall values reported here are considerably higher than those commonly reported in literature. For example, in his review paper on arc electrode phenomena, Guile (1971) reports voltage drops at the cathode of 8 V to 20 V for atmospheric pressure arcs. However, in the same paper the anode fall voltage for such arcs is reported to be between 10 V and 20 V. In the present analysis the anode fall voltage is assumed to be very small, based on the results of Dinulescu and Pfender (1980), and the total measured electrode voltage drop is assumed to be occurring at the cathode.

iii. Energy Distribution within the Transferred Arc Reactor

The total arc power distribution within a closed transferred arc reactor be described by the following energy balance:

$$V \times I = Pa + Pr + Pn + Pc + Pg + Pnb + Pi + Pab \qquad (5)$$

where the sum of the power transferred to the anode **Pa**, the reactor wall **Pr**, the nozzle assembly **Pn**, the cathode assembly **Pc**, the exiting plasma-gas **Pg**, the nozzle base **Pnb**, the electric insulator **Pi**, and the anode base **Pab** is equal to the total power input to the arc.

To measure the amount of the input power transferred to the various components within the reactor, thermocouples were placed strategically in the cooling water circuits. The inlet and outlet water temperatures from each section were measured using six K-type thermocouples connected to a Thermo Electric model Elph 4 digital temperature indicator through a 12-point rotary selector. The resolution of the indicator was 0.1°C. Four calibrated rotameters were used to monitor the cooling water's flowrate in various sections of the transferred arc reactor. The four water cooled sections were the anode, the reactor wall, the nozzle assembly, and the cathode assembly.

The nozzle base, the electric insulator, and the anode base were not water cooled. All energy input to these sections was transferred through conduction to surrounding water cooled sections (see Figure 5) or through natural convection to the ambient gas. The input energy to the nozzle and anode bases was relatively small since neither of these sections received any radiation directly from the arc. There were no measurements made of the energy received by the non-cooled sections of the reactor.

Furthermore, the temperature of the gas inside the reactor and consequently the energy transferred to the exhaust gas was obtained by inserting a thermocouple into the reactor, near the gas exit port, through one of the openings provided in the reactor wall. Through such measurements it was concluded that the energy content of the exiting gas represented only a small fraction of the total power input, typically less than 0.5 percent for pure argon and 1.5 percent for $TiCl_4$-rich plasma, and can be eliminated from Equation (5) without introducing a significant error. As such, Equation (5) was reduced to :

$$V \times I = Pt = Pa + Pr + Pn + Pc \tag{6}$$

In order to calculate the energy transferred to the various sections of the reactor, it was assumed that, at steady state, the energy removed by the cooling water was equal to the energy received by the section being cooled. Using this assumption, the amount of energy received by each section can be calculated from the simple expression:

$$Py = Fy \times \rho \times Cp \times (Tout - Tin)\, y \qquad (7)$$

where **Fy** is the measured cooling water flowrate to component **y** in cm^3/sec, and **ρ** and **Cp** are the water density and heat capacity, assumed constant with values of 1.0 g/cm^3 and 4.18 J/(g·K), respectively.

The results from the energy distribution calculations are shown in Table IV. The percent of the input power transferred to the various components, **n**, of the reactor system can be calculated by dividing both sides of Equation (6) by the total power input to the arc and multiplying by 100. The amount of power transferred to the cathode remained approximately constant for all experiments at about 0.3 - 0.4 kW. This represented between 3 and 5 percent of the total input power to the reactor. The measured values for **Pc** are not included in Table IV.

Experimental Runs 104-106 utilized a thoriated tungsten cathode and a 2-cm arc length, whereas Runs 1-S-1 and 1-S-2 utilized a thoriated TaC cathode, and Runs 1-S-7 to 1-S-9 a pure TaC cathode. All arcs of the 1-S series were 2.5-cm long, and all experiments shown in Table IV operated at an arc current of 200 A. The cumulative error, representing the difference between the sum of the power dissipated to each water-cooled component and the total input power, was less than seven percent of total power **Pt** . The source(s) of this error may be either due to the simplification of Equation (5) or due to systematic errors in the data.

TABLE IV. POWER DISTRIBUTION FOR $TiCl_4$-RICH TRANSFERRED-ARCS

RUN NO.	GAS FLOW (L/min)	$TiCl_4$ FEED (g/min)	POWER DISTRIBUTION							ARC DIAMETER (mm)
			Pt (kW)	Pa (kW)	ηa (%)	Pr (kW)	ηr (%)	Pn (kW)	ηn (%)	
(for runs with arc current = 200 A, arc length = 2.0 cm, cathode = ThO_2-W)										
104-1	Ar-15	0	5.2	3.8	73	0.7	13	0.6	12	7.0
104-2	Ar-30	0	5.6	3.9	70	0.9	16	0.6	11	7.6
106-2	Ar-30	6	9.6	5.0	52	2.0	21	2.2	23	7.6
105-3	H2-30	0	15.4	12.5	81	0.9	6	1.0	6	4.8
105-4	Ar-15 H2-15	0	11.4	9.3	82	1.1	10	0.9	7	5.2
105-5	Ar-15 H2-15	6	12.8	9.4	73	1.5	12	1.4	11	7.1
(for runs with arc current = 200 A, arc length = 2.5 cm, cathode = TaC)										
1-S-1	Ar-15	0	7.2	5.6	78	1.0	14	0.9	13	-
1-S-2	Ar-15	16	13.4	7.8	58	2.3	17	2.9	22	-
1-S-7	Ar-23	0	7.2	5.1	71	1.1	15	0.7	10	-
1-S-8	Ar-23	25	13.6	7.6	56	2.7	20	2.4	18	-
1-S-9	Ar- 8	25	14.8	7.6	51	3.0	20	3.1	21	-

By comparing the results in Table IV for arcs operating with pure argon plasmagas to those with a $TiCl_4$ rich plasmagas, some interesting observations emerge. It appears that the introduction of $TiCl_4$ favors the transfer of energy to the reactor wall and nozzle assembly over the anode. In Run 1-S-1 (Ar only), for example, the total power input to the arc was 7.2 kW. Of this power 78 percent went to the anode, 14 percent radiated to the reactor wall and 13 percent to the nozzle assembly. Run 1-S-2 by comparison, which utilized the same operating conditions but a $TiCl_4$-rich plasmagas, used almost twice the total power input due to its higher arc voltage. Yet the energy transferred to the anode increased only by 40 percent, whereas the energy transferred to the reactor wall and nozzle assembly increased by 130 and 220 percent respectively. Similar observations can be made by comparing Run 1-S-7 to Run 1-S-8, Run 104-2 to Run 106-2, and Run 105-4 to Run 105-5. On the average, in arcs operating with $TiCl_4$-rich argon plasmagas about 20 percent of of the total energy input to the reactor was transferred to each of the reactor wall and the nozzle assembly.

The relative increase of energy transferred to the reactor wall and nozzle assembly for $TiCl_4$ arcs may be explained by a number of factors. $TiCl_4$ has a much higher enthalpy than argon as it leaves the anode surface. Not only the heat capacity of $TiCl_4$ is higher than that of argon, the gas leaving the arc carries with it large amounts of chemical energy utilized in the vapourization and dissociation of the molecule. Once outside the arc, the temperature of the gas drops rapidly, resulting in recombination reactions and the release of energy to the surrounding walls. Furthermore, $TiCl_4$ recombines at relatively low temperatures which assures that much of the recombination energy is released away from the anode and closer to the nozzle assembly and reactor wall. At the end of each $TiCl_4$ run all exposed surfaces on the nozzle assembly and reactor walls were covered with a film of various titanium chloride powders.

A brief analysis was made on the energy distribution within the reactor used in this study for a variety of plasmagases. The results of this analysis for Ar, He, N_2, and H_2 are shown in Table V. From these results it appears that helium and hydrogen exibit smaller arc diameters than argon and nitrogen respectively, and transfer more of the input energy to the anode. The relationship between arc diameter and energy distribution should be obvious. The Ar and N_2 arcs can transfer more energy by radiation due to their larger radiating volumes. Since most of the energy transfer to the reactor wall and nozzle assembly is through radiation, the energy distribution in the reactor depends strongly on arc diameter.

The arc diameter of $TiCl_4$-rich arcs (see Table IV) is much larger than the diameter of H_2 arcs and roughly equal to that of Ar arcs. In essence $TiCl_4$ rich arcs exibit both the highest heat capacity and the largest arc diameter. It is, therefore, not surprising that such arcs would also exhibit the highest energy transfer to the surroundings.

TABLE V. POWER DISTRIBUTION IN TRANSFERRED ARC REACTOR *

RUN NO.	PLASMA GAS	ARC LENGTH (cm)	POWER DISTRIBUTION P_t (kW)	P_a (kW)	η_a (%)	P_r (kW)	η_r (%)	P_n (kW)	η_n (%)	ARC DIAMETER (mm)
110-2	Ar	2	5.6	4.2	75	0.7	13	0.6	11	7.2
110-3	He	2	8.0	7.0	88	0.6	8	0.3	4	6.6
110-4	N_2	2	10.2	7.9	77	1.0	10	0.9	9	5.1
110-5	H_2	2	15.4	13.7	89	0.8	5	0.8	5	4.7
110-6	Ar	3	6.6	4.2	64	1.2	18	0.7	11	-
110-7	He	3	9.6	8.1	84	0.9	9	0.3	3	-
110-8	N_2	3	12.6	9.2	73	1.9	15	1.0	8	-
110-9	H_2	3	18.2	15.0	82	1.5	8	0.9	5	-

* For all experiments in this Table, arc current = 200 A, plasmagas flowrate = 15 L/min, cathode = ThO_2 - W, anode = water-cooled Cu.

Since there is no information available on the emissivity or operating temperature of $TiCl_4$ rich plasmas, it is not possible to calculate radiative transfer directly.

iv. Chemical Reactions in a Transferred Titanium Tetrachloride Arc Reactor

No detailed analysis of the chemical reactions occurring in the transferred arc reactor was made in this study. However, general observations made during the operation of the system allowed for verification of results previously reported in literature. Of particular interest to the present observations are the results reported by Miller and Ayen (1969), who studied the reduction of $TiCl_4$ in a radio-frequency torch. They showed that $TiCl_3$ can be produced when hydrogen is introduced as the reducing agent, while in the absence of hydrogen there was no appreciable reduction of the $TiCl_4$ molecule.

The observations from the present study verify the results reported by Miller and Ayen. In experiments utilizing argon or helium as the main plasmagas, the exhaust gas was rich in $TiCl_4$, as evident by the accumulation of $TiCl_4$ liquid in a flask located at the bottom of the condenser (see Figure 2). Inside, the reactor was covered by a thin, powdery layer of titanium subchlorides, oxides and oxychlorides. Unfortunately, in the present set up it was not possible to determine how much of the material covering the reactor walls was formed during the experiment and how much was formed later, while the reactor was opened for inspection and cleaning. It is reasonable to expect that some of the recombined $TiCl_4$ would condense on the water-cooled reactor walls and remain there as a thin film until the reactor was opened. At that point, it would react quickly with the moisture in the ambient air to form at least part of the observed powder.

The amount of $TiCl_4$ collected from the exhaust gas was roughly the same for both argon and helium runs, and, at flow rates of 25 g/min, represented about 70 percent of the total $TiCl_4$ fed to the reactor. The remaining 30 percent may be attributed to the production of reduced compounds, losses through reactions with contaminants in the reactor and the plasmagas, and losses in the exhaust gas purification system. It should be pointed out that the exhaust gas entering the caustic scrubber (see Figure 2) contained significant amounts of $TiCl_4$ as evident by the formation of titanium oxides in the scrubber.

In experiments which contained hydrogen in the plasmagas, no $TiCl_4$ liquid was collected after the condenser. Furthermore, the inside reactor walls were covered with a thick layer of dark violet powder. Based on X-ray difraction analysis the titanium-to-chlorine ratio in the powder was determined to be about 1:2.7, indicating that the majority of the chloride was $TiCl_3$ The remaining powder probably consisted of oxides and oxychlorides formed due to the presence of contaminants in the reactor and the plasmagas.

Some of the contamination occurred after the completion of the experiment while the reactor was being opened for inspection. This suggests that at least some of the $TiCl_4$ molecules had fully recombined, since $TiCl_3$ does not decompose spontaneously in ambient air. Some fully recombined $TiCl_4$ may have also left the system in the exhaust gas. It was not possible to measure the yield of $TiCl_3$ in the present set-up.

CONCLUSIONS

A number of important operating characteristics of transferred arcs utilizing titanium tetrachloride-rich plasmagas were experimentally studied. The results from the study suggest the following:

1. Transferred arc reactors employing thoriated tungsten as the cathode forming material are not stable when utilizing $TiCl_4$-rich plasmagas. The source of instability appears to be the chemical reactions occurring at the cathode surface between the plasmagas and the cathode material. These reactions result not only in the deterioration of the cathode but also in the "suffocation" of the electron emission process by the formation of a liquid titanium film on the emitting surface.

2. Stable $TiCl_4$ transferred arcs can be maintained if the commonly-used thoriated tungsten cathode is replaced by a tantalum carbide cathode. Tantalum carbide does not react with the chloride in the plasmagas, has a relatively low thermionic work function and very high melting and boiling temperatures. The introduction of small amounts of thoria in the TaC cathode did not significantly influence the operation of $TiCl_4$-rich arcs, though it did lower the cathode spot temperature in argon arcs.

3. The introduction of $TiCl_4$ into the plasmagas of a transferred arc results in the formation of a luminous light blue sheath around the plasma column. It appears that the temperature within the sheath is high enough to allow the ionization of Ti atoms yet low enough to prevent the ionization of the atoms in the main plasmagas. Diffusion may also be contributing in concentrating titanium ions and chlorides within the sheath. The diameters of the hot central region and of the cooler sheath depend on the concentration of $TiCl_4$ in the plasmagas.

4. The total arc voltage of a 2-cm arc utilizing $TiCl_4$-rich plasmagas is roughly twice that of a similar arc utilizing pure argon as the plasmagas. Some of the increase in voltage can be attributed to the higher arc column voltage gradient (about 7 V/cm higher) for $TiCl_4$-rich plasmagas compared to the gradient for Ar arcs. The measured arc column voltage gradient for $TiCl_4$ arcs is about the

same as that of pure nitrogen arcs. Most of the increased voltage requirements in $TiCl_4$ arcs, however, are due to a sharp increase in the cathode fall potential.

5. When $TiCl_4$ is introduced into an argon plasma the voltage increases quickly until a $TiCl_4$ molar concentration of about 12 percent is reached. Further increases in $TiCl_4$ feed rate or in $TiCl_4$ concentration have a much smaller effect on the arc's voltage.

6. The introduction of $TiCl_4$ into the plasmagas decreases the fraction of the total input power transferred to the anode and increases energy transfer to the reactor wall and nozzle assembly.

7. The arc column diameter of $TiCl_4$-rich plasmas is about the same as that of argon and significantly larger than that of nitrogen, helium and hydrogen.

8. It is possible to produce $TiCl_3$ through the reduction of $TiCl_4$ with hydrogen in a transferred arc reactor. In the absence of hydrogen some reduction occurs, but the amount of $TiCl_3$ condensing on the eactor walls is much smaller.

REFERENCES

Akashi, K., S. Ohno, R. Ishizuka and T. Yoshida, "The Characteristics of Titanium Microcrystals Formed from a Mixture of Titanium Tetrachloride and Hydrogen in an Argon Plasma Jet", Communications-Symposium International de Chimie des Plasmas, Fauchais, P (ed), 3rd paper S.4-6, Limoges, France (1977).

Aubreton, J. and P. Fauchais, "Les Fours à Plasma", Rev. Gen. Therm. Fr, N . 200-201, p. 681 (1978).

Bonet, C.C., "Thermal Plasma Processing", C.E.P., p. 63 (December 1976).

Choi, H.K. and W.H. Gauvin, "Operating Characteristics and Energy Distribution in Transferred Plasma Arc Systems", Plasma Chemistry and Plasma Processing, Vol. 2, No. 4, pp 361-387 (1982).

Dinulescu, H.A. and E. Pfender, "Analysis of the Anode Boundary Layer of a High Pressure-High Current Arc", J. Appl. Phys., Vol. 51, p. 3149 (1980).

Gauvin, W.H. and H.K. Choi, "Plasmas in Extractive Metallurgy", Materials Research Society Symposia Proceedings, Szekely, J. and Apelian, D. (ed.), Vol. 30, pp.77-89, North-Holland Publishers (1983).

Guile, A.E., "Arc-Electrode Phenomena", Proc. IEE, IEE Reviews, Vol. 118, No. 9R, pp. 1131-55 (Sept. 1971).

Hamblyn, S.M.L., "A Review of Applications of Plasma Technology with Particular Reference to Ferro-Alloy Production"", National Inst. for Metall., Rep. No. 1895 (1977).

Handbook of Chemistry and Physics, Robert C. Weast (ed.), 58th edition, CRC Press, Inc. (1977-78).

JANAF Thermochemical Tables, D.R. Stull et. al. (ed.), Clearinghouse for Federal Scientific and Technical Information (1960), (1965).

Kikukawa, N., M. Makino, H. Matsumoto and M. Itorie, "Study on the Reduction of Titanium Compounds in a Hydrogen Plasma Jet", Kogai Shigen Kenkyusho Iho, Vol. 13, No. 2, pp. 13-22 (1983).

Kubaschewski, O., H. Villa and W.A. Deuch, Trans. Far. Soc., Vol. 52, p. 214 (1956).

Kyriacou, A., "Characteristics of a Thermal Plasma Containing Zirconium Tetrachloride", M. Eng. Thesis, McGill University, Montreal (1982).

Lowke, J.J., "Simple Theory of Free-Burning Arcs", J. Phys. D: Appl. Phys., Vol. 12, pp. 1873-86 (1979).

Maske, K.U and J.J. Moore, "The Applications of Plasmas to High Temperature Reduction Metallurgy", High Temp. Technol., Vol. 1, No. 1, p. 51 (1982).

Matskevich, T.L., "Thermionic Emission Properties of Metal Alloys (Survey)", Soviet Physics-Technical Physics, Vol. 13, No. 3, pp. 295-307 (Sept. 1968).

Mehmetoglu, M.T. and W.H. Gauvin, "Characteristics of a Transferred-Arc Plasma", A.I.Ch.E.J., Vol. 29, No. 2, pp. 207-15 (1983).

Miller, Reid Clarc, "Energy Transfer Processes and Reactions of Titanium Tetrachloride in an Inductively Coupled Argon Plasma", Ph.D. Thesis, University of California, Berkeley (1968).

Miller, R.C. and R.J. Ayen, "Reactions of Titanium Tetrachloride in a Radio-Frequency Plasma Torch", I and EC Process Design and Development, Vol. 8, p. 371 (1969).

Ramakrishnan, S. and B. Nuon, "Prediction of Properties of Free Burning Welding Arc Columns", J. Phys. D. Appl. Phys., Vol. 13, pp. 1845-53 (1980).

Rykalin, N.N., "Plasma Engineering in Metallurgy and Inorganic Materials Technology", Pure and Appl. Chem., Vol. 48, pp. 179-94 (1976).

Saye, I.G., "Some Applications of Thermal Plasma to Material Processing", paper presented at World Electrotech. Congress, Moscow, U.S.S.R., Sect. 4A, No. 107 (July 1977).

Sheer, C., S. Korman, T.J. Dougherty and H.Y. Chen, "Development and Application of the High Intensity Convective Electric Arc", Chem. Eng. Commun., Vol. 19, No. 1 (1982).

Spiliotopoulos, P.Z., "Characteristics of Zirconium Tetrachloride Thermal Plasmas", M. Eng. Thesis, McGill University, Montreal (1983).

Szekely, J., "Plasma Phenomena and Plasma Metallurgy.... an Overview", Proc. of 1983 MRS Annual Meeting (1983).

Tsantrizos, P. and W.H. Gauvin, "Operating Characteristics and Energy Distribution in a Nitrogen Transferred Arc Plasma", The Canadian Journal of Chemical Engineering, Vol. 60, No. 6, pp. 822-30 (1982).

U.S. National Materials Advisory Board, "Plasma Processing of Materials Report Number NMAB-415, Washington (1985).

Vacquie, S., "L'Arc électrique et ses applications", Chpt. IV, pp. 130-132, Edition du Centre National de la Recherche Scientifique, Paris (1984).

Yean, D.H. and J.R. Riter Jr., "High Temperature Heterogeneous Equilibriums in the Unit Activity Approximation II. Titanium Tetrachloride-Hydrogen System", Metallurgical Transactions, Vol. 1, No. 5, p. 2473 (1974).

PART II

CATHODE DETERIORATION PHENOMENA IN A TRANSFERRED-ARC REACTOR

ABSTRACT

Phenomena occurring on the surface of a thoriated tungsten cathode operating in a transferred-arc reactor were investigated. The effects of cathode geometry (pointed-tip vs. flat-tip) and plasmagas composition (argon vs. helium) on the rate and mechanisms of cathode erosion were studied experimentally by examining the morphology of the surface before and after runs of prespecified duration. Results from the study showed that on flat-tip cathodes operating in argon, thoria migrated through the tungsten matrix and concentrated on the surface. In longer duration runs, the thoria was consumed from the surface, resulting in extensive melting of the tungsten and the subsequent release from the surface of molten tungsten nodules. The surface temperatures of pointed-tip cathodes operating in either argon or helium and flat-tip cathodes operating in helium were higher than the boiling point of thoria and substantial vapourization of cathode material, both thoria and tungsten, was observed. Some of the vapourized material redeposited on the cathode surface, forming crystals whose morphology and composition depended on their distance from the arc root and the plasmagas composition. This redeposition mechanism resulted in relatively low erosion rates despite the extensive vapourization of cathode material. In the case of pointed-tip cathodes operated in argon, a large molten tungsten sphere was formed and subsequently released from the tip. The release of this sphere, which typically occurred after 40 minutes of operation, was responsible for most of the erosion observed in these

cathodes. Only phenomena occurring during the first hour of operation were investigated in this study.

BACKGROUND INFORMATION

Electrode lifetime has long been recognized as one of the most important considerations affecting the viability of a plasma process. Rapid electrode deterioration can diminish the value of a process both from an economic and a technical point of view. Consequently, parameters such as the frequency of reactor "down-time" for electrode replacement, the cost of electrodes, process instabilities due to poor electrode performance, and the contamination of products with materials emitted from the electrodes, are crucial in determining the ultimate success of plasma technology in general and that of the transferred arc reactor in particular.

Early recognition of the importance of electrode phenomena has provided incentive for much research in this field during the past fifty years. Yet, despite this intensive effort, the phenomena occurring at the electrodes, and especially the cathode, remain for the most part unexplained. In 1971, A. E. Guile, who has been one of the leaders in this field, published a review of arc-electrode phenomena in which he stated that "electrode erosion remains one of the least understood arc problems..." and "even when cathode material and arrangement normally giving acceptable level of erosion have been found, large differences in erosion rates can sometimes develop with apparently identical operating conditions." Guile's statements are as true today as they were seventeen years ago.

MECHANISMS OF CATHODIC ELECTRON EMISSION

The lack of a comprehensive theory for the cathode phenomena of an arc is partly due to the apparent existence of basically different mechanisms of electron emission for different types of arcs is partly due to the absence of a reliable body of empirical experimental data on which a quantitative theory could be based. Reliable data on cathode current densities and on cathode voltage drops are largely missing, making verification of existing models impossible. The problems in determining the current density, for example, lie in the fact that so far no direct measurements, e.g. with probes, have been made and there are no techniques so far available for doing so with the required degree of accuracy.

The techniques presently available for determining the cathode current density rely primarily on indirect methods. Such methods may consist of either measuring photographically the size of the visible cathode root (spot) and calculating the area of attachment by assuming that the optical root is equal to the electrical one, or determining the area of the root based on the magnitude of molten metal tracks left on the cathode in magnetically rotated arcs. Either of these two techniques offers highly questionable results. Errors may be introduced during the transition from an optical to an electrical root diameter, the molten tracks may be more representative of the thermal conductivity of the cathode material and of the time of contact, and the current density may not be uniform throughout the root area.

Despite the obvious shortcomings in our understanding of cathode phenomena, some theories have been developed and used with some success to explain empirically-attained data. Most of them begin by assuming a mechanism of electron emission and assessing the state of the cathode surface during such emission. Finnkelnburg and Maecker (1956) described the three traditionally-proposed mechanisms of cathodic electron emission as follows:

1. For sufficiently high temperatures at the cathode surface and low field strength, the current can be carried exclusively by electrons which have been thermally emitted from the cathode. This method of electron emission is commonly referred to as "thermionic emission" and is characterized by cathode surface temperatures above 3 500 K and current densities of around 10^3 to 10^4 A/cm^2. Only refractory materials such as tungsten and carbon have high enough boiling points to allow for thermionic emission.

2. For a sufficiently high field strength in front of the cathode surface, emission can occur at relatively low temperatures (below 3 000 K), with the cathode material releasing electrons whose energy is below the Fermi level. This mechanism is commonly referred to as "field emission" and is characterized by current densities higher than 10^6 A/cm^2. Non-refractory materials such as copper and

aluminum are used in field-emitting cathodes.

3. A third possibility is that, near the cathode surface, the arc's current is carried exclusively or chiefly by positive ions. In this case the cathode surface must be at sufficiently high temperature to permit the release of the required ion current density.

Today, most workers in the field agree that none of the three traditional theories is solely responsible for electron emission in real arcs. In general, one deals with a combination of thermal and field emissions while a smaller ionic component is also active. In fact, researchers such as Murphy and Good (1956) provided early attempts at the development of a unified emission theory by extending the Richardson-Dushman Equation, which describes the current density for thermionic emission, and the Fowler-Nordheim Equation, which is used in field emission, to the regions of temperature and field strength in between the two (i.e. the transition region). However, despite such efforts, there does not yet exist an acceptable unified theory on electron emission, prompting some to claim that there is no such thing as a typical cathode spot mechanism, while others argue that the cathode spot mechanism is the same for any metal (Guile and Juttner, 1980).

Despite the apparent differences between those who suggest the existence of thermionic, field and ionic emissions and those who search for a singular electron emission mechanism, all theoretical considerations on cathode phenomena are based on certain macroscopic properties of the cathode surface (e.g. work function, temperature, thermal conductivity, etc.). Hidden in these theories is the assumption that one can distinguish sharply between a solid or liquid cathode surface and the plasma state just ahead of it. Loeb (1939) was the first to point out that in view of the extraordinary concentration of power in the cathode spots of high cathodic current density arcs, the application of such macroscopic concepts and data is extremely questionable. Loeb used as an example an arc whose cathodic current density is 10^6 A/cm^2, in which 10 percent of the current was carried by ions. Under these conditions, 6×10^{23} ions strike the cathode unit surface per second, each possessing a kinetic energy of 5 to 10 eV and a potential energy of the same order of magnitude, which they release at the cathode upon neutralization. Each of these 6×10^{23} ions transports to the cathode material an amount of energy which is several times the binding energy of the building stones in the cathode lattice. Furthermore, since one cm^2 of cathode surface has only about 10^{15} surface atoms, each surface atom is struck about 10^8 times per second. Under these circumstances, it is obviously impossible to maintain the ordered lattice structure of the cathode material in the region of the cathode spot. In fact, according to Loeb, the spot must exist, to a depth of several atomic layers, in a state of such extreme looseness that it is doubtful whether one should refer to it as a state of strongly disturbed solid/liquid or a state of highly complex plasma.

An energy balance on the cathode surface is quite complex, requiring consideration of both the energy arriving and the energy leaving the surface. The energy arriving through ion impact is, to some degree, dissipated through electron emission, vapourization of the cathode material, radiation losses, and both water and gas cooling of the cathode. Furthermore, there have been studies (Benjamin and Jenkins, 1940) to show that the atoms on the cathode surface are in perpetual motion, constantly forming new crystals that assist the electron emission process by reducing the material's work function and increasing the emitting surface area. Nonetheless, if Loeb's analysis is correct and if on the cathode surface one deals with a transition state between a highly heated solid/liquid and a plasma, then the concept of cathodic work function along with the proposed mechanisms of thermionic and field emission lose most of their meaning.

Thermionic Work Function

The most important parameter used to measure a material's ability to emit electrons is its thermionic work function, ϕ. The relationship between electron current density, j, and thermionic work function, ϕ for refractory cathodes is given by the Richardson-Dushman Equation:

$$j = A \cdot T^2 \cdot \exp(-\phi/kT) \qquad (8)$$

where A is a constant whose theoretical value is 120 ($A/cm^2.K^2$) but whose measured value has been reported anywhere from less than 10 to over 1 000 ($A/cm^2.K^2$), k is the Boltzmann constant, and T is the cathode surface temperature in K. It can be clearly seen from the Richardson-Dushman Equation that an increase in the cathode's thermionic work function either decreases the current density, resulting in poor arc stability, or increases the surface temperature, resulting in excessive electrode erosion.

The thermionic work functions for refractory metals at temperatures near their melting points have been experimentally determined by many researchers. Unfortunately the reported results vary widely, as do the explanations on the factors influencing their value. It appears that the measurements of the work function suffer from the same limitations as those described earlier for cathodic electron emission mechanisms. Nonetheless, reported empirical data do provide important insights on the phenomena occurring at the cathode surface and should thus be carefully reviewed.

Gordon and Chapman (1972) used metal wires of various compositions as cathodes in an argon direct-current arc discharge. During operation a molten sphere was formed at the tip of the cathode whose diameter could be measured upon terminating the arc. By assuming that the diameter of the emitting area was the same as that of the molten sphere, they calculated the current density of the cathode at various operating temperatures. Using the Richardson-Dushman Equation, they plotted **$1/kT$ vs $\ln (j/T^2)$** and thus measured both the thermionic work function (slope of plotted line $= -\phi$) and the emission constant **A** (intercept of plotted line $= \ln A$).

The results obtained by Gordon and Chapman for the thermionic work function varied from 4.1 eV for tantalum to 5.1 eV for rhenium and were in reasonable agreement with results reported in handbooks for these metals. The observed agreement may be somewhat surprising considering the methodology used in these experiments. There is little support, for example, for the assumption that the emitting area is accurately represented by the area of the molten sphere. Other factors, such as the physical properties of the metal wire (surface tension, melting temperature, thermal conductivity, etc.) may have more to do with the size of the droplet than the emitting area.

Furthermore, Gordon and Chapman calculated the current density using the ratio **I/A** where I was the total arc current and A was the emitting area determined from the measured sphere diameter by the relation $A = \pi D^2$. They not only assumed that the current density was evenly distributed throughout the entire surface of the droplet exposed to the arc, a doubtful assumption at best, but also included the area of attachment between the sphere and the metal wire which cannot possibly emit electrons. Considering the additional uncertainty that must have been introduced during the temperature measurements at the cathode surface, the apparent agreement between their results and handbook values is surprising indeed.

Most of the thermionic work function data reported in the literature have been determined from the value of the thermionic current in zero field as described by Dyubua et al. (1966). In essence, the cathode material under investigation is placed in a vacuum chamber facing the anode. A heating element is used to raise the sample's temperature up to about 2 300 K, while a diode is used to measure its emission. The work function can then be calculated using the Richardson Dushman equation, in which the constant <u>**A**</u> is assumed equal to 120 ($A/cm^2.K^2$).

A complete survey of the thermionic emission properties of metals and alloys, measured by the above mentioned technique, was published by Matskevich in 1968. He presented extensive data of the thermionic work function of alloys as a function of composition, temperature and heating time, and offered an interesting discussion on phenomena relevant to cathode emission. In assessing the usefulness of Matskevich's data in the analysis of transferred arc cathodes, one may reasonably argue that the methodology used to calculate these thermionic work functions does not represent accurately the events occurring at the cathode surface during arc operation. However, it may also be true that the parameters affecting the work function of a material are the same no matter the circumstances under which electron emission is occurring. If such consistency is true, then parameters, such as the emitting material's composition, temperatu[illegible], surface characteristics and method of preparation, identified by Matskevich as having strong influence on emission characteristics, must also be important in transferred-arc cathodes.

1. Effect of Cathode Composition on Work Function

Early recognition that cathodes composed of pure refractory metals exhibit rapid erosion rates encouraged researchers to examine the possibility of using alloyed materials instead. In 1933, Brattain and Becker reported that a monolayer of electropositive atoms adsorbed on a metal constitutes a system with a work function lower than that of the metal. Their results, in which tungsten was used as the substrate and thorium as the adsorbed species, were verified that same year by Taylor and Langmuir who studied a tungsten-cesium cathode, and were later expanded to include alloyed cathode materials. Today the use of alloys to reduce the cathode's work function and consequently increase its thermionic emission, is practiced widely. Yet, there still exists considerable controversy concerning the mechanism responsible for this phenomenon.

Results obtained from measuring the thermionic work function of several alloys containing the same components but in various concentrations are represented in the form of the so-called "concentration graphs of the work function". Typical concentration graphs for W - Ta and Re - Ta alloys are shown in Figure 1. It should be pointed out that the alloy composition shown along the abscissa in Figure 1, is the composition of the specimen prior to use and as we shall discuss later does not necessarily correspond to the composition of the cathode surface during operation.

From the results presented in Figure 1 and others like them available in the literature, a rather interesting observation is possible. Consider the thermionic work function of the homogeneous alloy containing a small amount of tantalum in tungsten. The work function of this alloy is about 3.8 eV, smaller than the work function of either pure tungsten (4.55 eV) or pure tantalum (4.25 eV). On the other hand, the alloy composed of a few percent of tungsten in tantalum has a work function equal to that of pure tantalum. After a complete analysis of such data, Matskevich (1968) concluded that only alloys containing a small amount of the component with the lower work function possess work functions lower than that of either component. The addition of small amounts of a higher work function component, however, has no such effect.

While the above hypothesis holds true for the W - Ta alloys, it fails to explain the data presented for the Re - Ta alloys. In fact the addition of a small quantity of tantalum (the component with the lower

FIGURE 1

WORK FUNCTION CONCENTRATION GRAPH FOR W - Ta AND Re - Ta ALLOYS

Line 1: W - Ta Alloy

Line 2: Re - Ta Alloy

Source: Matskevich (1968)

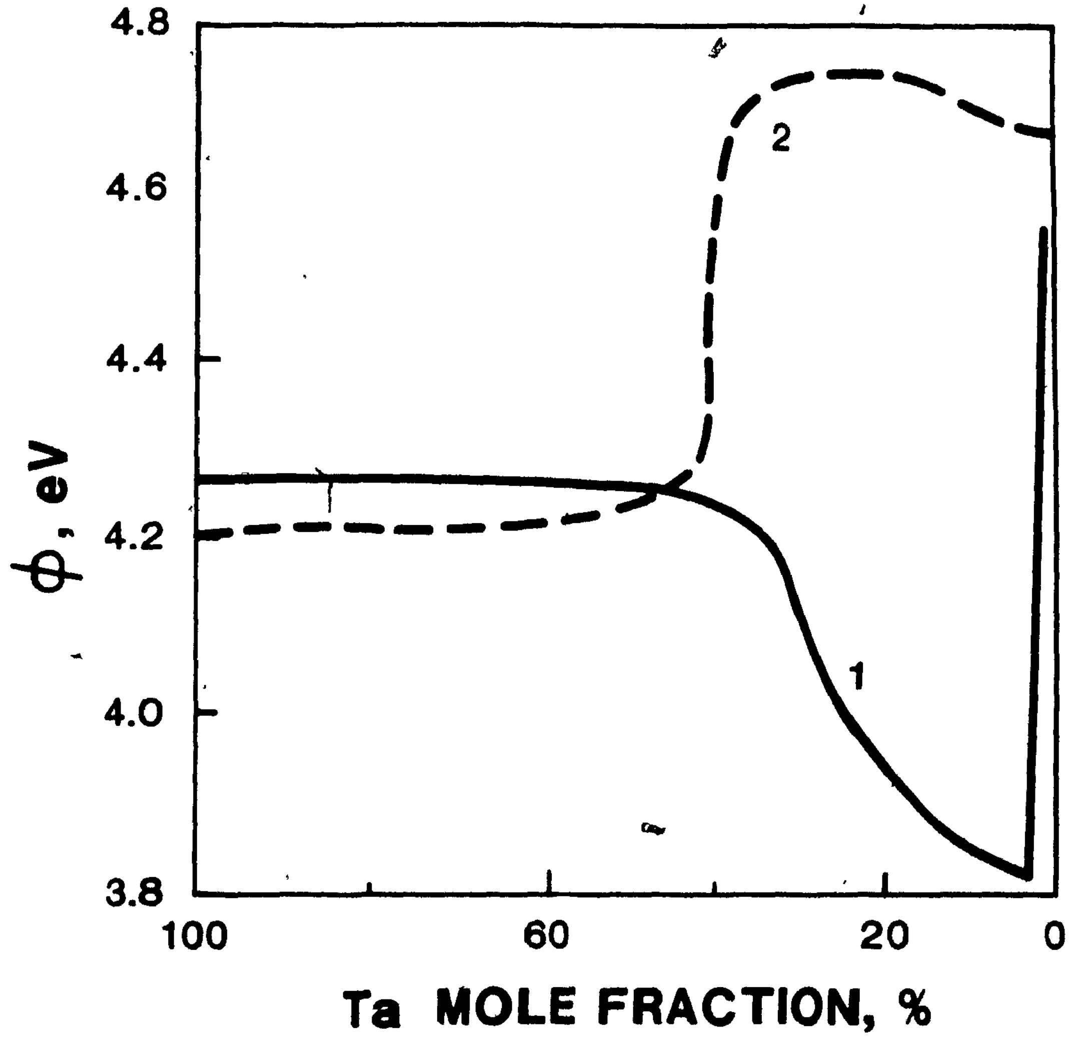
4.8
4.6
4.4
4.2
4.0
3.8
φ, eV
100
60
20
0
Ta MOLE FRACTION, %
1
2

work function) to rhenium causes little change in the work function. It appears that whether the work function of the main component will decrease, increase or remain the same upon the addition of a small quantity of a component with a lower work function depends on properties yet to be identified.

One of the properties that some consider important in determining the work function of binary metal alloys is the melting point of each constituent. This consideration stems from a proposed electrode phenomenon commonly referred to as the "film hypothesis". Proposed by many, including Dyubua et al. (1962), the film hypothesis suggests that when heated, the surface of binary alloys becomes coated by a thin adsorbed film of the lower melting point component, and thus, the thermionic emission properties of such alloys become similar to those of film emitters described earlier by Brattain and Becker. Furthermore, the change in work function depends on the thickness of the surface film, the thermionic emission properties of the film emitter and the emitter's surface density.

Anderson et al. (1963) investigated the thermionic properties of pure rhenium, and rhenium with an adsorbed layer of thorium atoms. They discovered that the work function decreased with increasing thorium coverage from 4.85 eV for pure rhenium to a minimum of 3.15 eV for a thorium surface density of 4.2×10^{14} atoms/cm^2. Upon further increasing the surface density to 8×10^{14} atoms/cm^2, the work function increased to about that of pure thorium (3.3 eV) and remained constant thereafter. They concluded that the surface density exibiting the minimum work function represented a true monolayer of metallic thorium and suggested that the lowering in work function is caused by interactions between thorium's valence electrons with rhenium. When the film thickness increased such interactions were prevented, and the system performed essentially as pure thorium.

The film hypothesis suggests that alloys whose minor component is surface active will exibit work functions lower than either component while alloys whose minor component is not surface active will have work functions equal to that of the major component. Thus, based on the data shown in Figure 1, tantalum is surface active in tungsten but not in rhenium. Unfortunately, an adequate understanding of the relationship between the properties of materials and their ability to perform as film emitters does not yet exist. However, it is known (Matskevich, 1968) that the addition of a third component to a binary alloy can in some cases facilitate the formation of the emitting film by changing the diffusion rate of the surface active component.

Although not everyone agrees with the film hypothesis, it is generally accepted that minimum work function can be achieved by using a ternary metal alloy. This alloy should consist mostly of a high-melting-point material known as the base (e.g. W), a lower-melting-point material known as the mobilizer (e.g. Zr, Hf), and a rare-earth metal known as the emitter (e.g. Th). Using methods earlier described the thermionic work function of a W - Hf - Th ternary alloy is given by Matskevich at 2.88 eV compared to 3.15 eV for a W - Th binary alloy.

The formation of films on the cathode's surface was partially confirmed by Shishkin and Bakhtiyarov (1974) in their study of Mo - Pt alloys. They clearly observed the formation of a film of the lower melting component (Pt) on the surface of an alloy containing 1% Pt in Mo. The Pt emerges onto the surface of the alloy along grain boundaries and at structural defects and forms a multilayer film.

Although the observations reported by Shishkin and Bakhtiyarov confirm the role of a film mechanism in the emission of the Mo - Pt alloy, there is some doubt as to their applicability to other alloys. It should be noted that the work function of platinum is significantly higher than that of molybdenum (5.36 eV for Pt and 4.22 eV for Mo). Thus, when the platinum film is formed, the work function increases as does the temperature of the cathode surface. This is contrary to the properties of common cathode alloys (e.g. W - ThO_2) in which the emitter is used specifically because of its ability to lower the thermionic work function. It is not clear how this difference affects the phenomena observed at the cathode surface.

While there is much ambiguity regarding the role of films on the surface of cathodes and the mechanism of electrode emission from binary alloys, there is substantial evidence for the preferential migration of components in cathode alloys. Along with the studies already mentioned, the work of Chiang and Maley (1984) is worth noting. Their study focussed on the migration of chromium through nickel in a field-emitting cathode. They observed that chromium, which originally was present only in the bottom layer of the cathode base metal (nickel), diffused rapidly throughout the cathode. The diffusion took place through easy diffusion paths such as grain boundaries that were present in the nickel portion of the cathode. Consequently, the composition of the cathode before use was very different from its composition during use.

ii. Effect of Cathode Temperature on Work Function

Variations in the temperature of the cathode's surface can affect the performance of the cathode in at least two ways. The first way, made obvious by the Richardson-Dushman Equation, is by changing the current density of the emitting surface. The second way, which will be reviewed here, is by changing the cathode's thermionic work function.

Although the thermionic work function of a cathode material is frequently reported as a constant, its value can change considerably due to variations in temperature. As one might expect, this is especially true for the work function of alloys. In the previous section the role of migration of the emitter within the base material of an alloy was discussed. It was shown that such migration results in the formation of a thin film of the lower melting point constituent on the surface of the emitting cathode, which strongly influences its effective work function. Since the migration rate is determined to a large degree by the temperature of the cathode, one may expect a strong relationship between the operating temperature and the effective work function. This relationship for W - Ta and W - Mo alloys is shown in Figure 2.

The data shown in Figure 2, first presented by Dyubua et al. (1966), were determined from measurements of the thermionic current in zero electric field based on the methodology described in the previous section. They are limited to the temperature range between 1 300 and 2 300 K, which is very much lower than the actual operating temperature of refractory cathodes. As such, their relevance to operating cathodes is highly questionable. Unfortunately, similar data for the temperature range commonly associated with refractory cathodes (over 3 500 K) do not exist.

Matskevich (1968) notes that not only the temperature dependence of the work function varies between alloys containing different components, but it also varies for alloys containing the same components but in different concentration. Thus, the work function of an alloy containing a small amount of tantalum in tungsten (see Figure 2) increases rapidly with increasing temperature, whereas the work function of an alloy containing 40 % tantalum in tungsten remains about constant within the

FIGURE 2

TEMPERATURE DEPENDENCE OF THE WORK FUNCTION FOR W - 3% Ta AND W - 3% Mo ALLOYS

Line 1: W - Ta Alloy

Line 2: W - Mo Alloy

Source: Dyubua et al., (1966)

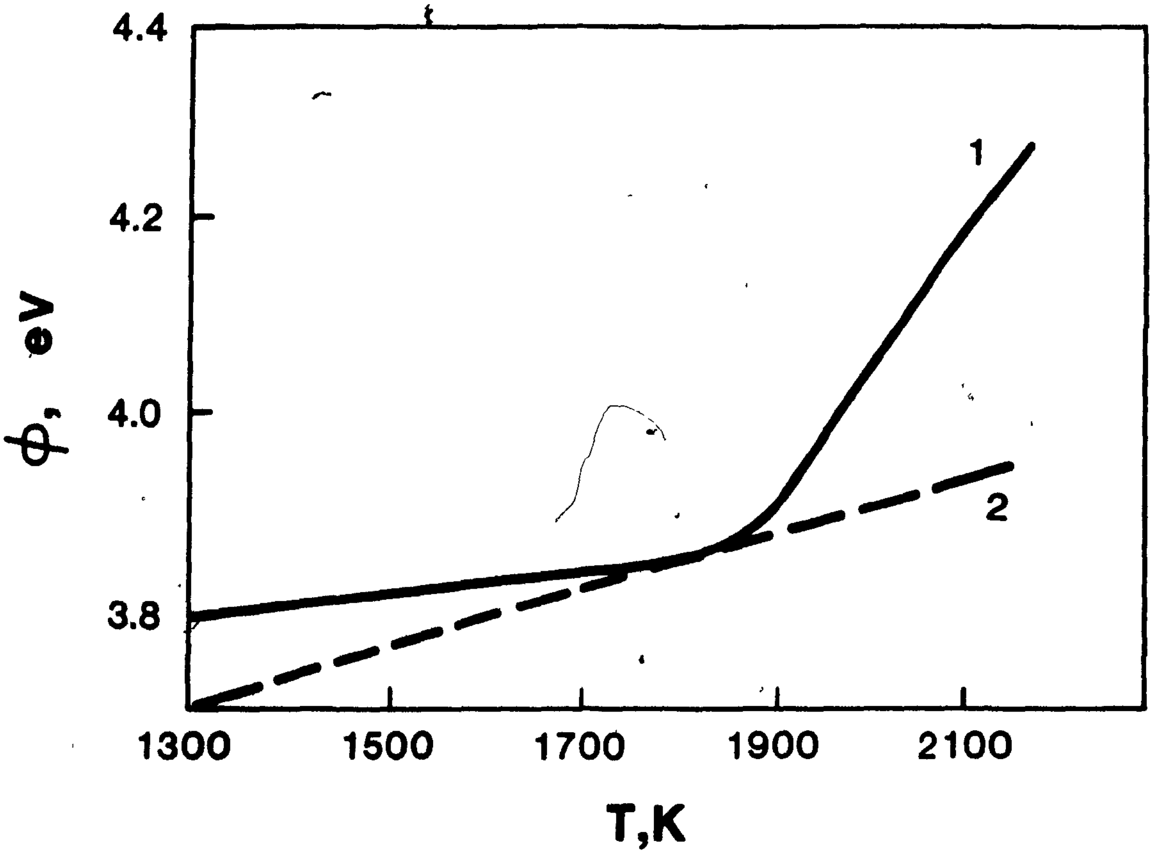
4.4
4.2
4.0
3.8
φ, eV
1300
1500
1700
1900
2100
T,K
1
2

temperature range of 1 300 to 2 300 K.

Furthermore, the work function of several alloys containing small amounts of one constituent (e.g. Ta - 1% Hf) changes slowly with time when exposed to a sharp change in temperature. The work function becomes stable only 5 to 30 minutes after it reaches a steady temperature, and this stable value depends upon the time and preliminary-heating temperature. For some alloys heating to high temperatures causes irreversible changes in their work function. Thus, the work function of a W - 3% Mo alloy at 1 500 K is about 4.1 eV after heating at 2 000 K for 50 hours but only 3.8 eV after heating to 2 300 K for 15 hours.

Although no comprehensive theories for the effects of alloy concentration and thermal pretreatment on the relationship between work function and cathode temperature have been offered, it would appear that they are related to the migration patterns of the lower boiling point component within the alloy. Since migration is not likely to be a completely reversible process, it is not surprising that Guile (1971) observed large differences in cathode performance under apparently identical operating conditions.

iii. Effect of Cathode Surface Characteristics on Work Function

The characteristics of the emitting surface are crucial in determining the operating performance of the cathode. In fact one may claim that cathode phenomena are essentially surface phenomena since only the first few atomic layers are influencing electron emission. Beyond the formation of thin films, whose effect on the thermionic work function has already been reviewed, crystal structures, shape and minor contaminations on the cathode's surface can also influence its performance.

As early as 1938, Muller showed that the angular distribution of field emission from fine points could be related to the crystal structure of the metal. He also suggested that the modifications in the surface pattern of tungsten, which took place when the temperature of the point was raised, could be attributed to a movement of the surface atoms which caused local changes in the work function. Later, Benjamin and Jenkins (1940) provided further evidence of surface mobility using tungsten, molybdenum and nickel cathodes. They showed that surface mobility occurs above 1 170 K for tungsten, 770 K for molybdenum and only 370 K for nickel. Surface mobility changes the geometric shape of the cathode point, which in turn changes the emission distribution. Both Muller's and Benjamin and Jenkins' studies dealt with field emission from cold cathodes. Unfortunately, no similar study is available for high temperatures and the applicability of the field emission results to transferred arcs can not be assessed.

Neurath and Gibbs (1963) experimented with different cathode geometries in a d.c. arc discharge operated at atmospheric pressure, using either argon or helium as the plasma generating gas. They discovered that a "flat-tipped" cathode (i.e. a conical cathode whose tip has been cut to form a flat surface 2 mm in diameter) operated at about half the current density of a pointed tip and at a much lower temperature. The current density was determined by dividing the total arc current by the area of the luminous section of the cathode which was recorded photographically immediately after arc extinction. This method may introduce large errors in the determination of current density. Furthermore, there may have been significant mobility in both geometries during arc operation whose influence on current density and work function were not analyzed by Neurath and Gibbs. Nonetheless, their results indicate that the geometry of the cathode surface is an important parameter in electron emission.

Finally, it is suggested by a number of researchers (e.g. Hitchcock and Guile, 1977) that the cathode spot of an arc consists of a number of emitting sites. The number of these sites and their ability to emit electrons is partly determined by the presence of surface impurities such as oxides, nitrides etc. Various mechanisms for electron emission in the presence of oxide films have been proposed for copper cathodes. A proposed mechanism for thick oxide films suggests that emission is due to electroforming of copper filaments and occurs with relatively long spot lifetime. A parallel mechanism for thin oxide films suggests that emission is due to tunneling and occurs with shorter lifetimes.

However, there is much ambiguity concerning such mechanisms, and there is no evidence regarding the role of such films in refractory cathodes.

CATHODE DETERIORATION MECHANISMS

Cathode deterioration can be the result of either thermal erosion or chemical corrosion. Thermal erosion refers to mass loss due to evaporation or particle emission from the cathode spot. Chemical corrosion, on the other hand, is the result of reactions occurring at the cathode surface between the cathode material and the plasmagas. Such reactions can produce compounds whose boiling point is lower than the operating temperature of the cathode or whose electron emission properties result in an increase of the surface temperature, and thus, contribute to the loss of cathode meterials. Since in this study only inert plasmagases were used (Ar and He), only research relevant to thermal erosion will be reviewed in this section. It should, however, be pointed out that even relatively small amounts of impurities in the plasmagas can have a significant effect on the rate of cathode deterioration. For example, Hardy and Nakanishi (1984) working with a thoriated tungsten cathode in a transferred arc system found that the mass loss rate for 99.5 percent nitrogen plasmagas was more than four times that of 99.95 percent nitrogen plasmagas.

Mechanisms of Thermal Erosion

For many years, the observed deterioration of the cathode has been explained using simple energy balances at the cathode spot. Holm (1949) carried out calculations which showed that, because of the smallness of the cathode spot area, the cathode is not able to dissipate by conduction all the energy generated during arc operation. He concluded that vapourization of the cathode material is necessary in order to complete the energy balance, and that the rate of vapourization per coulomb increases with increasing arc current. A model very similar to Holm's was proposed later by Augis et al. (1971).

Both the Holm model and the Augis et al. model considered only the largest contributions to the energy balance and attempted to estimate the energy dissipated at the cathode within an order of magnitude. According to these studies, the energy going to the cathode is primarily due to the ionic current, which includes both kinetic energy and the energy of recombination. The contributions from the electrode joule heating, the impact of the neutrals, radiation, and chemical reactions on the cathode surface were considered small and disregarded. The incoming energy can be dissipated within the cathode through conduction, utilized in phase changes of the cathode material (melting and vapourization), and provide the required electron emission to sustain the arc current.

Thus, the two positive terms of the energy balance are: (a) the kinetic energy of the ions, $Wa = I_i \cdot V_s \cdot A^+$, and (b) the ion recombination energy, $Wi = I_i (V_i - \phi) A^n$, where $\underline{I_i}$ is the ionic current, $\underline{V_s}$ is the cathode fall voltage, $\underline{V_i}$ is the ionization potential of the ion species, $\underline{\phi}$ is the thermionic work function of the cathode material, and $\underline{A^+}$ and $\underline{A^n}$ are the respective coefficients of accommodation. The two negative terms are: (a) the heat dissipated to the metal, $\underline{W_c}$, and (b) the power spent in extracting the electrons from the cathode surface, $\underline{W_d} = I_e \cdot \alpha \cdot \phi$, where $\underline{I_e}$ is the electronic current, and $\underline{\alpha}$ is the fraction of electrons contributed through thermionic emission.

Therefore, the energy balance becomes:

$$Wc = I_i (V_s \cdot A^+ + V_i \cdot A^n - \phi \cdot A^n) - I_e \cdot \alpha \cdot \phi \qquad (2)$$

Unfortunately, there are such large uncertainties regarding the value of these terms that Augis et al. concluded that the best order of magnitude approximation would be to simplify Equation (2) to the form:

$$W_c = I_i \cdot V_s \qquad (3)$$

which suggests that the heat absorbed by the metal is roughly equal to the kinetic energy coming from the ionic current.

The approximations used by Augis et el. introduce serious doubt about the value of their approach. Furthermore, there are no sufficiently accurate data available on the ionic current and the cathodic fall potential to make use of Equation (3). In fact, Augis et al. claim that any analysis of the plasma electrode interactions which uses only a continuous medium model and such macroscopic concepts as temperature and pressure, is destined to produce results of marginal value. A more exact treatment of the cathode erosion should focus at the atomic level and be based on interparticle collisions. Unfortunately, this type of analysis is not possible in light of our present understanding of cathode phenomena.

While some of the mass loss from cathodes has been attributed to vaporization, other mechanisms of electrode erosion have also been proposed. Gray and Pharney (1974), for example, studied the electrode damage caused by various types of low-current ($<$ 5 A) atmospheric pressure arcs. They concluded that most of the erosion in these arcs occurs by an explosive release of molten metal from the cathode surface. They observed that during operation craters were formed on the electrode surface and small droplets of the cathode material were found on the anode. It was assumed that the craters were formed during the discharge due to the impinging momentum of the ions acting on the molten cathode. This impinging jet of ions forces matter out from the bottom of the molten bath forming a high ridge at the crater's perimeter. Uppon abrupt cessation of the local ion bombardment, the unbalanced recoil force acts to form a small droplet in the center of the crater. Whenever the surface tension force is smaller than this recoil force, the droplet is released in the direction of the anode. According to Gray and Pharney the material ejected from the cathode due to this pressure release mechanism accounts for most of the electrode mass loss in short-duration arcs. The effect of such mechanism on the electrodes of long-duration, high-current arcs was not investigated.

Guile and Hitchcock (1975) disagreed with the mechanism offered by Gray and Pharney. They proposed that the rims on the cathode craters are not formed by molten pool displacement but rather by positive ions which have neutralized and condensed upon the cathode together with large numbers of back-scattered excited and neutral atoms. They estimated that over 95 percent of all the matter leaving the cathode craters returns and condenses back on the cathode's surface. Thus, they concluded that a larger portion of the cathode material is lost through evaporation rather than through the formation of droplets. Guile and Hitchcock made their observations while studying erosion on non-refractory cathodes having oxide films of different thickness. The application of their findings to refractory arcs can not be clearly assessed.

Gray and Augis (1971) studied the damage on silver, gold, palladium and tungsten cathodes in short-duration, low-current arcs at atmospheric pressure. While they observed many craters in a variety of patterns for the silver, gold and palladium cathodes, few craters were present on tungsten. Instead, the damage on tungsten appeared to be within a large diffuse area which contained protuberances having an average height of about one mm. They concluded that the presence and distribution of craters depend on the metal properties, including the melting point, the thermionic work function, and others. The relationship between the metal properties and the mechanism of cathode erosion is not well understood. An interesting observation made by Gray and Augis is that, based on ionic momentum transfer calculations, pressures of 10^3 atm may be acting on the cathode spot. If this is true, temperatures much greater than the boiling point of the cathode material may exist within the cathode spot.

Gray (1978) also studied the erosion of graphite electrodes in short duration low-current arcs at atmospheric pressures. He observed two types of cathode damage. In one type, the damage consisted of a multitude of microcraters separated by largely thermally-undisturbed areas. This type of damage was associated with high current density (about 6×10^7 A/cm^2) arcs and resulted in relatively low electrode erosion rates. The second type of damage had much larger spot area (lower current density), and the total surface within the spot was affected thermally. This type of damage was associated with thermionic arcs.

Gray's work seems to support the electrode erosion mechanism he proposed earlier (Gray and Pharney, 1974) against the mechanism proposed by Guile and Hitchcock. Although craters were formed in the graphite electrodes, no rims were observed. Gray claims that if ion backscattering occurred with metal electrodes, a similar process could be expected to occur with graphite electrodes. If that was the case, raised rims should be observed around the craters. The fact that this does not occur, and that graphite cathodes (which sublime) have no molten phase, is offered by Gray as support for the molten pool-displacement cathode erosion mechanism.

Gray's argument on the mechanism of cathode erosion is not completely convincing. The properties of graphite are very different [illegible]m those of most metal electrodes, and there is little understanding [illegible] the effect of the material's properties on erosion mechanism. For example, most metals have very low ionization potential compared to carbon. Copper's ionization potential is 7.7 eV, very close to that of tungsten (8.0 eV) and much lower than carbon's 11.3 eV. The effect of this difference is not understood. One could speculate that atoms from the cathode will become highly ionized in the cathode fall region of the arc and return to the cathode. However, the degree of ionization of carbon atoms may be much smaller than copper or tungsten atoms due to the difference in ionization potential. In any case, the relevance of either of the proposed cathode erosion mechanisms to long duration transferred-arc systems is not obvious.

Another research area that has received little attention is the effect of plasmagas composition on cathode erosion mechanism. The plasmagas composition is crucial in determining the temperature of the plasma directly in front of the cathode as well as the current density at the cathode spot. As such, one may expect that different plasmagases will have different cathode erosion rates and perhaps even different cathode erosion mechanisms. Such information is not yet available. Some work using nitrogen, oxygen, carbon monoxide and air has been published by researchers such as Szente et al. (1987), George (1985), Hardy and Nakanishi (1984), An'shakov et al. (1971), and Belkin (1971). Unfortunately these studies dealt exclusively with erosion rates and did not address the issue of erosion mechanism. Currently, R. N. Szente, working within the Chemical Engineering department of McGill University, is studying the mechanisms of cathode emission and erosion in magnetically rotated arcs.

Considering the ambiguities existing in our understanding of cathode electron emission and cathode erosion mechanisms, and the unavailability of both empirical experimental data and instrumentation for directly measuring the relevant parameters, it is not likely that any one study will provide definitive solutions to the uncertainties surrounding cathode phenomena. Yet, much can be gained by studying the changes that occur at the cathode's surface during arc operation. The approach taken in the present study was to examine carefully the cathode of an atmospheric-pressure, transferred-arc reactor before and after use. It is assumed that by varying the operating time the phenomena occurring during different periods of operation can be accurately identified. This assumption can not be fully verified until methods become available for measuring parameters related to cathode phenomena during arc operation. Until then, the accuracy of this critical assumption remains open to speculation.

EXPERIMENTAL

APPARATUS

The same apparatus was used for all the experimental work relevant to each of the four Parts of this thesis, including the work relevant to this study. A complete description of the apparatus was provided in Part I.

EXPERIMENTAL PROCEDURE

Prior to all experiments described in this study, the cathode was machined to the desired geometry, polished to assure a smooth surface, cleaned and dried. The cathode's surface was then examined and photographed using an Electron Scanning Microscope (JOEL JSM-35CF). The microscope used images from a Secondary Electron Detector for the photographs. The concentration of thoria on the cathode surface could also be measured semi-quantitatively using an Energy Dispersive X-Ray Mapping method. Unfortunately, the method used to determine the concentration of thoria was not sensitive to the presence of oxygen. As such, it could not be determined with certainty whether the identified thorium atoms were in fact bonded with oxygen. Nonetheless, this was assumed to be the case throughout this study and therefore references made within the discussion regarding thoria concentration should be qualified accordingly.

The procedure for examining the composition and characteristics of the cathode's surface was repeated after the completion of each experiment. By comparing the characteristics of the surface before and after an experiment, the electrode phenomena occurring during arc operation were investigated.

Cathode erosion rates were measured by weighing the cathode before and after each experiment and dividing the total mass loss by the duration of the experiment. A digital Mettler AE163 balance was used to weigh the cathode. The balance had a range of 0 - 30 grams and a precision of 0.01 mg. Each cathode was weighed at least seven times before and after the experiment. The weight reported in this study is the average weight from all readings. The systematic error for each reading was approximately 0.02 mg.

Once the preparation and characterization of the cathode was completed, the transferred arc reactor was assembled, sealed and purged with argon for about 15 minutes. After the completion of each experiment, the reactor was allowed to cool down for five minutes while being purged with argon. A water-cooled molybdenum disc was used as the anode in the transferred arc reactor. There was no visually noticeable damage to the anode during arc operation. As such, the anode was cleaned in between experiments and used repeatedly.

Since there was no need to preheat the plasmagas prior to its injection into the reactor, as was the case for all experiments in Part I, the plasmagas preheater shown in Figure 1 (Part I), was disconnected and removed. All parts shown in Figure 1 (Part I) that were relevant to the feeding of titanium tetrachloride were also disconnected from the reactor system in an effort to minimize plasmagas contamination. Fortunately, plasmagas contamination was easily detectable due to the formation of dark-blue colored oxides and nitrides on the cathode. The results from experiments in which cathode contamination was suspected were discounted. However, very few experiments showed such contamination. Prepurified grade helium and argon cylinders were used as the plasmagas source.

DISCUSSION AND RESULTS

The discussion and results from this study have been divided into two sections. The first deals with observations relevant to changes occurring in the appearance of the cathode's surface during arc operation. Experimental data on cathode erosion are presented in the second section.

The independent variables for both sections of this study were the cathode tip geometry (flat vs pointed) and the plasmagas composition (argon vs helium). All cathode tips were conical in shape using a cone angle of 60° with the horizontal. However, for the flat-tip cathodes the tip of the cone was cut to form a flat circular surface with a diameter of about 1.5 millimeter. The arc's current, length and plasma-gas flowrate were maintained constant for all experiments at 200 A, 2.5 cm and 15 L/min, respectively.

Cathode Surface Characteristics

The phenomena observed on the surface of cathodes operating in helium were essentially the same for both flat and pointed-tip geometries. Consequently, the two cathode geometries used in helium arcs will be discussed together. However, the same approach is not possible for argon arcs. The phenomena observed on the surface of flat cathode tip operating in argon were quite different from both those observed in helium arcs and those observed on pointed-tip cathodes operating in argon. Furthermore, while the pointed-tip cathodes operating in argon shared some of the characteristics observed in helium arcs they also exibited some unique phenomena. As such, the two cathode geometries used in argon arcs will be discussed separately.

1. Flat-Tip Cathodes Operating in Argon

The appearance of the flat-tip cathode operating in argon depended to a large degree on the arc current and the duration of the run. At relatively low currents (about 50 A) there was little visible damage on the cathode and no measurable weight loss. Furthermore, the concentration of thoria on the cathode surface remained at less than one percent and was evenly distributed throughout the surface. In essence, the cathode maintained its pre-operation appearance and composition, suggesting that the temperature of the cathode spot was well below the melting temperature of tungsten and that there was little or no diffusion of thoria through the tungsten matrix.

The appearance of total stability that characterized the cathode at low currents disappeared when the arc current was increased to about 200 A. By examining the surface of the cathodes used in experiments of varying durations, the sequence of events occurring at the cathode was identified. It was discovered that during the first five minutes of operation the tungsten maintained its solid state. However, the thoria was mobilized, moving primarily through tungsten grain boundaries to the cathode surface. Once on the surface, thoria concentrated in small regions forming a well defined mosaic on the tungsten base.

A magnified photograph (x1000) of a typical cathode surface after five minutes of operation is shown in Figure 3-a. Figure 3-b depicts a concentration map of the same photograph. The dark shaded areas indicate high concentrations of tungsten (over 99.5 %) whereas the light areas indicate the presence of thoria. The concentration of thoria

FIGURE 3

PHOTOGRAPH OF SURFACE FROM FLAT-TIP CATHODE OPERATING IN ARGON FOR 5 MINUTES

Photograph 3-a: Cathode Spot Area

Photograph 3-b: Thoria Concentration Map of Cathode Spot Area (3-a).

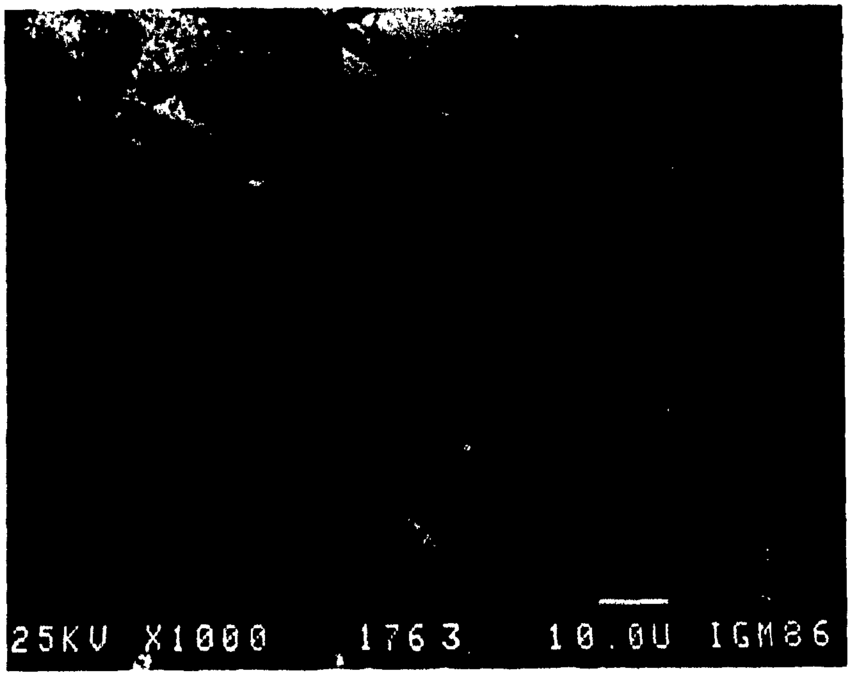

(a)

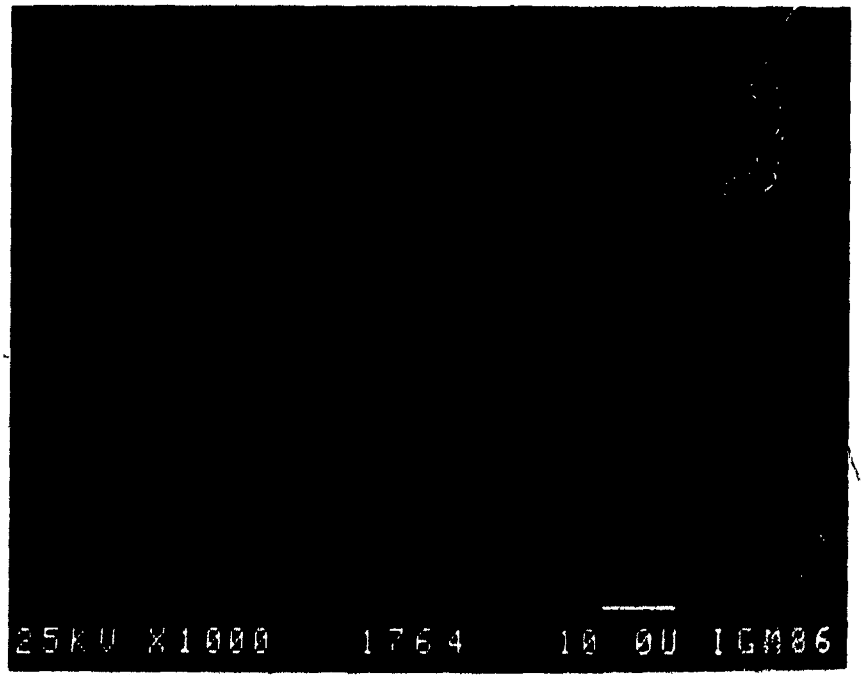

(b)

within the thoria-rich regions varied from 70 to 95 percent. Thin light shaded lines, indicating the presence of thoria, appeared on the concentration map corresponding to the tungsten grain boundaries. Based on these photographs, one may speculate that thoria, which was present deep within the cathode material at the beginning of the experiment, became mobile during operation of the arc. Thoria moved towards the surface, following the path of least resistance which would have had to be the boundaries of the tungsten grains. Once on the surface, thoria moved laterally to form rich thoria regions resulting in the mosaic shown in Figure 3.

It is not clear why the thoria moves through the cathode material or why it concentrates within such clearly defined regions. However, the observations are in close agreement with earlier observations by Shishkin and Bakhtiyarov (1974). They reported similar mobility of the low-melting component (Pt) to and on the surface of platinum-molybdenum alloy cathodes. On the surface of the binary alloy, platinum formed multi-layer films which led to an increase in the value of the cathode's thermionic work function.

Thoria, which is the lower melting component in the ThO_2-W alloy, must have moved through the cathode material in a manner similar to that observed in the Shishkin and Bakhtiyarov study. However, unlike the increase in thermionic work function caused by the formation of platinum films on the surface of the Pt-Mo cathode (Pt has a higher work function than Mo), the concentration of thoria on the surface of the ThO_2-W cathode likely decreases the cathode's work function.

No measurements of the cathode's thermionic work function were made in this study. Yet, qualitative information relevant to the cathode's emitting properties may be derived from the following observation. Whenever a new cathode was used, the total arc voltage at the begining of an experiment was about 29 V. From this value it decreased constantly throughout the first 10 minutes of operation until it reached about 26 V. Once at this new low value, the voltage remained constant throughout the remaining duration of that experiment. Furthermore, if the arc was terminated and the cathode reused for another experiment, the total arc voltage at the beginning of this run was only slightly higher (about 0.5 V) than the voltage at the time of termination.

Since the arc's current, length, anode material and plasmagas were maintained constant, variations in the total arc voltage were likely caused by variations in the cathode fall voltage. This suggests that changes occurring on the cathode surface, such as the concentration of thoria or the increase of the cathode spot temperature which shall be discussed later, facilitate the emission of electrons and reduce the fall potential. Once the surface has reached a desirable composition and morphology, corresponding to a minimum fall potential, the cathode can maintain most of these favorable characteristics even through the termination and reignition of the arc.

The above speculations can explain some of the observations made in this study. They may also serve to explain why thoria concentration above 0.5 percent have little effect on the performance of thoriated tungsten cathodes. If the cathode concentrates thoria during arc operation, one may expect that increasing the initial concentration of thoria beyond a certain minimum value would have little effect on the emitting properties of the cathode. However, the effect of increased thoria concentration on the longevity of the cathode may be significant. Further studies are required to confirm these speculations and identify the exact role of the thoria-rich regions in electron emission.

The concentration of thoria on the surface seems to continue for at least the first ten minutes of arc operation. By the end of this period most of the central region of the cathode was covered by a thin film of higly concentrated (over 80 %) thoria. Furthermore, the tungsten melted to form a liquid phase on the cathode surface nearest the cathode spot. Photographs of the cathode's surface after 10 minutes of operation are shown in Figure 4. The photograph shown in Figure 4-a depicts a thoria concentration map of the entire cathode surface. The average concentration of thoria on the cathode surface after ten minutes of operation varied between 30 and 45 percent. However, as shown in Figure 4-a the thoria was not evenly distributed throughout the entire cathode surface.

FIGURE 4

PHOTOGRAPHS OF SURFACE FROM FLAT-TIP CATHODE OPERATING IN ARGON FOR 10 MINUTES

Photograph 4-a:	Thoria Concentration Map of Entire Cathode Surface
Photograph 4-b:	Border Between Thoria-Rich and Pure-Tungsten Regions
Photograph 4-c:	Segregated Thoria-Rich Regions Outside Molten Tungsten Periphery

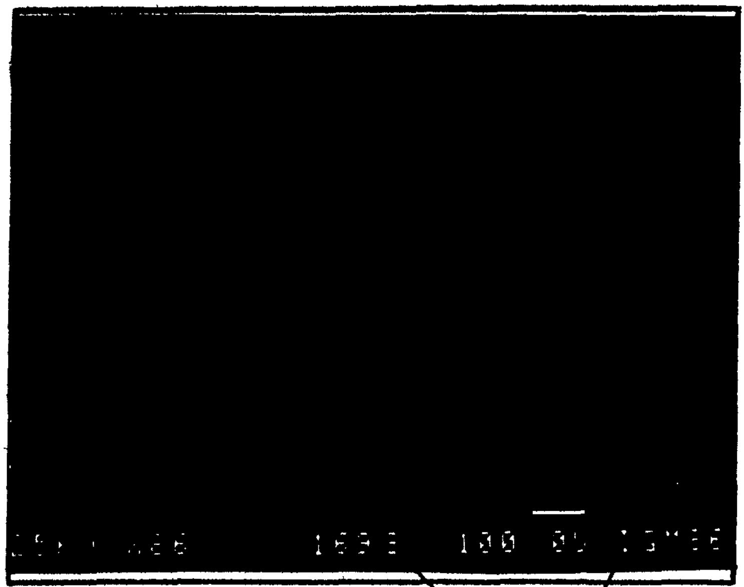

(a)

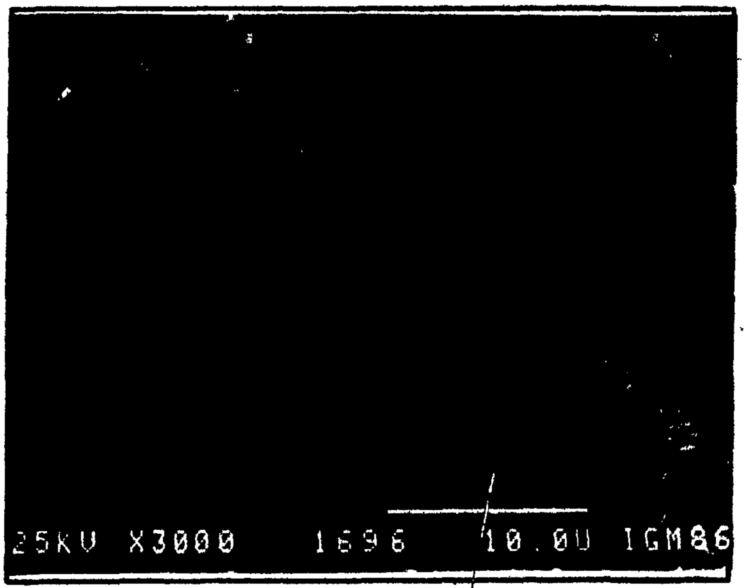

(b)

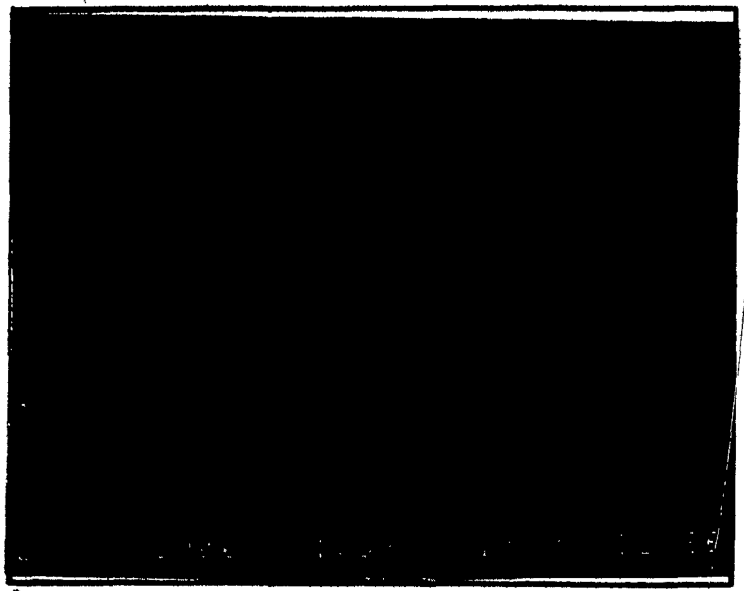

(c)

There are three clearly identifiable regions in the photograph shown in Figure 4-a. The central region is almost entirely covered with thoria as indicated by the light shaded, almost circular pattern. Surrounding this region is a dark area, indicating the presence of mostly tungsten and very little thoria. Still further away from the center of the cathode, a mosaic of light and dark areas can be observed. This mosaic is very similar to the one observed on the cathode surface after only five minutes of operation. It indicates the presence of many small regions some rich in thoria and some consisting of only tungsten.

The presence of these three regions may be explained as follows. The cathode spot was located in the center of the flat cathode tip. Within and nearest the cathode spot area, the temperature of the surface was above the melting point of tungsten (3 680 K) as demonstrated below. In this region, the cathode was in its molten state thus facilitating the mobility of the thoria molecules. Consequently, the thoria, which appears to be immiscible in liquid tungsten, concentrated in a single agglomerate on the surface of the molten tungsten. This concentration was responsible for both the formation of the thoria-rich region in the center of the cathode and the absence of thoria from the immediately surrounding region.

Evidence of the existence of a molten tungsten phase within the central region of the cathode are presented in Figure 4-b. This photograph was taken on the border between the thoria-rich and the pure-tungsten regions of the cathode surface. Thoria can be seen to form a thin, smooth layer on top of a re-solidified tungsten base. The extensive presence of dendrites, whose composition is over 99 percent tungsten, verifies the existence of a molten phase during arc operation. Some cracks appear on the surface, probably caused by thermal contraction stresses on the metal during the post-operation cooling.

Further away from the cathode spot region, the temperature of the cathode surface remained below the melting point of tungsten. Consequently, thoria was less mobile and could not agglomorate into the central region. Instead, it formed many distinct thoria-rich regions resulting in the mosaic seen in the periphery of Figure 4-a. The photograph shown in Figure 4-c was taken within this periphery. In this photograph the tungsten grains appear as perfectly smooth slabs with no evidence of dendrite formation. Thoria can be seen within distinct elevated regions and in the boundaries of the tungsten grains. The appearance of this region was basically the same as the appearance of the cathode spot region of a flat-tip cathode operating for five minutes in argon (see Figure 3).

Thus, the events occurring on the surface of a flat-tip cathode operating in argon during the first 10 minutes of operation were identified quite clearly. First, the thoria was mobilized, moving through grain boundaries to the surface where it agglomerated into small, distinct regions. Concurrently, the cathode spot temperature rose until it surpassed the melting point of tungsten forming a molten metal phase on the central region of the surface. Once the tungsten base was molten, the segregated thoria regions combined to form one large thoria-rich spot in the center of the molten tungsten pool. Regions outside the molten pool remained segregated forming a thoria-tungsten mosaic. During this transformation the total arc voltage was reduced by approximately 3 volts. It is speculated that most of this voltage reduction occurred within the cathode fall region of the arc.

Unfortunately, the repeatable, well-defined pattern of changes that occured on the cathode surface during the first 10 minutes of operation disappeared when the duration of the experiment was extended to 20 minutes or longer. Cathode tips used in these relatively long experiments exhibited highly disturbed surfaces, sometimes containing few if any clearly identifiable thoria-rich regions. Other times, large thoria regions were identified but not in the center of the cathode tip as was expected. Frequently, a thoria-rich ring surrounded the flat surface of the cathode. Such rings were consistently observed in experiments which utilized helium as the plasmagas and will be described in detail in the following section. In general, the appearance of the cathode surface suggested rapid movement of the cathode material which likely included vapourization and recondensation.

Frequently, large clusters of tungsten particles would form a sponge like shape on the cathode surface. A photograph of a cathode surface containing such clusters is shown in Figure 5. These sponges were identified in various regions of the flat-tip surface suggesting perhaps an extensive mobility for the cathode spot. Their shape and surface characteristics provided evidence of both melting and vapourization occurring on the cathode surface.

It is interesting to note that the presence of these sponge-like clusters was not necessarily a prelude to a high erosion rate in the particular cathode. Neither did such sponges cause noticeable variations in the total arc voltage. There were, however, some experiments that exhibited an unusually high erosion rate. In some of those experiments the cathode surface included smooth regions highly concentrated in thoria. These regions, which typically occupied only a fraction of the total cathode surface (their diameter varied widely around 0.3 mm as compared to a diameter of 1.5 mm for the flat-tip cathode surface), were similar in appearance to regions identified earlier on the cathodes of short duration (10 min) experiments.

The combination of the above observations could lead to the following speculation. It could be that the particular geometry, thermal conductivity and cathode cooling mechanisms created large temperature gradients within the cathode. These gradients limited the cathode's ability to mobilize thoria to a very small depth within the

FIGURE 5

SURFACE OF FLAT-TIP CATHODE OPERATING IN ARGON FOR 60 MINUTES

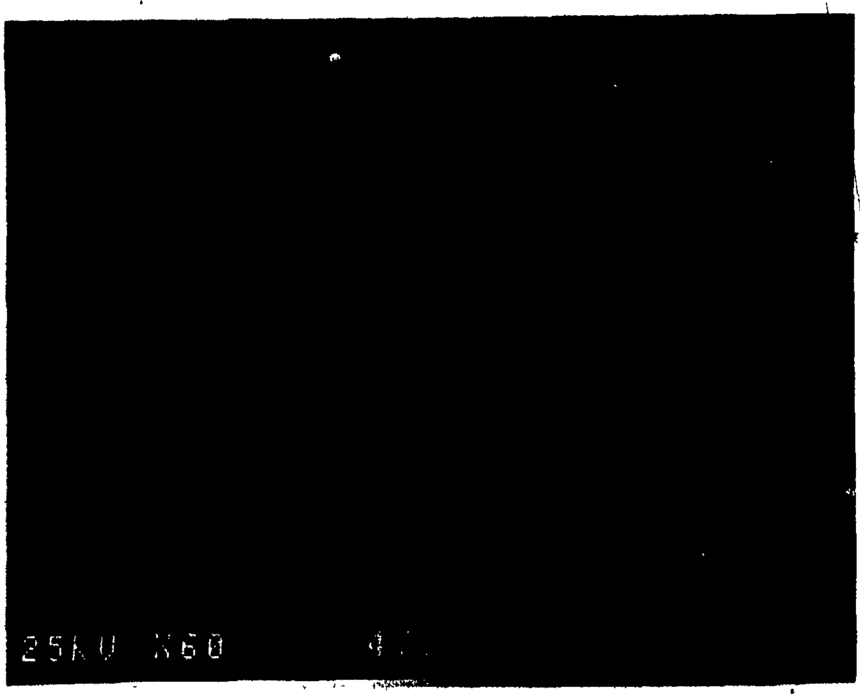
25KU X60

tungsten matrix. When the mobilized thoria reached the surface of the cathode, it left behind a layer of tungsten containing little thoria. Once the surface thoria was consumed or eroded, the cathode's temperature increased rapidly resulting in extensive melting and the formation of the observed sponges. The sponges increased in size until they suddenly broke away from the cathode, exposing fresh cathode material rich in thoria where the process could have begun all over again.

This speculation suggests that the cathode used in this study never really reached a steady state. Instead it operated on a cyclical pattern of thoria enriched/thoria-starved periodes each characterized by its own electron emission and electrode erosion phenomena. Clearly, the evidence presented in this study for this speculation is rather inconclusive. However, it does offer a possible reason for the large variations in erosion rate under apparently identical plasma operating conditions observed both in this and other studies (Guile, 1971). Furthermore, a similar cathode erosion mechanism was observed in pointed-tip cathodes operating in argon. In any case more studies in this area are clearly needed.

ii. Flat-Tip and Pointed-Tip Cathodes Operating in Helium

The appearances of both flat-tip and pointed-tip cathodes operating in helium were essentially the same. In both geometries, three distinct regions were identified on the cathode surface following its use in the transferred arc plasma. The three regions, shown schematically in Figure 6, consisted of a relatively large circular central region and two surrounding concentric rings. This configuration was perfectly repeatable for all helium experiments. Furthermore, the appearance and composition of these regions did not vary significantly with the duration of the experiment. Consequently, the appearance of a cathode operating in helium for 10 minutes was the same as the appearance of a cathode operating under the same conditions for 60 minutes.

The central region, which extended about one millimeter from the center of the cathode tip, consisted of highly distorted molten tungsten particles. The shape and arrangement of these particles, whose photographs are shown in Figure 7, suggest that the region was operating at a temperature near the boiling point of tungsten (5 930 K), and that rapid evaporation of the cathode material was occurring. It also appears that the molten particles had been separated into specific shapes prior to melting, suggesting that the particles were formed on the surface through the recondensation of vapourized cathode material (Williams, 1987). No thoria could be identified within this region.

In the case of flat-tip cathodes a small protuberance of molten particles was formed in the center of the cathode surface having a diameter of about one millimiter and a height of less than 0.1

FIGURE 6

SCHEMATIC DRAWING OF REGIONS ON FLAT AND POINTED-TIP CATHODES AFTER 40 MINUTES OF OPERATION IN HELIUM

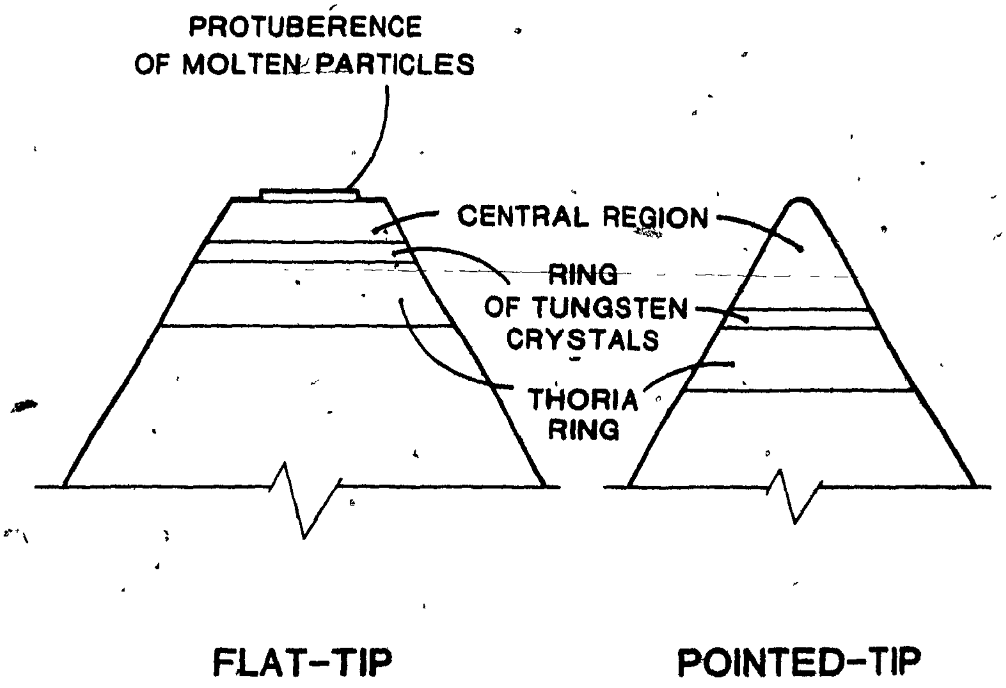
PROTUBERENCE
OF MOLTEN PARTICLES
CENTRAL REGION
RING
OF TUNGSTEN
CRYSTALS
THORIA
RING
FLAT-TIP
POINTED-TIP

FIGURE 7

PHOTOGRAPHS OF MOLTEN TUNGSTEN PARTICLES WITHIN CENTRAL REGION OF CATHODE SURFACE IN HELIUM ARCS

Photograph 7-a: Particles on Surface of Flat-Tip Cathodes

Photograph 7-b: Particles on Surface of Pointed-Tip Cathodes

(a)

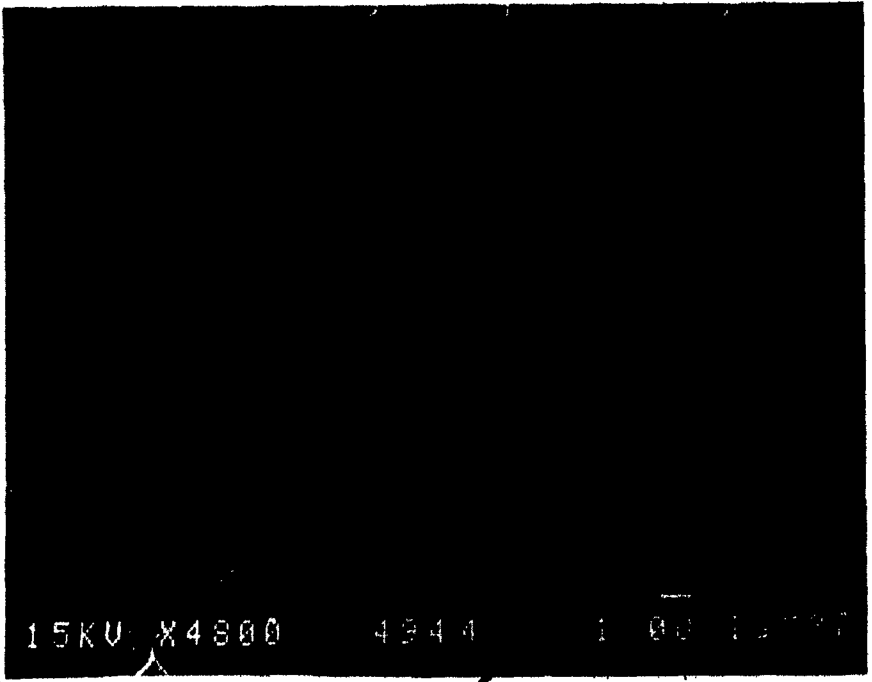

(b)

millimeter. The composition and appearance of the particles on the surface of the protuberance were the same as those of the particles in the rest of the central region. In some experiments an indentation was observed in the center of the protuberance probably marking the location of the cathode spot. Photographs of the protuberance on two such cathodes, one with and the other without an indentation, are shown in Figure 8. It is not clear whether the protuberance was caused by tungsten displacement due to melting or reflected a higher redeposition rate of vapourized tungsten on the cathode surface.

The particles identified within the central region of pointed-tip cathodes (see photograph in Figure 7) had essentially the same appearance as those identified on flat-tip cathodes. Furthermore, the perimeter of this region was about one millimeter from the center of the tip, a distance approximately equal to that measured on flat-tip cathodes. However, no protuberance was observed on the pointed tip cathodes.

Surrounding the central region in both flat and pointed-tip cathodes a ring of large tungsten crystals was observed and photographed. These highly regular, multifaceted crystals, whose photographs are shown in Figure 9, varied in diemeter from about 5 to more than 20 microns. The ring containing these crystals was about 0.1 millimeter wide for both cathode geometries. The shape and general appearance of these crystals are typical of crystals formed through the

FIGURE 8

PHOTOGRAPHS OF FLAT-TIP CATHODES OPERATED IN ARCS WHICH UTILIZED HELIUM AS THE PLASMAGAS

Photograph 8-a: Tip Showing Indentation in Center (Operating time = 20 minutes)

Photograph 8-b: Tip Showing no Indentation in Center(Operating time = 10 minutes)

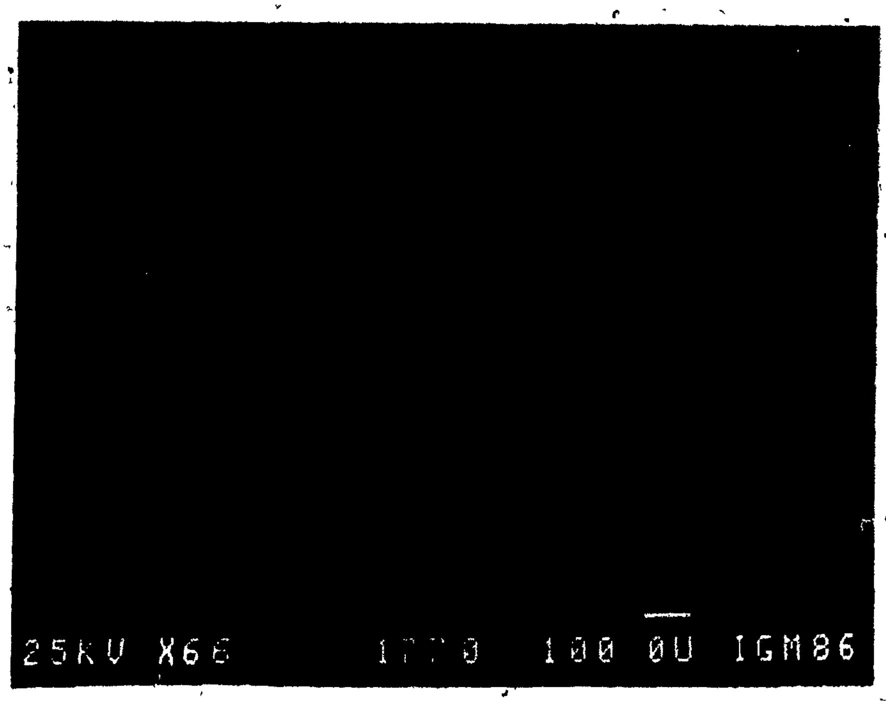

(a)

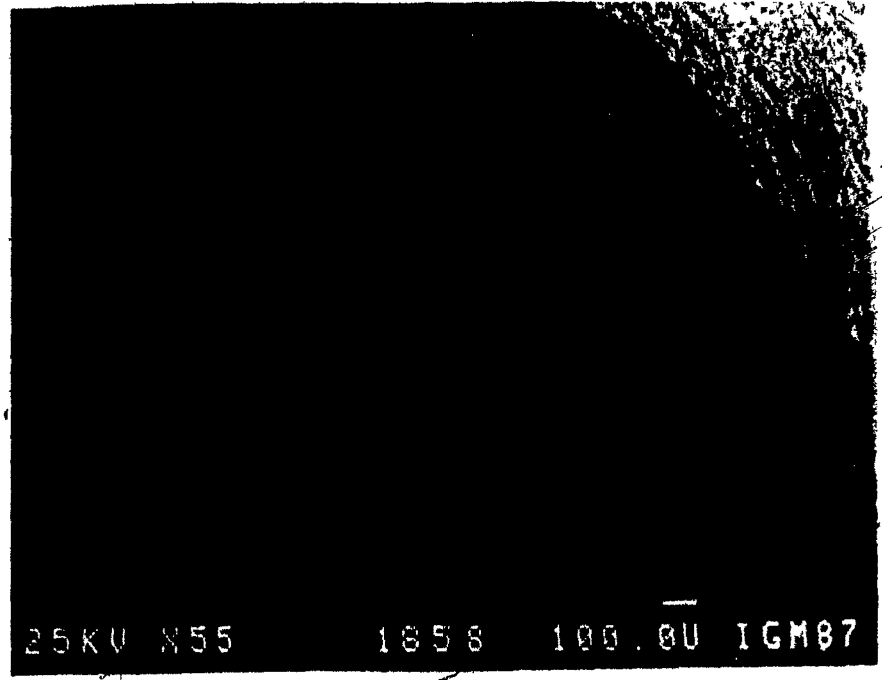

(b)

FIGURE 9

TUNGSTEN CRYSTALS FORMED ON THE SURFACE OF CATHODES OPERATING IN HELIUM PLASMAS

Photograph 9-a: Ring of Tungsten Crystals Which Surrounds Central Region of Cathode Surface

Photograph 9-b: Highly Magnified Photograph of Crystals

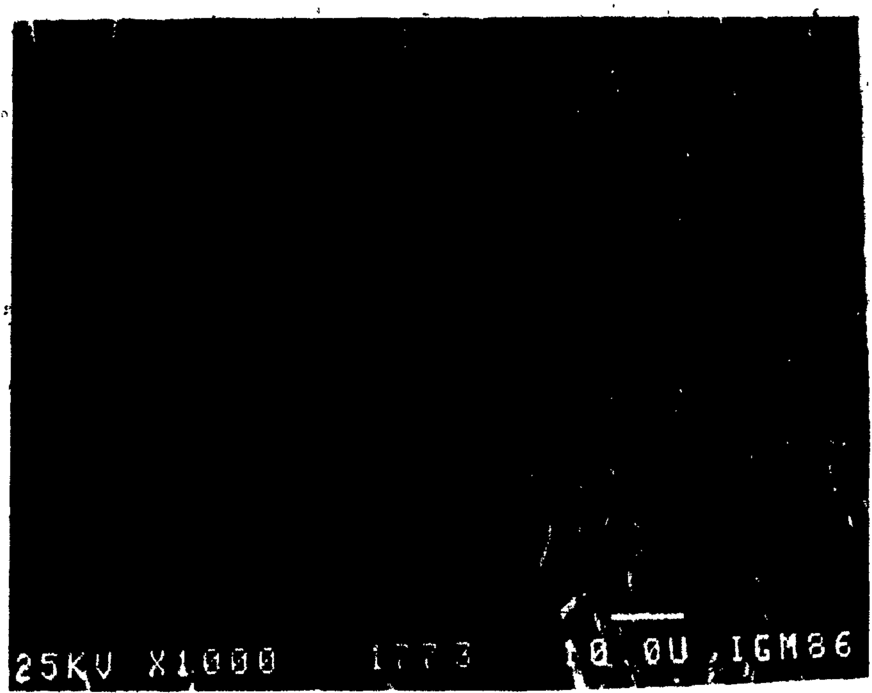

(a)

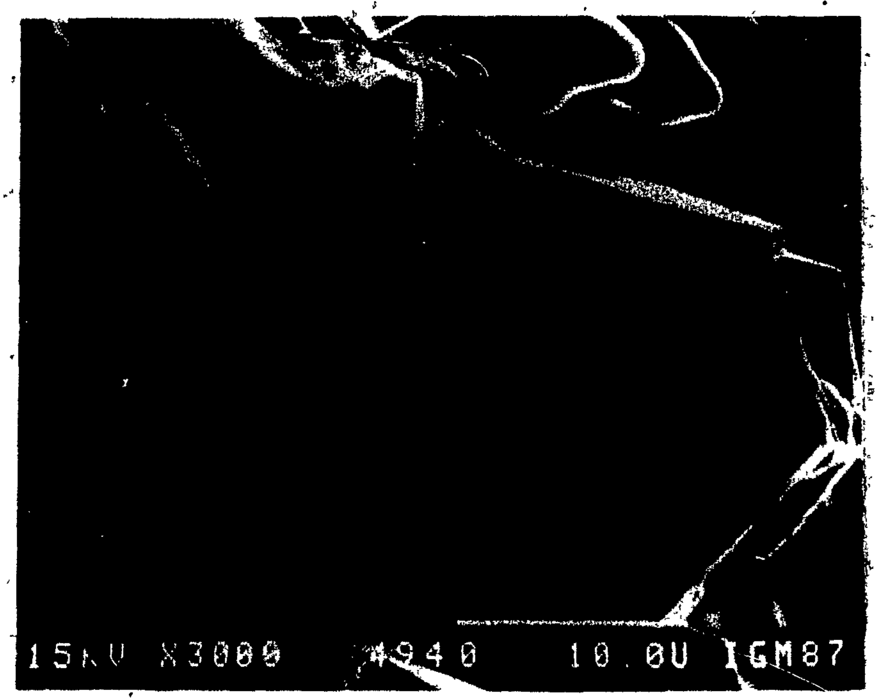

(b)

condensation of metals from a vapour into a solid phase (Williams, 1987). This suggests that they were formed from the recondensation of tungsten vapour on the cathode surface. Similar to the composition of the central region, no thoria was found in this region.

The absence of thoria from both the central region and the first concentric ring was reversed in the second ring. This ring occupied an area about 300 microns wide and surrounded the ring with the large tungsten crystals. It consisted of much smaller crystals highly concentrated in thoria. The average diameter of these crystals was around one micron while their composition included over 80 percent thoria. The ring was perfectly concentric, uniform in width and had the same dimensions and appearance in both pointed and flat-tip cathodes. Typical photographs of these crystals are shown in Figure 10. Just as was the case with the larger tungsten crystals, the shape and general appearance of the thoria crystals suggests that they were formed from the condensation of thoria vapour on the cathode surface.

In summary, the appearances of both flat and pointed-tip cathodes operating in helium were very similar. They were characterized by the formation of a relatively extensive central region consisting of molten and volatilizing tungsten particles, surrounded by two concentric rings. The ring nearest the central region was composed of large tungsten crystals, whereas the outside ring was composed primarily of smaller thoria crystals. The shape and appearance of both the crystals

FIGURE 10

THORIA CRYSTALS FORMED ON THE SURFACE OF CATHODES OPERATING IN HELIUM PLASMAS

Photograph 10-a: Region Containing Over 80 Percent Thoria Crystals

Photograph 10-b: Highly Magnified Thoria Crystals

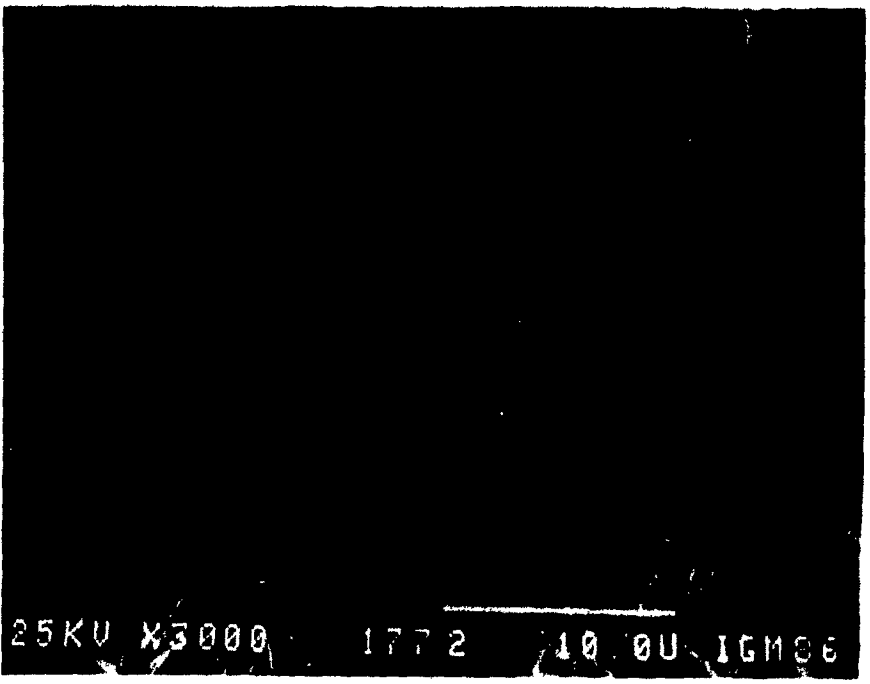

(a)

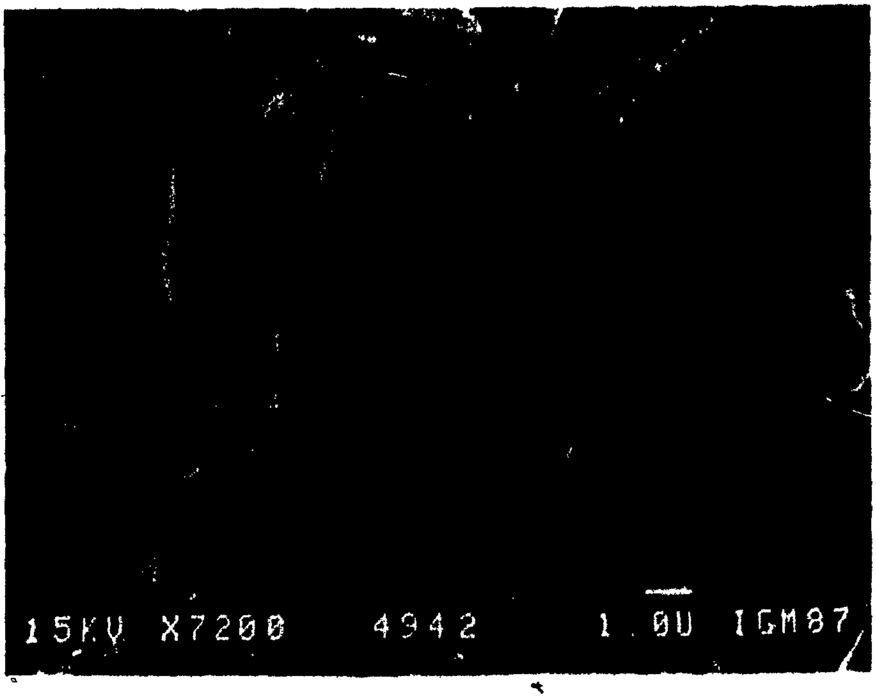

(b)

in the rings and the molten particles in the central region suggest that they were formed through the condensation of the cathode material from a vapour phase.

The observations reported here were highly repeatable and reflect phenomena occurring at the cathode surface. It is not clear, however, what exactly these phenomena are. One could speculate, based on Guile and Hitchock's (1975) hypothesis on the cathode erosion mechanism, that both the central region and the surrounding rings were formed by positive ions which condensed and neutralized upon the cathode together with large numbers of backscattered excited and neutral atoms. Based on their results, which were derived from experiments on non-refractory cathodes, over 95 percent of all the matter leaving the cathode returns and condenses back on the surface.

The above hypothesis is consistent with the observed formation of the concentric rings on the cathode surface whose shape and composition depended on their distance from the center and the plasmagas composition. Since both the distance from the cathode spot, which is presumed to be in the center of the cathode, and the composition of the plasmagas are important factors in determining the temperature profile on the cathode surface, the combination of the observed results with the Guile-Hitchock hypothesis suggests the following sequence of events:

1. Cathodes operating in helium plasmas had cathode spot temperatures

near or equal to the boiling point of tungsten. Consequently, large amounts of cathode material were vapourized into the arc.

2. Once in the arc, some of the cathode material (whose ionization potential is well below that of the plasmagas) became ionized and returned to the cathode surface along with large numbers of neutral atoms and molecules.

3. On the surface the returning particles condensed at various rates according to the recondensation temperature they experienced, resulting in the formation of the observed concentric rings. Thoria, which has a relatively low boiling point could condense only on the outside perimeter of the cathode surface where the temperature was relatively low. Thus, a thermal separation of tungsten and thoria occurred.

4. Tungsten atoms that condensed within the central region were quickly melted and partly vapourized, along with any thoria that may have migrated from inside the cathode material to the surface. This resulted in the formation of the observed highly porous surface.

The above sequence of events is consistent with another experimental observation from this study. Using flat-tip cathodes and helium as the plasmagas, the plasmagas flowrate was increased from 15 L/min to 45 L/min. Similar increases in plasmagas flowrate for flat-tip cathodes operating in argon had resulted in lower erosion rates and made no difference in the appearance of the surface. With helium as the plasmagas, however, the erosion rate was generally higher. Furthermore, the diameter of the central protuberance was about 50 percent smaller in the case of the high plasmagas flowrate. Since increasing the plasmagas flowrate results in a more constricted arc, which in turn may reduce the evaporated material's ability to return to cathode surface, the observed results offer further support for the Guile-Hitchock hypothesis. However, caution should be exercised in using this observation since both the erosion rates and the diameter of the protuberance varied significantly even for experiments which employed apparently identical operating conditions.

Further evidence of an active recondensation mechanism was provided from the fact that although the surface of cathodes operating in helium were highly disturbed when compared to similar cathodes operating in argon, their erosion rates were not measurably higher. Based on the extend of the disturbance on the surface, it would appear that the amount of cathode material vapourization was significantly greater for helium. Since the net cathode mass loss for helium is about the same as that of argon and the rate of vapourization higher there must exist one or more mechanisms which allows the helium operated cathode to regain some of its losses. Redeposition of cathode material from the arc is the most obvious of such mechanisms. In addition, the shape of the crystals within the concentric rings and the complete absence of dendrites from the surface of these crystals are clear indications that they were formed through a direct transition from a vapour to a solid phase.

A redeposition mechanism driven by the presence of positively charged tungsten and thorium ions may also explain the differences between argon and helium operated flat-tip cathodes. Based on their relative ionization potential and electrical conductivity it may be speculated that the argon plasma temperatures near the cathode were much lower than those of helium plasmas. Consequently, the degree of ionization of tungsten and thorium in argon are much lower than in helium resulting in a relatively weak redeposition force. A weaker redeposition force combined with a lower rate of vapourization may explain the absence of the tungsten-crystals ring from the surface of flat-tip cathodes operated in argon.

A similar argument can be used to explain the differences between pointed and flat-tip cathodes operating in argon. Pointed-tip cathodes are generally characterized by higher current densities and higher plasma temperatures near the cathode. Therefore, the smaller ring of tungsten crystals observed on pointed-tip cathodes operating in argon may reflect the presence of a redeposition mechanism which although not as strong as in the case of helium plasmas is still much stronger than the one operating in flat-tip cathodes.

These observations, which will be discussed in more detail in the following sections, agree qualitatively with the observations reported earlier by Neurath and Gibbs (1963). Although Neurath and Gibbs reported temperatures much lower than the ones suggested in this study, they similarly concluded that flat-tip cathodes operating in argon are characterized by lower current densities, and consequently lower temperatures, than pointed-tip cathodes or cathodes operating in helium. No direct measurement of cathode tip temperature were made in this study.

Despite the consistency of the above observations, some questions remain. Implied in the proposed redeposition hypothesis was the presence of tungsten and thoria vapour over one millimeter upstream from the center of the cathode spot. Although no measurements of the cathode spot area were made, it is probably safe to assume that at that distance the tungsten and thoria atoms were being rapidly cooled by the incoming plasmagas. That some of them should remain ionized long enough to attach themselves to the cathode surface is indeed surprising. Furthermore, it is not clear what percentage of the vapourized cathode material was redeposited on the cathode surface. The effect of the tungsten-thoria cloud, that must exist near the cathode surface, on the electron transmission characteristics of the arc must be investigated. The function of the redeposited crystals in the cathode's electron emission process was also not determined.

In any case, a spectroscopic analysis of the concentration of tungsten in the arc column, especially very near the cathode surface, is needed to positively verify the redeposition hypothesis and provide answers to some of the above questions. Unfortunately, due to the mobility of the cathode spot and the sharp gradients in the properties of the plasma that are characteristic of the cathode fall region, such analysis would be extremely difficult.

iii. Pointed-Tip Cathodes Operating in Argon

Pointed-tip cathodes operating in argon exibited most of the characteristics described earlier for cathodes operating in helium. These included the formation of a central region of molten tungsten particles surrounded with two concentric rings. Just as was the case for helium-operated cathodes, the first ring consisted of tungsten crystals whereas the second was highly concentrated with thoria crystals. However, the size and shape of these crystals were quite different in the case of argon from those found on helium-operated cathodes.

A unique characteristic of the pointed-tip cathode operated in argon was the formation and subsequent release of a small (about 0.2 mm in diameter) molten sphere of tungsten at the point of the tip. The formation of the sphere commenced immediately after arc ignition and grew gradually during operation. It appears to have been caused by the melting of cathode material on the tip. As the molten sphere grew in size, it eventually reached a point at which the force of gravity exceeded the surface tension of the cathode material and the shere was released from the cathode. The released sphere passed through the arc and landed on either the anode or the reactor wall from where it could be collected. Photographs of a cathode tip with an attached sphere (1) and one from which the sphere has been released (2) are shown in Figure 11. A photograph of the sphere itself is also shown in Figure 11-b. A pointed-tip cathode (3) which was operated in helium for 60 minutes is included for the purpose of comparison.

Using the geometry and operating conditions described earlier, the molten tungsten sphere was released sometime between 30 and 60 min into the experiment. It resulted in an immediate mass loss from the cathode ranging between one and three milligrams and an increase in the arc's voltage between one and two volts. The voltage increase was temporary and followed the same pattern as the one observed and described earlier for new cathodes. It likely reflected an increase in the cathode fall voltage while the operating temperature and surface characteristics of the newly exposed cathode material were being adjusted to facilitate electron emission.

An interesting observation from Figure 11 pertains to the fact that a similar molten sphere was not formed on the tip of cathodes operated

FIGURE 11

PHOTOGRAPHIC EVIDENCE OF SPHERE FORMATION ON POINTED-TIP CATHODES OPERATING IN ARGON

Photograph 11-a: Tip (1) - Operated in Argon for 40 min.

Tip (2) - Operated in Argon for 60 min.

Tip (3) - Operated in Helium for 60 min.

Photograph 11-b : Molten Tungsten Sphere Released from Tip

(a)

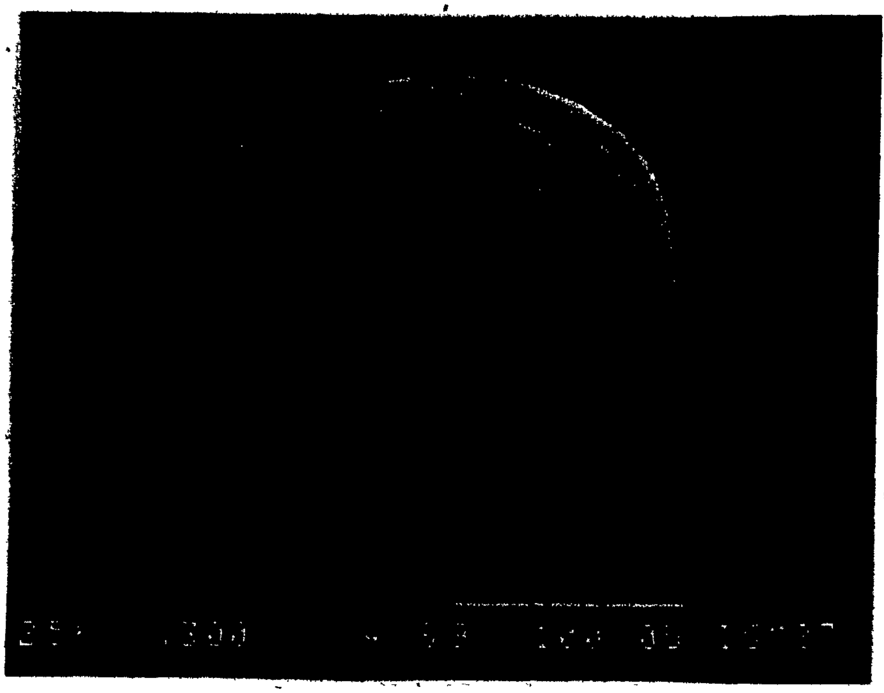

(b)

in helium. This may be due to differences in the heat transfer phenomena occurring on the respective cathode surfaces. In helium arcs the temperature near the cathode was likely higher resulting in a rapid vapourization of cathode material. This high rate of vapourization removed as latent heat much of the energy received by the cathode. The constant removal of energy, combined with the low thermal conductivity that typically characterizes sintered materials (such as the thoriated tungsten rods used for cathodes) and highly porous surfaces (such as those shown in Figure 7), may have prevented the formation of a molten layer. Argon arcs, on the other hand, heated the cathode more gradually, resulting in lower levels of vapourization and allowing for the formation of a relatively large molten region. A similar phenomenon, namely a reduction of the molten layer due to excessive increases in the temperature of the heating medium, has been observed in other low thermal conductivity materials (Mucciardi, 1987).

The surface of the sphere was covered with molten tungsten particles very similar in appearance with the particles identified within the central region of cathodes operated in helium. Magnified photographs of the sphere's surface are shown in Figure 12. Once again the particles were separated from each other, suggesting that they were formed through recondensation of vapourized tungsten. However, unlike the helium operated cathodes, the base on which these particles were attached was rounded in a rather uneven fashion (see photograph 12-a). These surface protrusions were probably caused by uneven melting within

FIGURE 12

SURFACE CHARACTERISTICS OF MOLTEN SPHERE ON POINTED-TIP CATHODES OPERATED IN ARGON

Photograph 12-a: Surface of Molten Sphere.

Photograph 12-b: Molten Tungsten Particles on Surface of Sphere

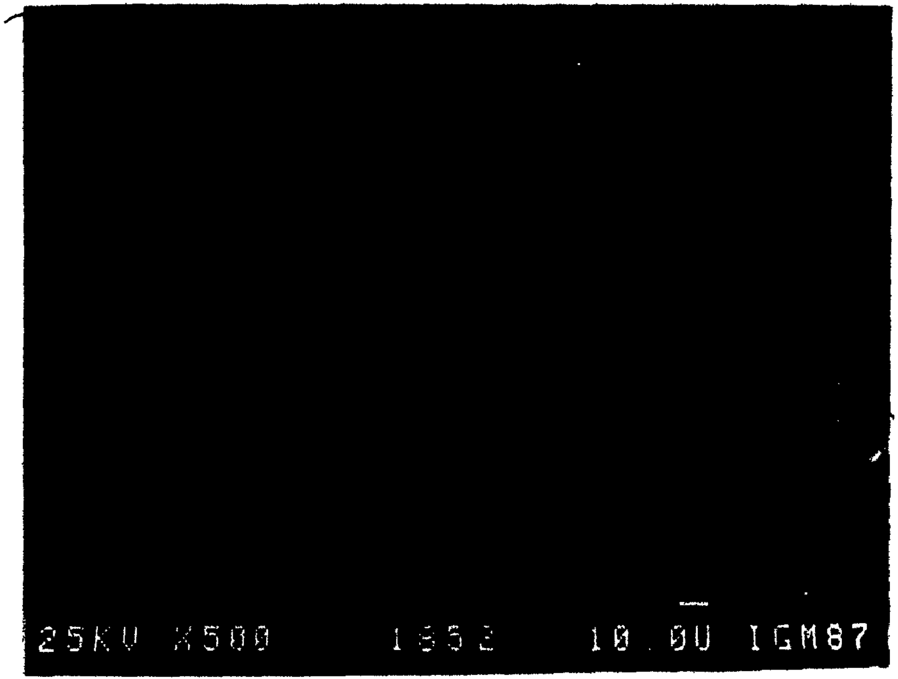

(a)

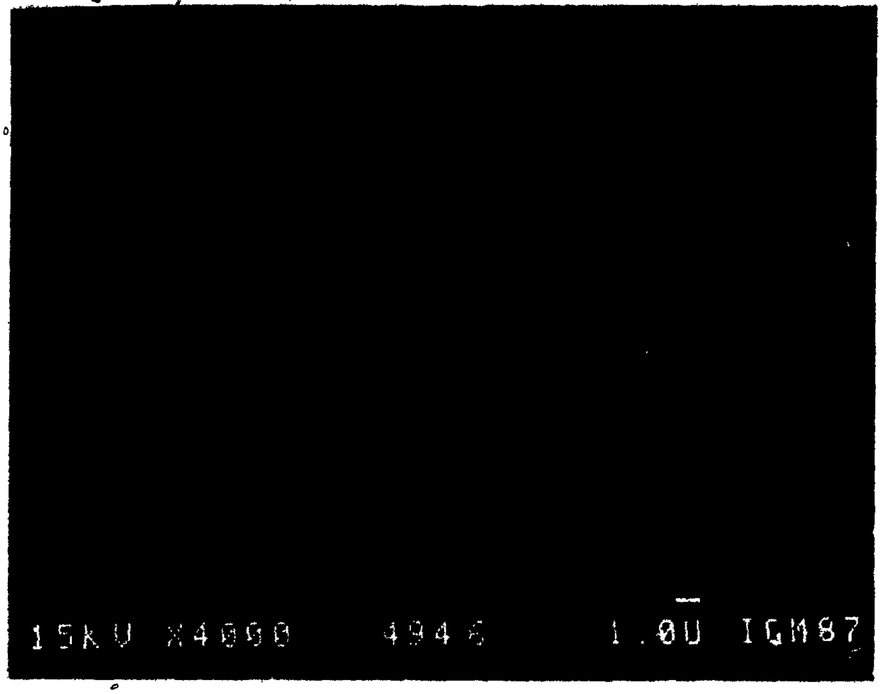

(b)

the sphere.

Upstream of the sphere, on the non-molten portion of the cathode the concentric rings appeared. In argon the rings were not as easily identifiable as they were in helium-operated cathodes and the crystals on them were significantly smaller. However, their compositions were exactly the same in both cases as was the evidence that they have been formed through redeposition. A photograph of the two rings is shown in Figure 13. The rectangular tungsten crystals, whose magnified photograph is also shown in Figure 13, were between 2 and 10 micron in length and were deposited on what appears to be a partially molten surface. In fact, as can be seen in photograph 13-a, the cathode surface appeared molten even beyond the area where the majority of the tungsten crystals were attached. Still further away from the cathode tip, in the extreme right of photograph 13-a, the thoria-rich ring appeared.

Worth noting is the fact that the distance between the center of the cathode tip and the beginning of the tungsten-crystals ring was about 0.5 mm, roughly half the equivalent distance measured on the helium operated cathodes. This may reflect differences in the cathode surface temperature gradients that characterized the two arcs. Since the location of the tungsten crystals likely indicates an operating temperature around the melting point of tungsten (3 680 K) it may be assumed that the area exposed to temperatures higher than this was about

FIGURE 13

CRYSTALS FORMED ON SURFACE OF POINTED-TIP CATHODES OPERATING IN ARGON

Photograph 13-a: Rings of Tungsten and Thoria Crystals

Photograph 13-b: Tungsten Crystals

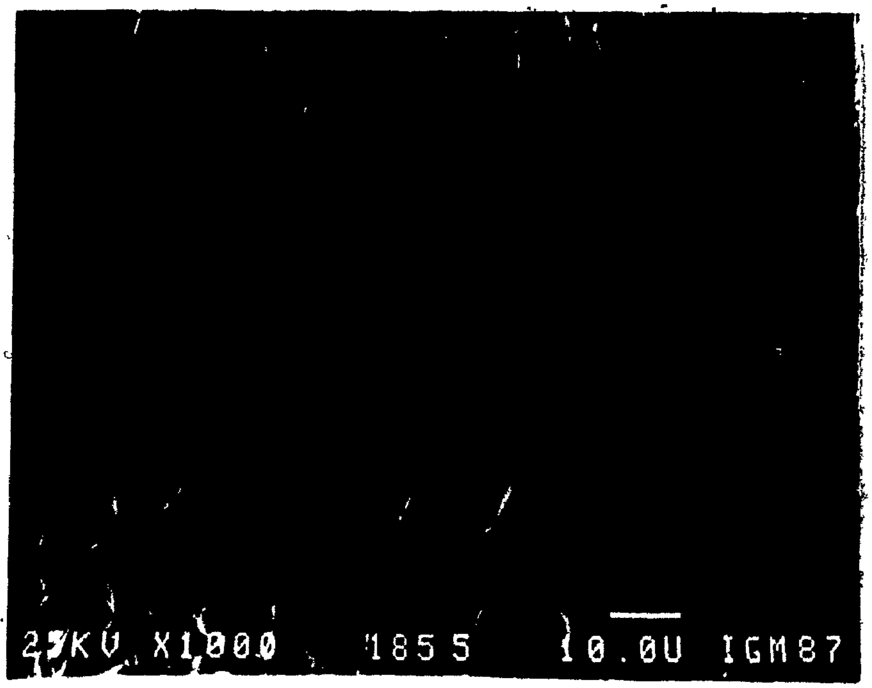

(a)

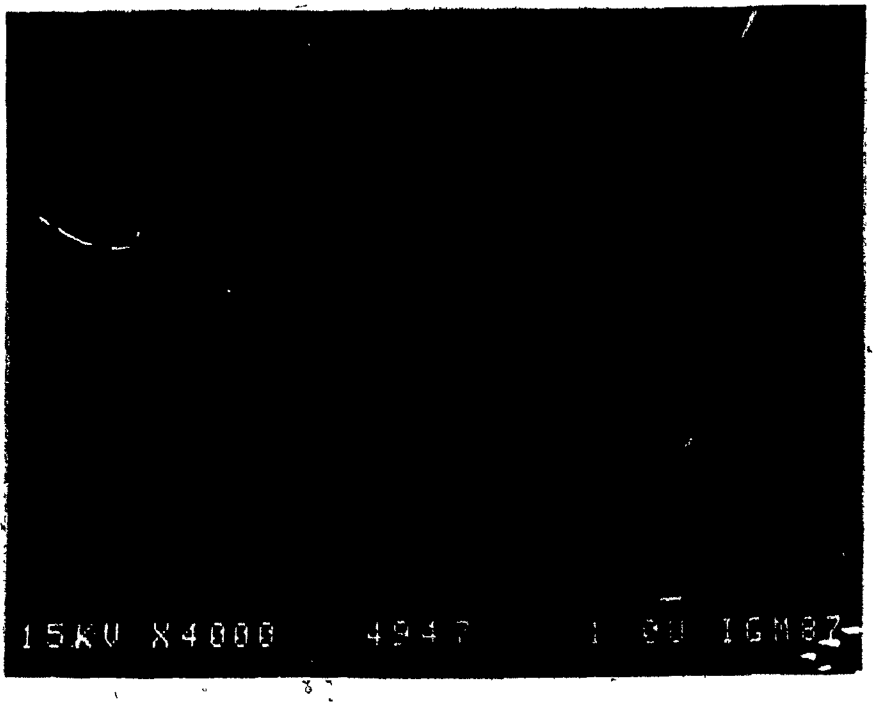

(b)

four times bigger in helium than in argon.

Cathode Erosion Characteristics

A total of 109 experiments were conducted in order to assess the erosion rates of thoriated tungsten cathodes operating in inert plasmagas atmospheres. The experiments were divided into four sets (two tip geometries, each operated in two plasmagases) on an approximately equal basis. Each set was further divided into five subgroups according to the duration of each experiment. All experimental data are shown in Table I.

As can be seen from Table I, the experimental data showed wide variations even for apparently identical operating conditions. As such, a statistical analysis was performed in an effort to identify any significant difference between the erosion rates measured for each set of operating conditions. The results of the statistical analysis are shown in Table II. For the statistical analysis the sample mean $\underline{Y}$ and standard deviation $\underline{s}$ were calculated separately for each subgroup. For the purpose of calculating the population mean $\underline{\mu}$ a 90 percent confidence interval was used along with a two pooled standard deviations $\underline{s_p}$. The first pooled standard deviation was calculated from the sample deviations of all experiments whose duration was less or equal to 10 minutes. Its value was 4.0 μg/min. The second pooled standard

TABLE I. EXPERIMENTAL DATA ON CATHODE EROSION

RUN DURATION (min)	EROSION RATE, (μg/min)			
	SET 1 (Ar-Flat)	SET 2 (Ar-Pointed)	SET 3 (He-Flat)	SET 4 (He-Pointed)
5	14, 8, 4, 0, 10, 2	16, 6, 4, 2, 12, 4	2, 4, 8, 2, 2	10, 0, 6, 2, 4, 12, 4
10	2, 7, 4, 10, 10, 8, 12, 6	4, 10, 11, 8	5, 7, 3, 3, 4, 10	7, 5, 2, 13, 3
20	7, 7, 3, 6, 8	5, 14, 8, 6, 3	2, 4, 6, 2	5, 6, 2, 2, 3
40	5, 5, 6, 1, 3	38, 2, 30, 62, 42	4, 1, 4, 7, 5	2, 3, 5, 2, 6
60	3, 8, 1, 2, 2, 4	54, 40, 36, 42, 23	2, 5, 1, 2, 1, 3	1, 3, 2, 1, 3, 5

*For all experiments: Arc Current = 200 A, Plasmagas Flowrate = 15 L/min and Arc Length = 2.5 cm.

TABLE II. STATISTICAL ANALYSIS OF CATHODE EROSION DATA

RUN DURATION (min)	EROSION RATE, (μg/min)			
	SET 1 (Ar-Flat)	SET 2 (Ar-Pointed)	SET 3 (He-Flat)	SET 4 (He-Pointed)
5	$Y = 6.3$ $n = 6$ $s = 5.3$ $3.6 < \mu < 9.0$	$Y = 7.3$ $n = 6$ $s = 5.5$ $4.6 < \mu < 9.0$	$Y = 3.6$ $n = 5$ $s = 2.6$ $0.6 < \mu < 6.6$	$Y = 5.4$ $n = 7$ $s = 4.1$ $2.9 < \mu < 7.9$
10	$Y = 7.4$ $n = 8$ $s = 3.3$ $5.0 < \mu < 9.8$	$Y = 8.3$ $n = 4$ $s = 3.1$ $4.9 < \mu < 11.7$	$Y = 5.3$ $n = 6$ $s = 2.7$ $2.6 < \mu < 8.0$	$Y = 6.0$ $n = 5$ $s = 4.4$ $3.0 < \mu < 9.0$
20	$Y = 6.2$ $n = 5$ $s = 1.9$ $4.8 < \mu < 7.6$	$Y = 7.2$ $n = 5$ $s = 4.2$ $3.2 < \mu < 11.2$	$Y = 3.5$ $n = 4$ $s = 1.9$ $1.9 < \mu < 5.1$	$Y = 3.6$ $n = 5$ $s = 1.8$ $2.2 < \mu < 5.0$
40	$Y = 4.0$ $n = 5$ $s = 2.0$ $2.6 < \mu < 5.4$	$Y = 35$ $n = 5$ $s = 22$ $14 < \mu < 56$	$Y = 4.2$ $n = 5$ $s = 2.2$ $2.8 < \mu < 5.6$	$Y = 3.6$ $n = 5$ $s = 1.8$ $2.2 < \mu < 5.0$
60	$Y = 3.3$ $n = 6$ $s = 2.5$ $2.0 < \mu < 4.6$	$Y = 39$ $n = 5$ $s = 11$ $28 < \mu < 50$	$Y = 2.3$ $n = 6$ $s = 1.5$ $1.0 < \mu < 3.6$	$Y = 2.5$ $n = 6$ $s = 1.5$ $1.2 < \mu < 3.8$

deviation was calculated from all experiments whose duration was 20 minutes or more excluding experiments in set 2. Its value was 1.9 μg/min.

The separation of the data in the above manner was necessary in order to account for the relative influence of the systematic error in the measurements. The balance used to measure mass loss from the cathode produced a systematic error of about 0.02 mg. The absolute value of this error remained the same for all experiments. However, its relative influence on the standard deviation was obviously higher in short duration runs.

The erosion rates of relatively long runs within set 2 (Ar-Pointed) were influenced greatly by the release of the molten tungsten sphere from the tip. The release of this sphere, which was described in detail in the previous section, had such an overwhelming effect on the erosion rate that each subgroup within this set had to be considered separately. By assuming that the erosion caused by vapourization was roughly equal for both flat and pointed-tip cathodes operating in argon, an assumption substantiated rather well by erosion rate data for shorter runs, the weight of the released sphere was calculated. The weight of the released tungsten sphere varied between 1 and 3 mg with an average value of 1.9 mg. Thus, for pointed-tip cathodes operated in argon, the erosion caused by vapourization during the first hour of operation was at least an order of magnitude smaller than the erosion caused by melting.

When the data from set 2 are excluded, the results of the statistical analysis suggest that there is no significant difference (based on a 90 % confidence interval) in the cathode erosion rates occurring under the various operating conditions used in this study. It appears that although the helium operated cathodes are exposed to higher temperatures and therefore higher rates of vapourization, the rate of redeposition compensates enough to maintain a low erosion rate. The effect of this cathode material recycling mechanism on the erosion rates of very long duration arcs was not investigated.

The erosion rates measured for short duration arcs (less than 10 minutes) was somewhat higher than the rates exhibited by longer duration arcs. This may suggest that relatively rapid erosion was occurring during the early stages of arc operation. It may also reflect mass loss due to attrition during the processes of installing and removing the cathode tip from the cathode assembly. In any case, the difference in erosion rates are rather small.

CONCLUSIONS

By examining the composition and characteristics on the surface of flat or pointed-tip cathodes operated in either argon or helium and by measuring the weight of cathode tip before and after an experiment, phenomena occurring on the cathodes of transferred-arc systems were investigated. The following conclusions resulted from the study:

1. Whenever a new cathode tip was used, during the first 10 minutes of operation the cathode fall voltage gradually reduced by approximately 3 volts as the temperature and morphology of the cathode's surface were changing to facilitate electron emission.

2. On flat-tip cathodes operated in argon these changes involved the mobilization of thoria which by moving through the tungsten grain boundaries concentrated on the surface where it agglomerated into small distinct regions. Concurrently, the cathode spot temperature rose above the melting point of tungsten forming a molten metal pool in the center of the tip. Within the molten pool, the thoria combined to form a large thoria-rich spot (over 80 % thoria) whereas outside the pool the thoria agglomerates remained segregated forming a thoria-tungsten mosaic. In longer duration arcs, the thoria was consumed from the surface, resulting in further increases in the surface temperature and significant tungsten melting. The molten tungsten formed small sponges on the cathode surface. The sponges increased in size until they broke away from the cathode exposing new cathode material to the arc, rich in thoria, where the thoria concentration-tungsten melting cycle was repeated.

3. On either flat or pointed-tips operated in helium the cathode surface temperature was much higher than that observed on flat tip cathodes operated in argon, probably near the boiling point of tungsten, resulting in extensive vapourization from the surface. Once in the arc, some of the cathode material became ionized and returned to the cathode surface possibly carrying with it some neutral atoms and molecules. On the surface the returning particles condensed forming a central region consisting of partially molten tungsten particles, a surrounding ring of tungsten crystals and an outside wider ring of smaller thoria crystals.

4. Pointed-tip cathodes operated in argon were characterized by the formation and subsequent release of a molten tungsten sphere at the point of the tip. Outside the sphere formation, the surface of these cathodes contained all of the characteristics identified on helium operated cathodes including the presence of the three concentric regions formed from the apparent redeposition of vapourized thoria and tungsten on the surface.

5. During the first hour of operation, the erosion rates of flat-tip cathodes operated in either argon or helium and of pointed-tip cathodes operated in helium were approximately equal. Pointed-tip cathodes operated in argon exhibited significantly higher erosion rates due to the release of the molten tungsten sphere.

REFERENCES

Anderson, J., W. E. Danforth, and A. J. Williams III, "Work Function and Thermal Desorption in the System Thorium-on-Rhenium", Journal of Applied Physics, Vol. 34, No. 8, p. 2260 (Aug. 1963).

An'shakov, A. S., G-N. B. Dandavon, M. F. Zhukov, and M. I. Sazanov, "Study of Tungsten Cathode Erosion in Nitrogen", Proc. Sixth International Confrence on Phenomena in Ionized Gases, Oxford, p. 103-4 (1971).

Augis, J. A., F. J. Gibson, and E. W. Gray, "Plasma and Electrode Interactions in Short Gap Discharges in Air", Int. J. Electronics, Vol. 30, No. 4, pp. 31532 (1971).

Belkin, G. S., "Dependence of Electrode Erosion on Heat Flux and Duration of Current Flow", Soviet Physics-Technical Physics, Vol. 15, No. 7 (Jan. 1971).

Benjamin, M., and R. O. Jenkins, "The Distribution of Autelectronic Emission from Single Crystal Metal Points. I. Tungsten, Molybdenum, Nickel in the Clean State", Proc. Roy. Soc. (A), Vol. 176, pp. 262-79 (1940).

Brattain, W. H., and J. A. Becker, Phys. Rev., Vol. 43, p. 428 (1933).

Chiang, K. T., and J. J. Maley, "Operating Mechanism of the One-Piece Cathode", RCA Review, Vol. 45, pp. 379-96 (Sept. 1984).

Dyubua, B. C., O. K. Kultashev, and L. V. Gorshkova, "Work Function of Solid Solutions of Tungsten with Molybdenum and Tantalum", Soviet Physics-Solid State, Vol. 8, No. 4, pp. 882-5 (Oct. 1966).

Dyubua, B. C., A. I. Pekarev, B. N. Popov, and M. A. Tylkina, Radiotekhnika i electronika, Vol. 7, p. 1566 (1962).

Finkelnburg, W., and H. Maeker, "Electric Arcs and Thermal Plasma", Handbuch der Physik, Vol. 22, pp. 254-444, Springer-Verlag, Berlin (1956).

George, A. P., "The Effect of Cathode Surface Temperature on Erosion Rate in a Schoenhen Type Arc Heater Operated on Oxygen", ISPC-7, paper P-4-3 (July 1985).

Gordon, W. A., and G. B. Chapman II, "Determination of Work Function Near Melting Points of Refractory Metals by Using a Direct-Current Arc", NASA TN D-6888 (Aug. 1972).

Gray, E. W., "On the Electrode Damage and Current Densities of Carbon Arcs", IEEE Trans. on Plasma Science, Vol. PS-6, No. 4, pp. 384-93 (Dec. 1978).

Gray, E. W., and J. A. Augis, "The Effects of Nanosecond Atmospheric Arcs on Various Metallic Surfaces", Inter. J. Electronics, Vol. 30, No. 6, pp. 533-41 (1971).

Gray, E. W., and J. R. Pharney, "Electrode Erosion by Particle Ejection in Low Current Arcs", J. Applied Physics, Vol. 45, No. 2, pp. 667-71 (Feb. 1974).

Guile, A. E., "Arc-Electrode Phenomena", Proc. IEE, IEE Reviews, Vol. 118, No. 9R, pp. 1131-55 (Sept. 1971).

Guile, A. E., and A. H. Hitchcock, "Oxide Films on Arc Cathodes and Their Emission and Erosion", J. Physics D : Appl. Phys., VOl. 8, pp. 663-9 (1975).

Guile, A. E., and B. Juttner, "Basic Erosion Processes of Oxidized and Clean Metal Cathodes by Electric Arcs", IEEE Trans. on Plasma Science, Vol. PS-8, No. 3, pp. 259-69 (Sept. 1980).

Hardy, T. L., and S. Nakanishi, "Cathode Degradation and Erosion in High Pressure Arc Discharges", NASA Technical Memorandum 83638 (1984).

Hichcock, A. H., and A. E. Guile, "Effect of Copper Oxide Thickness on the Number and Size of Arc-Cathode Emitting Sites", IEE Proc., Vol. 124, p.488 (1977).

Holm, R., "The Vaporization of the Cathode in the Electric Arc", J. Applied Physics, Vol. 20, p. 715 (July 1949).

Loeb, L. B., "Fundamental Processes of Electrical Discharge in Gases", John Wiley and Sons, Inc. (1939).

Matskevich, T. L., "Thermionic Emission Properties of Metal Alloys (Survey)", Soviet Physics-Technical Physics, Vol. 13, No. 3, pp. 295-307 (Sept. 1968).

Mucciardi, F., Assoc. Prof., Physical Metallurgy, McGill University, Private Communication (1987).

Muller, E., Z. Phys., Vol. 108, p.668 (1938).

Murphy, E. L., and R. H. Good Jr., "Thermionic Emission, Field Emission and the Transition Region", Physical Review, Vol. 102, No. 6, pp. 1464-73 (1956).

Neurath, P.W., and T. W. Gibbs, "Arc Cathode Emission Mechanisms at High Currents and Pressures", J. Applied Physics, Vol. 34, No. 2, pp. 277-83 (1963).

Shishkin, B. B., and R. S. Bakhtiyarov, "Electron-Microscope and X-Ray Study of Thermionic Emitters Made from Mo-Pt Alloys", Sov. Phys.-Techn. Phys., Vol. 19, No. 2, pp. 243-50 (Aug. 1974).

Szente, R. N., R. J. Munz, and M. G. Drouet, "The Effect of Low Concentration of a Polyatomic Gas in Argon on Erosion on Copper Cathodes in a Magnetically Rotated Arc", Plasma Chemistry and Plasma Processing, Vol. 7, No. 3, pp. 349-64 (1987).

Taylor, J. B., and I. Langmuir, Physical Review, Vol. 44, p. 423 (1933).

Williams, W. M., Birks Prof. of Metallurgy, McGill University, Private Communication (1987).

PART III

AN ASSESSMENT OF THE POTENTIAL OF RECOVERING TITANIUM METAL IN THE MOLTEN ANODE OF A TRANSFERRED TITANIUM TETRACHLORIDE ARC

ABSTRACT

An investigation was conducted into the possibility of producing titanium metal by dissociating titanium tetrachloride molecules in a transferred-arc reactor and collecting the titanium atom in a molten metal bath before it could recombine with the chlorine. The main plasmagen gas consisted of either pure argon or equi-molar mixtures of argon and hydrogen. Titanium tetrachloride vapour was introduced into the plasmagen gas, upstream of the plasma-forming region of the reactor, at a rate of 6 g/min. The mass and composition of the metal forming the molten bath, which also served as the anode of the transferred-arc system, was assessed before and after each run. The net gain of titanium metal was calculated and used to assess the technical feasibility of the process.

Three molten metal bath compositions were used in this study. In the first two, the molten bath at the beginning of the experiment consisted of titanium and zirconium, respectively. Using these initial compositions, the feasibility of producing titanium metal through the plasma dissociation of $TiCl_4$ and the subsequent diffusion of the free titanium atoms into the molten bath, was investigated. The third molten bath used in this study consisted initially of aluminum. Thus, the feasibility of employing a reducing agent in the high-temperature thermal reduction of $TiCl_4$ for the production of titanium metal was assessed.

Results from this study show that it is not possible to produce titanium metal through the simple dissociation of the tetrachloride molecule and the collection of titanium atoms in a molten titanium or zirconium bath. Although about 25 % of the titanium fed to the arc was collected in the molten bath, significantly more metal was removed from the bath through the formation of subchloride vapours. The observed losses of titanium metal from the molten bath were not attributable to vapourization of this metal. No chlorides were detected in the molten bath after the runs. The presence of hydrogen did not significantly affect the collection of titanium in the molten bath.

On the other hand, experimental results indicated that titanium metal or titanium aluminum alloys can be produced through the reduction of titanium tetrachloride in the presence of aluminum in a transferred-arc reactor using a molten bath consisting initially of pure aluminum metal. About 60 percent of all titanium fed into the reactor was recovered in the product. Just over three moles of aluminum were removed from the bath for each mole of titanium collected. No chlorine contamination of the product was observed when the temperature of the bath was maintained above the boiling point of $TiCl_2$. A thermodynamic analysis of the reduction process was also performed. However, it is not possible, using the existing apparatus, to determine how close the experimental results were to theoretical yields.

BACKGROUND INFORMATION

It has been shown (Akashi et al., 1977) that titanium tetrachloride can be dissociated completely into titanium atoms, titanium ions, chlorine atoms and chlorine ions when it is heated to temperatures higher than 5 000 K. Since transferred arcs operate at temperatures higher than 10 000 K, it can be assumed that any tetrachloride molecules entering the hot region of the arc will be completely dissociated. Accordingly, metallic titanium may be obtained by the prevention of back reactions causing the recombination of titanium atoms or ions with chlorine atoms or ions. These back reactions can be suppressed, to some extent, by rapid cooling or quenching of the high-temperature reaction products. However, perfect suppression of the back reactions may be impossible. Furthermore, some of the molten metal in the collection bath can react with chlorine, or vapourize, resulting in further product losses. Clearly, the ability to produce titanium metal through the thermal dissociation of its tetrachloride depends on reduction processes occurring within the reactor and on the phenomena occurring on the surface of the collecting target which in this study is the anode.

THE PRODUCTION OF TITANIUM THROUGH THE PLASMA REDUCTION OF ITS TETRACHLORIDE

Pioneering attempts to reduce a metal tetrahalide through thermal dissociation in a plasma reactor were made by DiPietro et al. (1950) at the National Research Corporation (NRC). The work involved the decomposition of ZrI_4 in a transferred-arc struck between a zirconium ingot and a hollow electrode through which the iodide vapour entered. As the iodide decomposed the zirconium remained in the molten pool formed in the ingot, while the iodine and undecomposed iodide were removed from the reactor. The metal was simultaneously produced and consolidated, using the same heat source, thus, substantially reducing both operating costs and contamination of the product. Representative operating conditions were: arc voltage: 22-30 volts, arc current: 700 - 1 000 amperes, and reactor pressure of about 250 torrs. The ZrI_4 feed rate was in the range of 0.45 - 1.8 kilogram per hour and the highest conversion rate accomplished was 97.7 %. Unfortunately, there was an inverse relation between the production rate of Zr metal and conversion. The maximum Zr production was 255 g/h corresponding to a conversion of only 16.4 %. The maximum conversion of 97.7 % corresponded to a production rate of only 41.2 g/h. The zirconium metal was produced with power expenditure of about 65 kWh per kilogram of zirconium.

The initial work at the NRC dealt with the thermal dissociation of zirconium tetrachloride. However, it was established that for the $ZrCl_4$ runs, zirconium was not deposited but, in fact, was removed from the starting ingot. It was suspected that this was the result of poor dissociation of the $ZrCl_4$ molecule and unfavorable thermodynamics in the metal deposition phase. Free energy change (ΔF) data as a function of temperature for various zirconium tetrahalides are shown in Figure 1. These data demonstrate that ZrI_4 is much less stable than $ZrCl_4$ and can, thus, be dissociated more easily. For this reason, emphasis was shifted from $ZrCl_4$ to ZrI_4.

DiPietro's work at NRC was followed by two other studies: Ingraham et al. (1957) and Newham and Watts (1960). Both research groups reported some success in reducing metal tetrachlorides with hydrogen in low pressure arcs. Ingraham's group produced finely-powdered $TiCl_3$ while Newman's group focussed their efforts on the production of $ZrCl_3$. Neither group produced any metal and the production rates in both cases were extremely low.

Miller and Ayen (1969) studied the reduction of $TiCl_4$ in a radio-frequency torch. It was shown that $TiCl_3$ can be produced with good yields (64 % to 87 %) when hydrogen is introduced as a reducing agent. In the absence of hydrogen, no appreciable reduction of $TiCl_4$ could be obtained with the quenching method employed. Power input and $TiCl_4$ feed rate appear to have had little effect on the percent conversion. The maximum $TiCl_4$ concentration in the argon plasma gas was less than 1 mole %. Higher $TiCl_4$ concentrations could not produce stable operating conditions in the r.f. torch. No titanium metal was obtained in this study.

FIGURE 1

FREE ENERGY CHANGE FOR THE DISSOCIATION OF ZIRCONIUM TETRAHALIDES AS A FUNCTION OF TEMPERATURE

Source: DiPietro et al. (1950).

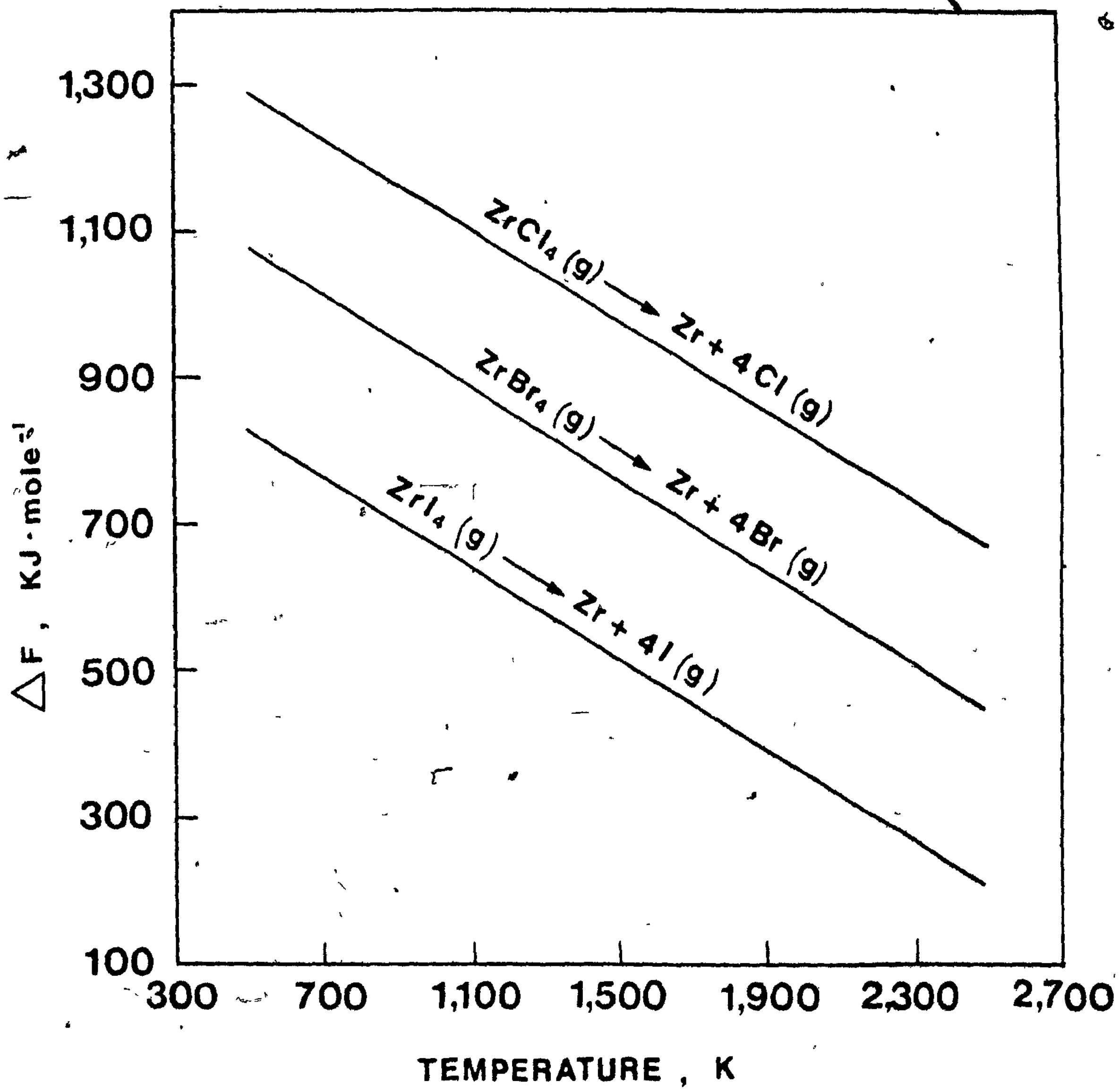

1,300
1,100
900
700
500
300
100
300
700
1,100
1,500
1,900
2,300
2,700
△F , KJ · mole⁻¹
TEMPERATURE , K
$ZrCl_4(g) \rightarrow Zr + 4Cl(g)$
$ZrBr_4(g) \rightarrow Zr + 4Br(g)$
$ZrI_4(g) \rightarrow Zr + 4I(g)$

Finally in 1969 a British patent was awarded to Ciba Ltd. (1969) for the production of niobium in a plasma reduction process. The patent claims that the production of niobium could be obtained in 93 % yield by passing its pentachloride in argon through a 24-kW hydrogen d.c. jet plasma. Finely-powdered niobium was produced at the rate of 32 g/min which was then heated first in hydrogen and then in vacuum. The process removed undecomposed niobium halides and yielded non-pyrophoric niobium with a surface area of 6.5 m^2/g. It was also reported that tantalum, molybdenum, tungsten, zirconium and hafnium could be obtained in the same way with yields of 96 %, 90 %, 94 %, 65 % and 70 %, respectively.

Most of the recent research on the plasma reduction of tetrachlorides has been carried out in Japan and Europe. Akashi et al. (1977), Ohno et al. (1979), and Kikukawa et al. (1983) provide the most relevant published information on the Japanese work. Papers by Atamanov et al. (1979) and Behnke et al. (1983) are examples of the relevant research done in Eastern Europe, while the patent awarded to Voest-Alpine (1985) provided an example of relevant Western European research.

The papers by Akashi et al. (1977) and Ohno et al. (1979) describes the formation of titanium micro-crystals from a mixture of titanium chloride and hydrogen introduced into the tail flame of an argon plasma jet. Titanium tetrachloride mixed with hydrogen was supplied laterally into the argon plasma jet through an alumina tube. A small tungsten or silica plate was put on a water-cooled copper mold just under the plasma jet in order to condense and collect the titanium vapour from the reaction products. X-ray diffraction analysis and scanning electron microanalysis showed that the condensate on the plate consisted of titanium microcrystals of various complex shapes. When a small amount of molten titanium was used instead of the tungsten or silica plate, its mass increased gradually during the run. Thus, it was concluded that the selective absorption of titanium vapor into the molten metal under a plasma tail flame is technically feasible.

Akashi's group claimed that the addition of hydrogen to titanium tetrachloride changes the high temperature equilibrium relations among the chemical species and thus prevents the back reactions causing the formation of titanium sub-chlorides upon the quenching. A non-transferred type d.c. jet plasma torch was used to generate the argon plasma jet. The flow rate of argon, the electrical current and the voltage between the terminals were 9 L/min, 60 A and 20-25 V, respectively. The titanium tetrachloride feed rate was 0.4-0.5 g/min while the hydrogen (which served both as the reducing and the carrier gas) flow rate was 0.5 L/min. When molten titanium metal (about 1 g) was used as the quenching target, the weight of the titanium metal increased about 10 % after about 20 minutes of operation. No precipitation of compounds such as titanium nitride or oxide were observed and the purity of the metal was estimated to be above 99 %.

Assuming the data reported for metal purity, weight gain and $TiCl_4$ feed rate are correct the product yield can be calculated at about 3-5 %. Considering the very low yield, feed rate and recovery it seems rather premature to draw any conclusions regarding the feasibility of the project. Furthermore, there is little information on the reasons why the $TiCl_4$ and hydrogen concentrations in the arc were kept so low or of the potential reactions that may have occurred between the tungsten collector and the dissociated $TiCl_4$ molecule. As shown in Part I of the present thesis, such reactions occur readily and may be responsible both for Akashi's results and limitations. The reported flow rates correspond to a plasmagen molar chloride concentration of only 0.6 percent. Much more useful results would be obtained at higher chloride concentrations and feed rates.

In their 1979 paper, Akashi et al. described a similar study aimed at the reduction of titanium and silicon tetrachloride in a plasma process. An interesting plasma generating device was used in this study. It combined an r.f. plasma torch with a d.c. torch in an effort to generate a stable and enlarged argon plasma. The chemical reactions resulting from the introduction of a mixture of vapourized $TiCl_4$ and H_2 or $SiCl_4$ and H_2 into the argon plasma were examined. The reaction products deposited on the inner reactor wall and a water-cooled copper column inserted in the reactor. They consisted of a very fine powder of mostly titanium sub-chlorides (85 % $TiCl_3$, 14 % $TiCl_2$, and 1 % TiN and TiO) or silicon. The $TiCl_4$ feed rate was in the range of 0.4 - 1.3

g/min. The most remarkable result of this study was the change that occurred as a function of the volume, shape and length of the argon plasma jet by the coupling of the r.f. and the d.c. torches. The expansion of the arc and consequent increase in its cross-sectional area could have significant effects on the arc's current density, temperature and degree of ionization. This may be a way of stabilizing a $TiCl_4$ arc while increasing its mass flow rate. Unfortunately, no such data were reported in the Akashi study.

Kikukawa et al. (1983) reported on the reduction of TiO_2 and $TiCl_4$ in a hydrogen d.c. plasma jet. Various reactant feeding methods and product collecting methods were examined. Reaction products were analyzed by X-ray diffraction, EPMA, and chemical methods. In the case of TiO_2, the highest reduced product was TiO, and Ti metal was not obtained. In the case of the reduction of $TiCl_4$ two collecting methods were used. Both methods employed a molten metal substrate in a graphite crucible. In the first method tantalum was used as the metal substrate whereas the second used titanium. Consequently, the product collected on the tantalum substrate was TiN as compared to Ti metal that was collected on the titanium substrate. The results reported by Kikukawa's group are not surprising. Tantalum melts at about 3 270 K which is too hot for any significant condensation of Ti metal (boiling temp. = 3 550 K). Titanium nitride (melting temp. = 3 200 K), probably formed through the reaction between the Ti vapour and trace N_2 existing in the plasma-gas, is the only compound in the reactor with high enough boiling temperature to condense on the tantalum substrate. There is no data provided in this paper on $TiCl_4$ feed rates or Ti yields.

Whereas most of the Japanese work on the reduction of metal halides has focussed on atmospheric pressure arcs, the Eastern Europeans have concentrated their efforts on vacuum plasmas. Two recent papers, Atamanov et al. (1979) and Behnke et al. (1983), offer examples of these research efforts. Atamanov's group described their experimental attempts to reduce titanium tetrahalide in the plasma of a steady electron beam-plasma discharge. The electron beam power varied from 200 W to 5 kW at a beam current of 1 A and a voltage of 6 kV. The pressure in the reactor chamber was between 10^{-3} and 10^{-2} torr. The maximum $TiCl_4$ feed rate was 0.2 mole/h (0.65 g/min). The products were collected on a watercooled plate held 20 cm in front of the gas injection nozzle. The reported theoretical collection rate for Ti metal was only 140 mg/h. If both this value and the $TiCl_4$ feed rate are correct, the yield was less than 1.5 %. This production rate is far too small to draw any conclusions regarding the feasibility of this approach. Furthermore, there is no clear indication in Atamanov's et al.'s paper that the theoretical collection rate was reached experimentally. However, this paper is of interest due to a pertinent discussion regarding the relation between collection efficiency and the temperature and geometry of the quenching target.

Behnke et al. (1983) measured the amount of atomic Ti generated during the flow of a gas mixture of argon and titanium tetrachloride through a stainless steel hollow cathode 4 cm long and 8 mm in diameter. The linear velocity of the gas was 1.3 cm/s, the pressure of argon was 270 Pa and the discharge current 20 mA. The $TiCl_4$ concentration in the feed gas varied between 0.3 % and 1.5 %. The aim of the study was to obtain information about the degree of dissociation of the $TiCl_4$ molecule in hollow cathode discharges. The most relevant result of this study was the strong relation between current and degree of dissociation in the plasma. However, caution should be taken in extrapolating from Behnke's results to atmospheric pressure arcs. At higher pressures, increased arc current results in an increase in arc diameter without significantly changing the arc temperature and hence the degree of dissociation and ionization.

In 1985, a European patent was awarded to Voest-Alpine on a plasma process designed to produce metal from the thermal reduction of titanium tetrachloride with hydrogen. According to the description of the process, $TiCl_4$ vapour and hydrogen are fed into the plasmagas of a transferred-arc reactor. Within the arc the $TiCl_4$ is reduced producing titanium metal and HCl. The metal is collected in the molten titanium anode and the HCl leaves the reactor in the off-gas. The temperature of the collection bath is maintained at 3 000 K. The process described in the Voest-Alpine patent is very similar to the one being evaluated in the present study and is therefore particularly relevant to this review. Unfortunately, little information has been provided to support the scientific basis of the patent. For example, in one of the studies described in the Voest-Alpine patent, the reaction temperature is given as 4 000 K. Under these conditions it is claimed that a mixture of 4.3 kg of $TiCl_4$ and 8.9 Nm^3 of hydrogen will produce 0.9 kg of titanium metal at an energy consumption of 56 kWh. These numbers represent a yield of about 83 percent, a rather remarkable accomplishment if one assumes that it represents metal recovered in the molten bath. However, there is neither any information on what these numbers represent nor any actual experimental data. Furthermore, it is not clear how the titanium metal (which is in its vapour phase at this temperature) would be collected. In fact, it is not at all obvious that this patent represents any real experimental accomplishments.

While many researchers have attempted to produce titanium metal through the plasma dissociation of the $TiCl_4$ molecule and the selective absorption of titanium atoms into a molten bath others have taken a different approach. Research efforts in the plasma reduction of $TiCl_4$ to Ti metal through the use of a reducing agent, such as sodium or magnesium, have been initiated recently. In these processes the reduction of $TiCl_4$ is not due to the plasma dissociation of the $TiCl_4$ molecule but rather due to the high temperature reaction:

$$TiCl_4 + 4Na \rightarrow Ti + 4NaCl$$

or

$$TiCl_4 + 2Mg \rightarrow Ti + 2MgCl_2$$

In this sense the process resembles the conventional $TiCl_4$ reduction processes (Hunter and Kroll) and the plasma functions mostly as a heat source.

A thorough investigation of the titanium or zirconium reduction process by an arc heater was recently carried out at the Westinghouse Research and Development Center (Down, 1982). Their work led to a U.S. Patent in 1978 (Westinghouse Electric Corp., 1978). It included a thermo-chemical analysis and an experimental investigation. The apparatus used consisted of a 40-kW d.c. plasma torch, an injection system immediately adjacent to the torch through which Na and $TiCl_4$ vapours were introduced, and a refractory reaction tube made of silicon carbide or graphite. The main plasma gas was a mixture of H_2 and Ar in a 2:1 or 4:1 ratio.

The products were collected on the refractory tube and were analyzed using Scanning Electron and Energy Dispersive X-ray Microscopy. The conclusions of the study were as follows:

1. Calculations indicated that a plasma process operating in the range 1 700 -2 200 K should produce titanium yield close to 100 % of theoretical with little or no production of subchlorides.

2. Experimental verification of such a process succesfully demonstrated that an effective separation of the co-product sodium chloride could

be achieved at these temperatures.

3. It was demonstrated that collection of the titanium product from such a process could be achieved either as a liquid for continuous casting or directly as a powder suitable for powder metallurgical applications.

4. Economic projections, made on a conservative basis, indicate that a continuous plasma process could operate competitively with existing Kroll or Hunter batch processes.

Although many problems remain unanswered by the Westinghouse project, especially ones relating to the materials of construction for the titanium collection zone, a further series of tests at the 40-kW laboratory scale is under consideration. Another series of tests utilizing an intermediate scale reactor (200-500 kW) is planned for the near future.

The Westinghouse process offers many advantages over the conventional titanium production processes. It is continuous, produces marketable metal products rather than sponge which is characteristic of conventional processing and reduces the tetrachloride, separates the by-products, namely NaCl, from the useful metal and consolidates the metal in a single processing step.

Years earlier, Gyula (1966) showed that it was possible to produce a master alloy of aluminum-titanium by the thermal reduction of titanium tetrachloride with aluminum. The process proposed by Gyula occurs at relatively low temperature and thus is capable of producing only TiAl and $TiAl_3$ alloys. There was little information provided by Gyula as to the chlorine contamination of the final products. However, considering that the process operated at about 1 070 K and that the vapourization temperature of $TiCl_3$ and $TiCl_2$ are somewhat higher (1 100 and 1 400 K respectively) extensive contamination may be expected. A few years later a Japanese patent was awarded (Egi, 1973) on essentially the same process. In the Japanese patent only the production of titanium subchlorides was described.

When one combines the results from the Westinghouse study with the results from the Gyula study an interesting possibility emerges. What would happen if a plasma process was used to reduce $TiCl_4$ directly with aluminum. Should this be possible, the advantages offered by such chemistry are obvious. The process would maintain the advantages mentioned earlier for the Westinghouse process but would also produce a valuable by-product ($AlCl_3$ powder is a catalyst in the production of various aromatic compounds) and would be less sensitive to contamination by the reducing compound. Not only the boiling points of the various aluminum chloride by-products are significantly lower than those of the respective magnesium and sodium chlorides (and thus less likely to remain in the molten anode bath) but also the potential presence of some aluminum in the final product would not be detrimental. In fact, since most of the titanium marketed today is alloyed with aluminum, exact control of the operating conditions may allow the direct production of valuable alloys. Finally, the cost of aluminum reducing agent would likely be lower than that of either magnesium or sodium. A simplified comparison of the respective cost of the various reducing agents is shown in Table I. The cost estimates in Table I were calculated by assuming that only fully chlorinated by-products (i.e. NaCl, $MgCl_2$, and $AlCl_3$) are produced in the reaction and that the amount of reducing agent used reflects only stoichiometric requirements. As such, these cost estimates do not reflect the real needs of the reduction process and Table I offers only a qualitative comparison of the costs associated with each of the potential reducing agents.

ANODE PHENOMENA

Both the National Research Corp. and the various Japanese studies used basically the same collection method. The collection of the metal (Zr or Ti) was attempted in a molten metal bath placed below the plasma jet. In this way, the molten bath was not part of the plasma and the collection efficiency was governed by diffusion and thermodynamic balances in the vicinity of the molten surface.

In the present study, the situation is quite different. The

TABLE I. ESTIMATED COST OF REDUCING AGENTS IN THE PRODUCTION OF TITANIUM

	SODIUM	MAGNESIUM	ALUMINUM
Titanium Metal Produced, kg,	1 000	1 000	1 000
$TiCl_4$ Reduced, kg,	3 961	3 961	3 961
Reducing Agent Required, kg,	1920	1 051	751
Unit Cost of Reducing Agent*, $ U.S./kg,	1.95	3.43	1.70
Cost of Reducing Agent, $ U.S.,	3 744	3 605	1 277

* Chemical Marketing Reporter, Nov. 9, 1987.

collection bath is one of the electrodes in the transferred-arc system, namely the anode. Thus, electrode phenomena become more important than in the above studies. This is especially true for the region of the anode where the arc attachment occurs. A general understanding of phenomena occurring in the anode region is therefore pertinent to this project.

The anode region of an arc is defined as that portion of the discharge path which is influenced by the presence of the anodic electrode. It includes the anode, the zone of the net negative space charge immediately in front of the anode (sheath or anode fall zone) and an intermediate zone bordering the arc column known as the contraction zone (or the diffuse attachment zone).

The specific problems associated with the anode region of steady state, high intensity arcs were first investigated by Maecker (1951) and later by Ecker (1961). More recently, anode phenomena have been studied extensively by E. Pfender's plasma research group at the University of Minnesota (Chou and Pfender, 1973; Dinulescu and Pfender, 1980).

Depending on the experimental conditions, two modes of arc attachment at the anode have been observed by Pfender's group. The two attachment modes have been described as a "diffuse" and a "constricted" attachment. Electrode induced macroscopic flows are responsible for the two modes. In the case of the diffuse attachment, a plasma jet originating at the cathode impinges on the anode, forming a stagnation region in front of the anode. In the constricted attachment mode, a plasma jet is formed in the vicinity of the anode surface in which the gas flow is directed away from the anode.

High pressures and chemical reactions on the anode surface as, for example, encountered in arcs operated in atmospheric air or in other oxidizing plasma gases seem to favor a constricted attachment mode. It has also been shown experimentally that high intensity arcs, such as those operating in hydrogen or nitrogen atmosphere, display a more severe constriction on metallic, cooled anodes than less intense arcs such as argon. Although no direct observations have been made in this study, it is believed that the high intensity-oxidizing atmosphere titanium tetrahalide arc studied would likely exhibit a constricted attachment mode at the anode. However, due to the relatively short arc lengths used, the impingement of the cathode jet on the anode surface may be strong enough to induce a diffuse attachment.

The formation of plasma jet(s) at the anode, that are associated with a constricted attachment, are the result of a magnetic pinch at the electrodes of high pressure arcs (Finkelnburg and Maecker, 1956). Due to the contraction of the arc, the current lines are curved in the vicinity of the electrode attachment (spot) and thus an axial component of the magnetic force $\vec{j} \times \vec{B}$ arises which pumps the plasma away from the electrode. The plasma which departs with the jet is replaced by radial inflow of cold gas from the electrode periphery which cools the arc fringes further, causing more severe constriction and pumping. The electrode region reaches equilibrium when the cooling from the inflowing gas is balanced by the outward flow of heat from the arc's hot core.

Anode evaporation is another mechanism which may lead to anode jet formation. Pfender and Eckert (1976) claim that even small traces of anode vapour may have an appreciable effect on the operation of the arc in the anode region due to the low ionization potential of metal vapours and their effect on the electrical conductivity of the plasma column. This mechanism of anode jet formation may be more significant in this study than in previous work. It appears that the vapourization of anode material is controlled by two factors: the heat flux to the anode and the rate of melting and heat diffusion into the anode. An argon arc, for example, attached to a molten copper anode produces only a small amount of copper vapour (Choi and Gauvin, 1982), whereas a nitrogen arc operated under similar conditions generates large amounts of copper vapour (Tsantrizos and Gauvin, 1982).

The heat flux to the anode of a nitrogen arc is about twice that of an argon arc under similar operating conditions. Thus, one may speculate that when the heat flux to a cold anode is sufficiently high, the surface temperature at the anode spot rises quickly beyond the boiling point, resulting in evaporation of anode material without producing a large molten pool. The heat flux to the anode of a 2-cm nitrogen arc operating at 200 A has been reported by Tsantrizos and Gauvin (1982) at about 6.0 kW increasing to about 6.5 kW when the arc length is extended to 2.5 cm. Comparing these numbers to the data reported in Part I (Table IV) it can be shown that the heat flux to the anode of $TiCl_4$-rich argon arcs is similar to that of nitrogen arcs, whereas the heat flux of arcs formed from an equimolar mixture of argon and hydrogen and rich in $TiCl_4$ is about 50 percent higher.

The second factor controlling the vapourization of anode material is the rate of melting and heat diffusion into the anode. Since copper has a significantly higher thermal conductivity than titanium, diffusion into a Ti anode should be slower, resulting in increased vapourization. Counteracting the effect of lower thermal conductivity is the fact that titanium vapourizes at higher temperatures than copper thus permitting high temperature gradients within the anode pool and therefore increased heat diffusion rates.

The exact causes and conditions resulting in the formation of the constricted anode attachment (anode spot formation) are not yet understood. It is known however, that under certain conditions, the anode attachment occurs by the formation of one or more anode spots, each associated with an anode jet, and that these spots may move over the anode surface, sometimes at appreciable velocities.

As mentioned earlier, the anode region consists of the anode and two distinct zones: the contraction or diffuse attachment zone and the anode fall zone. The contraction zone is by far the thickest of the two and contains plasma under quasi-neutral conditions ($n_e = n_i$). The anode fall zone on the other hand is thin (between 0.1 and 1 mm for high pressure-high current arcs) and not electrically neutral. It is this zone of transition, also known as the "anode boundary layer", between the hot plasma and the relatively cold anode that remains the stumbling block for a full understanding of anode phenomena.

The anode boundary layer is the thin layer of plasma covering the anode, in which the temperature decreases from a value of about 10 000 K in the adjacent arc column to the temperature at the anode surface (about 3 500 K for a molten titanium anode). Knowing that the electrical conductivity of an equilibrium plasma decreases to near zero at the temperature occurring at the anode surface, it would appear that an insulating gas layer exists just in front of the anode, making it difficult to understand how current continuity is maintained at the electrode. The apparent dilemma is explained by the fact that a state of non-equilibrium exists in the anode boundary layer in which the species temperatures differ and the gradients of temperature and concentration play an appreciable role in the transport of electric charge carriers. While the heavy species temperature decreases to a low value in front of the anode, the electron temperature remains high enough (about 9,000 K for argon arcs) to maintain the required electrical conductivity.

The concentration of electrons results in the formation of a negative electrical field (relative to its orientation in the arc column) near the anode surface. Furthermore, the concentration and temperature gradients within the anode boundary layer push the electrons towards the anode extending the negative electric field from the anode surface to the entire anode boundary layer. This negative electrical field orientation in the anode boundary layer could have significant influence in the results of this study. The positive ion current, which outside the anode boundary layer is oriented in the direction from the anode to the cathode, changes sign within the boundary layer, and in the immediate vicinity of the anode surface is oriented towards the anode. The ions fall on the anode and recombine with electrons. This two-way flow of ions requires that ions are generated within the boundary layer, (Dinulescu and Pfender, 1980). The ion generation takes place by ionizing collision between the energetic electrons and the neutral particles. In the case of a titanium tetrahalide transferred-arc system, the titanium has by far the lowest ionization potential of all the atoms in the arc (6.8 eV compared to 13.0, 13.6 and 15.8 eV for Cl, H and Ar respectively). One could therefore speculate that if the tetrahalide molecule is completely dissociated upon entering the anode boundary layer, the titanium atoms will be ionized more easily than the chlorine or main plasmagas atoms. The positive titanium ions generated in the anode boundary layer could then fall on the anode, recombine with electrons and be captured in the anode molten bath.

There are potentially two titanium collection areas on the anode of a titanium tetrachloride transferred-arc system. The first area is the anode spot where the arc attachment occurs. As discussed above, collection efficiency in this area is governed by the rate of vapourization of titanium metal (anode jet formation), and the rate of arrival of titanium ion on the anode surface (boundary layer ionization).

The second titanium collection area is the surface that surrounds the anode spot and lies outside the path of charge carrying electrons and ions. The collection of titanium in this area occurs in the manner observed by DiPietro et al. (1950) and Akashi et al. (1977), described earlier in this review. Its collection efficiency depends on the diffusion of titanium atoms to the anode surface, and the selective condensation of such atoms in the molten bath before they have a chance to recombine with the halide. Considering the relatively low temperatures (3 500 K) encountered in this region of the anode, the availability of free titanium atoms may be limited. In fact, if the gas sweeping the anode surface is assumed to be at thermodynamic equilibrium, the calculations by Miller and Ayen (1969) have shown that no free titanium atoms can be expected at these temperatures, irrelevant of the presence of hydrogen.

An important consideration in this study, however, is the fact that the chemical species formed near the anode surface and outside the hot region of the arc are not likely to be in thermodynamic equilibrium. The gas leaving the plasma consists primarily of totally dissociated atoms which, while traveling at high velocities, are exposed to a rapid quench. This rapid quench may prevent the species from ever reaching thermodynamic equilibrium and thus allow for the presence of fully dissociated titanium atoms at the surface of the anode.

Except in the case where a reducing molten bath is used, the presence of free titanium atoms near the anode surface is an obvious precondition to any potential collection of titanium metal. However, the presence of such atoms does not necessarily indicate the feasibility of the proposed collection mechanism. It is not known what fraction of the free titanium atoms diffuse to the anode surface and condense in the molten bath. Furthermore, the presence of free titanium atoms implies the presence, in perhaps much larger concentrations, of free chlorine atoms. The chlorine atoms would also be sweeping the anode surface, reacting with the titanium in the molten bath and removing the metal from the desired product. The degree to which the concentration of free chlorine atoms can be limited by the use of hydrogen in the plasmagas is unknown.

In summary, the yield of titanium metal from the dissociation of the $TiCl_4$ molecule in a transferred arc system and the subsequent collection of titanium atoms in a non-reducing molten bath anode depends on the sum of three parameters: (1) the rate of vapourization of titanium metal from the bath, (2) the rate of diffusion of free titanium atoms into the bath, and (3) the rate of diffusion of free chlorine atoms into the bath which remove titanium metal through the formation of subchlorides. The magnitude of each of these parameters varies according to a number of factors including the plasmagas composition and the distance of the collection region under consideration from the center of the anode spot.

The use of a reducing molten bath introduces even more complexity to the phenomena occurring on the anode surface. In this case all molecules exposed to the material in the anode bath can react to form a variety of compounds. For example, when aluminum is used in the bath, free titanium atoms can react to form TiAl or $TiAl_3$, free chlorine atoms can react to form aluminum chlorides and titanium subchlorides can react to form titanium and aluminum chlorides. Furthermore, since aluminum chlorides have low boiling temperatures, it may be assumed that they would volatilize as soon as they are formed causing the formation of a strong anode jet. Based on presently available information, a theoretical analysis of the reactions, and heat and mass transfer phenomena occuring in the molten bath is quite impossible. However, useful information can be attained through a thermodynamic analysis of the thermal reduction of $TiCl_4$ with aluminum at high temperatures. Therefore, such an analysis has been included in the discussion section of this Part.

EXPERIMENTAL

APPARATUS

The apparatus used in the experimental studies relevant to this Part were for the most part identical to those used and described in Part I. The only modification introduced in this section involved the replacement of the flat, water-cooled copper plate with a copper water-cooled anode cup, shown schematically in Figure 2. A solid metal disc, whose mass and composition reflected the desired initial conditions in the molten bath, was placed inside the anode cup before each experiment. Heat from the arc was used to melt the metal disc, resulting in the formation of the molten bath. The anode cup was 10 cm in diameter and 1.5 cm in height. The initial size of the metal disc placed in this anode cup was 6.4 cm in diameter and 1.0 cm in height.

In some of the experiments it was deemed desirable to reduce the molten bath's diameter and increase the bath's temperature. For these experiments a bottomless boron nitride crucible (also shown in Figure 2) 2.0 cm in height and 4.0 cm in diameter was placed at the center of the anode cup. The initial metal disc (2.6 cm in diameter and 1.0 cm in height) was then placed inside the boron nitride cylinder. Boron nitride was used because it is inert to the chemical compounds under consideration in this study. It is also an electrical insulator and thus resistant to arcing and has a very high melting point and thermal conductivity and is thus capable of handling the high heat load that characterize operations in plasma reactors. Finally it has lubricating properties that allow for the relatively easy removal of the final solidified product, when cooled.

EXPERIMENTAL PROCEDURE

The experimental procedure used in this section was the same as that described in Part I. The only significant difference involved the use of the molten anode bath. The solid metal disc used to form the initial molten bath was prepared and installed in the desired anode configuration. A Mettler AE163 balance with a range of 0 - 162 grams and a precision of 0.01 mg was used to determine the mass of the metal disc before and after each experiment. The composition of the final product was determined by an Energy Dispersive X-Ray technique using the same Scanning Electron Microscope described in Part II. Since this technique was only able to provide semi-quantitative concentrations of various atoms within a specific surface area, it was neccessary to cut the final product which formed the anode bath into many small pieces and analyze the surface composition of each piece separately. In this manner, characteristic concentrations at the various locations within the bath were assessed and integrated over the volume of the bath to provide an estimate of the average bath composition.

Once the metal disc had been installed within the anode cup, the reactor was sealed gas-tight and was purged for 15 minutes with argon. During this period, the plasmagas preheater, the $TiCl_4$ vapourizer and the plasmagas feed lines were heated to such temperatures as to be able to provide the reactor with the required plasmagas at about 150°C. Following this, the arc was ignited, adjusted to the desired operating conditions, and maintained for at least 5 minutes prior to the injection of $TiCl_4$ to assure the formation of a molten anode bath.

Two main plasmagas compositions, one consisting of pure argon and the other of an equimolar mixture of argon and hydrogen, were used in the experiments relevant to this Part. Titanium tetrachloride was fed for 5 minutes at a rate of 6 g/min (about 3 % molar concentration of $TiCl_4$ in the plasmagas) for each experiment.

DISCUSSION AND RESULTS

The results from this experimental study can be divided into two main categories: those in which a non-reducing molten bath was utilized and those in which aluminum was used in the initial bath. In the first case (non-reducing), the chemical properties of the molten bath are such that there was no titanium metal production through the reduction of titanium subchlorides within the bath. Initial metal discs consisting of either titanium or zirconium formed non-reducing baths. In the conductivity and is thus capable of handling the high heat load that characterize operations in plasma reactors. Finally it has lubricating properties that allow for the relatively easy removal of the final solidified product, when cooled.

EXPERIMENTAL PROCEDURE

The experimental procedure used in this section was the same as that described in Part I. The only significant difference involved the use of the molten anode bath. The solid metal disc used to form the initial molten bath was prepared and installed in the desired anode configuration. A Mettler AE163 balance with a range of 0 - 162 grams and a precision of 0.01 mg was used to determine the mass of the metal disc before and after each experiment. The composition of the final product was determined by an Energy Dispersive X-Ray technique using the same Scanning Electron Microscope described in Part II. Since this technique was only able to provide semi-quantitative concentrations of various atoms within a specific surface area, it was neccessary to cut the final product which formed the anode bath into many small pieces and analyze the surface composition of each piece separately. In this manner, characteristic concentrations at the various locations within the bath were assessed and integrated over the volume of the bath to provide an estimate of the average bath composition.

Once the metal disc had been installed within the anode cup, the reactor was sealed qas-tight and was purged for 15 minutes with argon. During this period, the plasmagas preheater, the $TiCl_4$ vapourizer and the plasmagas feed lines were heated to such temperatures as to be able to provide the reactor with the required plasmagas at about 150°C. Following this, the arc was ignited, adjusted to the desired operating conditions, and maintained for at least 5 minutes prior to the injection of $TiCl_4$ to assure the formation of a molten anode bath.

Two main plasmagas compositions, one consisting of pure argon and the other of an equimolar mixture of argon and hydrogen, were used in the experiments relevant to this Part. Titanium tetrachloride was fed for 5 minutes at a rate of 6 g/min (about 3 % molar concentration of $TiCl_4$ in the plasmagas) for each experiment.

DISCUSSION AND RESULTS

The results from this experimental study can be divided into two main categories: those in which a non-reducing molten bath was utilized and those in which aluminum was used in the initial bath. In the first case (non-reducing), the chemical properties of the molten bath are such that there was no titanium metal production through the reduction of titanium subchlorides within the bath. Initial metal discs consisting of either titanium or zirconium formed non-reducing baths. In the second case (reducing), the initial metal disc was aluminum resulting in the formation of a bath capable of reducing titanium subchlorides, and therefore of producing titanium metal, within it.

Non-Reducing Molten Bath Experiments

In the experiments which utilized a non-reducing molten anode bath, the following three general mechanisms of mass transfer could have potentially occurred within the bath:

1. physical or thermal losses (**V**), such as sputtering and vapourization, from the bath due to excessive energy input from the arc;

2. physical gains from the arc's constituents (**D**) and specifically the collection of free titanium atoms either through diffusion or through currents induced by the electric field in the vicinity of the anode (for more information see relevant discussion in background section of this Part); and

3. chemical losses (**R**) resulting from chlorination reactions occurring in the molten bath between the molten metal and either free chlorine atoms and molecules or poly-chlorinated titanium molecules (for example $TiCl_3$ may react with Ti to form $TiCl_2$ and TiCl resulting in the loss of Ti from the bath).

The fourth potential mechanism of mass transfer, which might have contributed to chemical gains of titanium atoms from the reduction of titanium chlorides within the bath, could not occur in baths with non-reducing chemical properties. As such, the net change of titanium mass contained in the bath (**ΔG**) can be expressed in the form of the following generalized mass balance equation:

$$\Delta G = V + D + R \tag{1}$$

Experiments were conducted to assess the relative contribution of each of these mass transfer mechanisms under the various operating conditions. A summary of these experiments is shown in Table II.

1. Physical or Thermal Losses (V)

To determine the losses from the bath that may have resulted from sputtering or vapourization, experiments were conducted in which the main plasmagas (without any $TiCl_4$ feed) was utilized and the operating conditions were such as to insure that the amount of energy transferred to the molten bath was roughly the same as the amount transferred during experiments which utilized a $TiCl_4$-rich plasmagas. Thus, the amounts of energy transferred to the molten bath anodes of runs 121, 123, 126 and 131 were roughly equal to those of runs 120, 122, 125 and 130 respectively, although the former group contained no $TiCl_4$ in the

TABLE II. SUMMARY OF RESULTS FROM EXPERIMENTS USING A NON-REDUCING BATH

RUN No.	GAS FLOW (L/min)	$TiCl_4$ FEED (g/min)	ARC LENGTH (cm)	ARC CURRENT (A)	ENERGY TO BATH (kW)	BATH INITIAL COMPOS.	BATH FINAL COMPOS.	DISC DIAM. (cm)	ΔW (g)	ΔG[2] (g)
121	Ar-30	0	2.0	250	4.3	Ti	Ti	6.4	+ 0.5	0.0
120	Ar-30	6	2.0	200	4.2	Ti	Ti	6.4	- 1.8	- 2.3
123	Ar-15, H_2-15	0	2.0	220	7.0	Ti	Ti	6.4	+ 0.6	0.0
122	Ar-15, H_2-15	6	2.0	200	7.2	Ti	Ti	6.4	- 2.2	- 2.8
126	Ar-15, H_2-15	0	2.5	220	8.6	Ti	Ti	6.4	+ 0.6	0.0
125	Ar-15, H_2-15	6	2.5	200	8.4	Ti	Ti	6.4	- 1.2	- 1.8
131	Ar-15	0	2.5	250	4.9	Zr	Zr	2.6	+ 0.3	0.0
130	Ar-15	6	2.5	200	4.6	Zr[3]	Zr-Ti(5%)	2.6	- 1.7	+ 1.8

1. **ΔW** refers to the change in the overall mass of the molten bath. Changes observed in the experiments with no $TiCl_4$ in the plasmagas are assumed to be caused by contamination of the plasma with oxygen and nitrogen.

2. **ΔG** refers to the calculated change in the mass of titanium contained in the bath and includes changes in the overall weight due to contamination (assumed egual to mass gains in inert-gas experiments).

3. The initial weight of the zirconium disc was 33.5 g.

plasmagas and operated at somewhat higher currents. Furthermore, it was assumed that the losses due to vapourization or sputtering would reflect only the amount of energy transferred to the bath and would not be influenced by the composition of the plasmagas.

Based on the results presented in Table II it can be seen that there were no losses due to vapourization or sputtering. In fact, experiments which utilized no $TiCl_4$ in the plasmagas exhibited a slight gain (about 0.5 g) in the mass of the molten bath. This gain was probably attributable to the formation of oxides and nitrides within the bath from contaminants present in the reactor and in the plasmagas. Furthermore, in experiments which utilized argon only (either with or without $TiCl_4$) as the plasmagas and the larger diameter molten bath, the melting of the initial metal disc was incomplete. Only the central region, with a radius of about 2.5 cm was fully melted. Thus, the term V in Equation (1) can be eliminated and the changes in the mass of titanium contained in the bath (ΔG) can be assumed equal to the sum of terms D and R.

ii. Physical Gains from the Arc's Constituents (D)

In order to determine the amount of titanium collected in the molten bath due to the condensation of free titanium atoms within it, experiments were conducted in which the initial bath composition was pure zirconium metal (Experiments No. 130 and 131). Zirconium and titanium have similar chemical and physical properties. Thus, it was assumed that the replacement of titanium with zirconium did not change significantly the ability of the bath to collect titanium. Furthermore, since the reactivity of zirconium to chlorine is roughly equal to that of titanium, and since the concentration of titanium in the bath was very low (< 7 %) throughout the entire duration of the experiment, it can be assumed that most of the free titanium atoms collected in the bath will remain there.

Based on the above reasoning, the amount of free titanium atoms collected in the bath can be estimated from a simple analysis of the final composition of the bath. In run No. 130, the initial mass of the bath was 33.52 grams consisting entirely of zirconium metal. At the end of the run, the mass of the bath was 31.85 grams. Energy Dispersive X-Ray analysis showed that the final product contained on average 5.84 % titanium, with the concentration of titanium varying between 4.61 and 6.62 % depending on the location of the analyzed region within the bath. No chlorine was identified anywhere in the bath. By assuming that 0.31 gram of the final product was attributable to oxygen and nitrogen contaminants (same as the amount measured in run No. 131) which are not detectable by the analytical technique used in this study, the amount of titanium contained in the final product can be calculated at approximately 1.84 gram. This amount of titanium represents roughly 25 percent of all the titanium atoms fed into the reactor in the form of titanium tetrachloride. It should be pointed out, however, that this technique for calculating the term **D** in Equation (1) contains many approximations and is thus capable of producing only order of magnitude results. Furthermore, no experiments were conducted to determine the effect of hydrogen on the collection efficiency of the molten bath. The effects of arc length, molten bath diameter and plasmagas flowrate were also not investigated.

iii. Chemical Losses (R)

Having estimated the value of free titanium deposited into the bath during an experiment at about 25 percent of the titanium fed into the reactor, and having measured the change in the overall mass of the titanium molten bath (**ΔG**), Equation (1) was used to calculate the amount of titanium lost from the bath due to chemical reactions between the metal and chlorine. In all of the experiments in this section, $TiCl_4$ was fed into the arc for 5 minutes at a rate of 6 g/min. In all, the equivalent of about 7.5 grams of titanium were fed into the arc, of which 25 % (about 1.9 g) were assumed to have been collected within the bath.

Subtracting 1.9 gram from the final mass of the molten bath, as well as the appropriate mass contributed by the contaminants, the chemical losses from the titanium bath can be calculated at 4.2, 4.7 and 3.7 grams for run No. 120, 122 and 125 respectively. In other words, more than twice as much titanium was lost from the bath due to chemical reactions as was collected in the bath from condensing titanium atoms. Furthermore, the influence of hydrogen on this ratio was rather small, if any, and was therefore negligible within the accuracy of these experiments.

Having concluded from these results that the above approach was not likely to produce a technically or economically feasible process for the production of titanium metal, attention was focused on the use of a reducing molten bath. It should be mentioned, however, that the results presented here had a relatively narrow scope. By changing the operating conditions, it may be possible to change the ratio between collection gains and chemical losses to the degree where an overall gain in the mass of the bath could occur. It may also be possible to change this ratio significantly by substituting a more readily dissociated halide, such as the iodide used in the National Research Corporation study (DiPietro et al., 1950), for the tetrachloride used in this study. It is doubtful, however, that any such changes would produce a process of commercial interest.

Reducing Molten Bath Experiments

When a non-reducing molten bath was used, thermodynamic considerations within the bath favored the production of titanium subchlorides resulting in the loss of metal from the bath. This situation can be altered by substituting the non-reducing bath with a reducing one. In the case of a reducing bath, free chlorine will preferentially react with the reducing agent, allowing for the accumulation of titanium in the bath. Furthermore, any titanium chloride that may come in contact with the bath may be reduced to produce more titanium metal. In this study, an aluminum bath was used to investigate these possibilities.

i. Thermodynamic Considerations

The equilibrium concentration of products derived from the thermal reduction of titanium tetrachloride with aluminum were identified using the F.A.C.T./EQUILIBRIUM program of the McGill University computer library. The program is designed to calculate equilibrium concentrations as a function of the reacting system's temperature and pressure by minimizing the system's free energy. It is capable of producing results for temperatures up to 6 000 K, and a variety of pressures. However, in the present study, only temperatures up to 3 000 K, at atmospheric pressures were considered.

A simplified overall reaction may be written in the following form:

$$n\mathrm{TiCl_4}\ (v) + m\mathrm{Al}\ (l) = k\mathrm{TiCl_x}\ (v) + m\mathrm{AlCl}_y(v) + (n-k)\mathrm{Ti}$$

The reaction temperature and the aluminum-to-$TiCl_4$ ratio (m/n) are crucial parameters in determining the equilibrium concentration of the products. At low temperatures most of the titanium produced is in the form of solid TiAl or $TiAl_3$. Sample results from the F.A.C.T. analysis at relatively low temperatures are provided in Table III. These results indicate that at these temperatures the formation of TiAl or $TiAl_3$ necessitates the use of large aluminum to $TiCl_4$ ratios in order to assure the complete reduction of the titanium chloride. For example, at 700 K and an m/n ratio of 3.0 over 1/3 of the titanium remains chlorinated as most of the aluminum is bonded to titanium in the form of $TiAl_3$. At the same m/n ratio but a reaction temperature of 1 200 K, the formation of TiAl is favored resulting in the release of aluminum and subsequently the almost complete reduction of all titanium chlorides.

As the temperature increases further, the TiAl disappears and pure liquid titanium metal is formed (see Figure 3). Further increases in temperature result in the formation of TiCl vapour and Ti vapour, thus reducing the amount of recoverable titanium. For the reaction of one mole of $TiCl_4$ with three moles of aluminum the optimum temperature, defined by the maximum equilibrium yield of liquid Ti, is about 2 200 K. At that temperature about 90 percent of the titanium fed to the reactor in the form of $TiCl_4$ can (at equilibrium) be converted to liquid Ti metal. The effect of temperature on the equilibrium composition of products resulting from the reduction of one mole of $TiCl_4$ with three moles of Al is shown in Figure 3.

TABLE III. LOW TEMPERATURE EQUILIBRIUM PRODUCT COMPOSITION OF Ti - Al SYSTEM

TEMP. (K)	m/n RATIO	PRODUCT COMPOSITION, %										
		$TiAl_3$	TiAl	Ti	Al	Al_2Cl_6	$AlCl_3$	$AlCl_2$	AlCl	$TiCl_4$	$TiCl_3$	$TiCl_2$
1 000	10.00	12.7	0.0	0.0	71.1	1.6	12.0	2.6	0.0	0.0	0.0	0.0
930	1.35	0.0	21.8	0.0	0.0	3.7	40.3	2.6	0.0	0.3	1.3	29.9
700	3.00	40.2	0.0	0.0	0.0	31.9	4.9	0.0	0.0	0.0	0.0	36.3
1 200	3.00	9.0	30.2	0.0	0.0	0.2	35.8	23.7	0.8	0.0	0.1	0.0

FIGURE 3

EQUILIBRIUM COMPOSITION FOR THE $TiCl_4$ + 3 Al SYSTEM

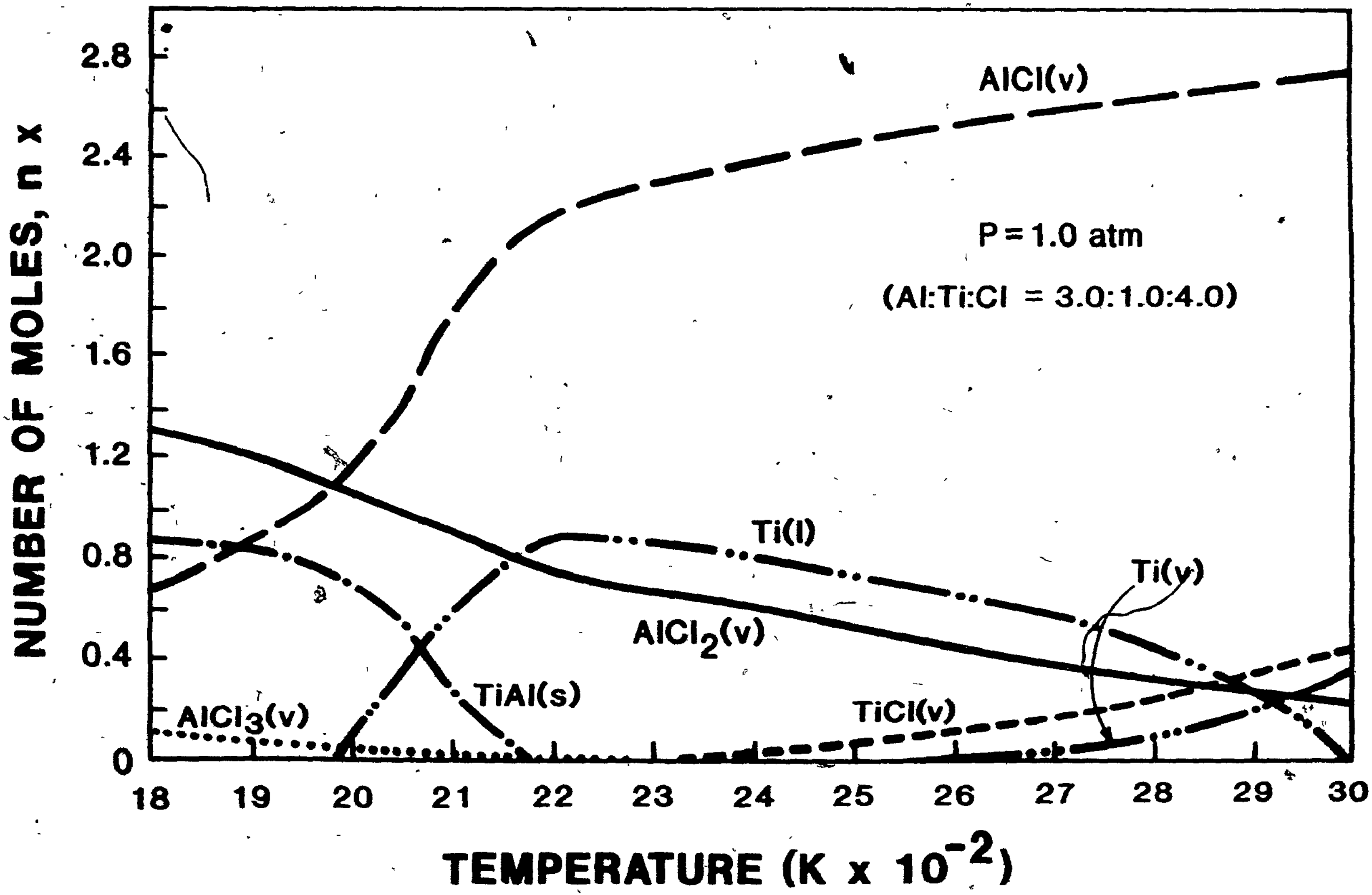
AlCl(v)
P = 1.0 atm
(Al:Ti:Cl = 3.0:1.0:4.0)
Ti(l)
Ti(v)
AlCl2(v)
TiAl(s)
AlCl3(v)
TiCl(v)
NUMBER OF MOLES, n x
0
0.4
0.8
1.2
1.6
2.0
2.4
2.8
18
19
20
21
22
23
24
25
26
27
28
29
30
TEMPERATURE (K x 10-2)

The operation of the proposed process at temperatures below 1 800 K was not considered promising in the present study. The factors contributing to this decision included: (1) the relatively high melting points of $TiAl_3$ and TiAl (1 613 K and 1 733 K, respectively) combined with the requirement to maintain a molten bath, and (2) the need to operate above the condensation temperature of all chlorides (chloride with highest boiling point: $TiCl_2$ at about 1 400 K) in order to minimize bath contamination. Consequently, all further thermodynamic considerations were limited to temperatures above 1 800 K, despite the fact that increases in operating temperature result in the formation of lower aluminum chlorides ($AlCl_2$ and AlCl instead of Al_2Cl_6 and $AlCl_3$) and therefore higher consumptions of aluminum metal.

The effect of the $Al/TiCl_4$ ratio is demonstrated in Figure 4. As the ratio increases both the maximum theoretical yield of liquid titanium and the optimum reaction temperature increase. The curves shown in Figure 4 represent the fraction of titanium tetrachloride reduced to liquid titanium at equilibrium and do not include other Ti products such as TiAl or Ti vapour. Evident from these curves is the fact that, theoretically at least, a substantial fraction of the titanium fed into a transferred-arc reactor should be collected in a molten aluminum bath anode. Furthermore, the actual yield of titanium metal is potentially higher than that indicated in Figure 4 since fewer titanium subchorides are likely to form from the reaction of a fully-dissociated $TiCl_4$ molecule with aluminum. In fact, it is likely that in

FIGURE 4

MAXIMUM THEORETICAL YIELD OF LIQUID TITANIUM METAL

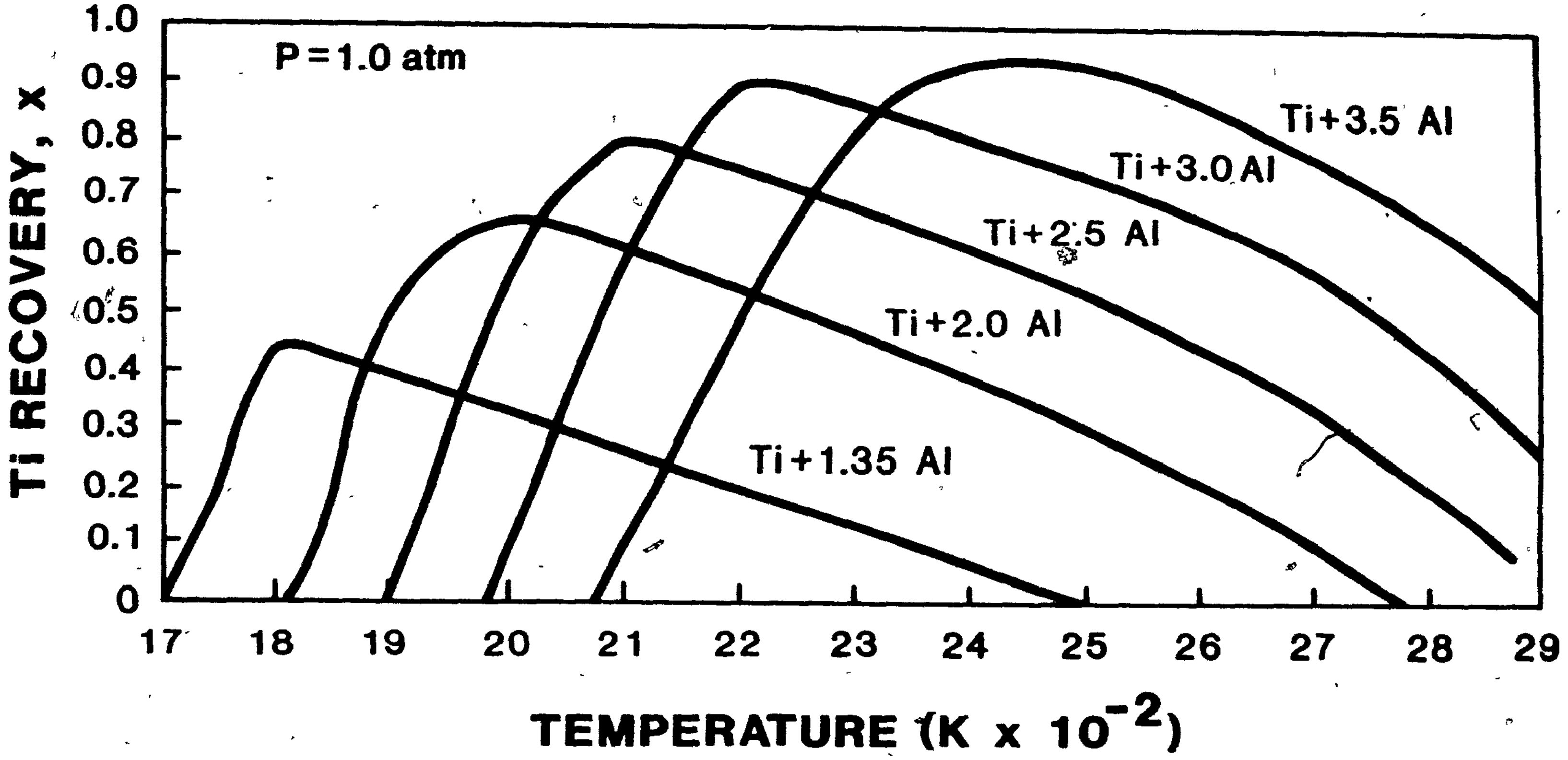

P = 1.0 atm
Ti RECOVERY, x
1.0
0.9
0.8
0.7
0.6
0.5
0.4
0.3
0.2
0.1
0
17
18
19
20
21
22
23
24
25
26
27
28
29
TEMPERATURE (K x 10^{-2})
Ti+3.5 Al
Ti+3.0 Al
Ti+2.5 Al
Ti+2.0 Al
Ti+1.35 Al

a reactor system that permits extensive intimate contact between the plasma and the aluminum, thermodynamic considerations will pose a less severe limit on the titanium yield than the ability to collect the liquid titanium produced.

ii. Titanium Collection Efficiency in a Molten Aluminum Bath

Using the transferred-arc reactor, which was originally designed to investigate the technical potential of recovering the dissociated titanium atoms from a $TiCl_4$ plasma in a molten titanium bath, it was possible to assess the titanium collection efficiency in a molten aluminum bath. However, some caution should be exercised when these results are used to assess the potential of a process based on the plasma reduction of $TiCl_4$ with aluminum. The transferred-arc system used in the present study was a batch reactor in which a finite amount of aluminum was used to form the initial molten bath. Since no means were available through which more aluminum could be added during operation, the composition of the bath was constantly changing reflecting the bath's initial mass, the $TiCl_4$ feedrate, the Ti collection efficiency and the duration of the experiment rather than the thermodynamics of the $TiCl_4$/Al reaction. Consequently, a comparison between the collection efficiency measured experimentally and the maximum efficiency predicted by the thermodynamic analysis is not possible.

Another limitation of the reactor system used in this study was caused by the absence of aluminum from the hot region of the plasma. Just as was the case with the titanium and zirconium baths, there was no measurable vapourization of aluminum from the molten anode and therefore, no potential source of aluminum atoms within the plasma. Hence, the chemical reduction of titanium chlorides could only occur within the molten bath. The effect of this configuration on the reacting system can be demonstrated by the fact that while the average titanium concentration in the bath remained well below 50 % for all experiments, the titanium concentration at the surface of the bath was as high as 90 %. Clearly, the ability to reduce and capture any titanium chloride molecules that did not penetrate the surface was severely limited. A plasma reactor which would both allow continuous aluminum feeding and intimate contact between the reacting compounds would significantly improve the results.

No attempt was made to either control or measure the molten bath temperature. Instead, the bath was allowed to operate at a steady state temperature which reflected the energy input from the arc and the energy losses to the anode cooling system and to radiation. The only precautions taken were to insure that the initial aluminum disc in the bath was fully melted and that the temperature of the latter was high enough to prevent the condensation of chloride within it. The complete melting of the initial aluminum disc was not a problem in either the water-cooled anode cup or the boron nitride crucible. However, some chlorine (likely in the form of titanium chloride) was identified in the molten bath contained by the water-cooled cup during the preliminary runs. This was corrected in later runs by replacing argon with helium as the main plasmagas whenever the water cooled anode cup was utilized. The resulting increase in the energy transferred to the anode raised the bath temperature to a point where the presence of chlorides in the final product was prevented. No measurable vapourization of aluminum occurred as a result of this change.

Despite the limitations expressed above, the results of this study provide useful and highly encouraging evidence of the possibility of producing dense titanium metal through the one-step reduction of $TiCl_4$ with aluminum in a plasma reactor. A summary of these results is shown in Table IV. Roughly 60 percent of all titanium fed into the reactor in the form of $TiCl_4$ was captured in the molten bath. The titanium yield (% of Ti fed into reactor that is captured in the bath) varied only slightly between runs. Runs which utilized a larger molten bath surface appear to have a somewhat higher yield, though the difference is too small (relative to the expected systematic error) to be conclusive.

The concentration of titanium was not evenly distributed within the bath. Regions closer to the center of the bath were characterized by higher titanium concentrations when compared to regions near the edge of the anode crucible. Based on this observation, it may be speculated that region of the bath near the center was agitated vigorously by the

TABLE IV. EFFICIENCY OF TITANIUM RECOVERY IN A MOLTEN ALUMINUM BATH

RUN No.	Al DISC DIAMETER (cm)	$TiCl_4$ FEED DURATION (min)	Ti BATH CONCENTRATION[1] (%)	TOTAL Ti RECOVERED (g)	Ti YIELD (%)	Al REMOVED (g)	m/n RATIO[2]
112	6.4	5	1 - 18 (5.5)	4.6	61	8.8	3.4
113	2.6	5	11 - 35 (19)	4.2	56	7.8	3.3
114	6.4	3	0 - 11 (3.3)	2.8	62	4.9	3.1
116	2.6	2	4 - 10 (6.4)	1.7	57	3.9	4.1
117	2.6	4	14 - 43 (27)	3.5	58	6.4	3.2

For all runs the arc current was 200 A, the arc length 2.5 cm, the main plasmagas flowrate 30 L/min and the $TiCl_4$ feedrate 6 g/min. In runs 112 and 114 helium was the main plasmagas whereas in runs 113, 116 and 117 argon was used.

1. Range indicates measured concentrations in various locations within bath whereas number in brackets indicate calculated average.

2. Moles of Al removed per mole of Ti recovered.

plasma resulting in the constant exposure of fresh aluminum to the chloride molecules of the plasmagas. Furthermore, some titanium atoms are likely to have diffused into the bath based on the mechanism described earlier for non-reducing baths. Near the edge of the bath, the mixing was much less vigorous and most collection of titanium occurred at the surface. Once the Ti concentration at the surface of these regions reached a high value there was little further Ti collection.

Experimental results seem to support the above speculation. Surface Ti concentration measurements were taken for a number of runs. In general, the surface concentration of Ti reflected the opposite pattern than the one observed deeper within the bath. For example, the measured Ti surface concentrations for Run No. 112 varied between 9 % and 24 % within a radius of 1.0 cm from the center of the bath but increased to values from 19 % to 38 % for the region lying between 1.0 and 2.0 cm from the center of the bath. In the peripheral region (beyond 2.0 cm from the center) Ti surface concentrations between 31 % and 86 % were measured. Immediately below the surface of these peripheral regions, the average concentration of Ti was only about 1 %.

Due to the large concentration gradients within the bath, an integrative technique was used to calculate the average titanium concentration of the bath. This technique involved the accumulation of sufficient measurements to allow for the segregation of the bath into smaller volumes of approximately equal concentration. By determining the mass of each of these volumes and their respective average Ti concentration, an integrated average Ti concentration was calculated. The total titanium recovered was estimated by multiplying the integrated average to the total mass of the bath.

Aluminum losses from the bath were calculated by comparing the mass of the initial aluminum disc to the mass of the final product minus the mass of the recovered titanium. No adjustments were made to reflect either mass gains due to contamination or mass losses due to vapourization. Results from experiments in which the plasmagas contained no $TiCl_4$ indicated that these two terms were small and approximately equal. Consequently, the final mass of molten aluminum in the inert-plasmagas experiments was roughly the same as the mass of the initial disc. If it is assumed that the amount of oxide and nitride contamination in the aluminum bath was about equal to that measured for non-reducing baths (about 0.5 g) the values shown in Table IV for "Al Removed" and "m/n Ratio" would be slightly higher.

CONCLUSIONS

An experimental study was used to assess the technical feasibility of dissociating $TiCl_4$ in a transferred-arc reactor and collecting titanium metal in a molten bath anode. Both non-reducing (titanium or zirconium) and reducing (aluminum) metals were used to form the initial molten bath. The results of this study led to the following conclusions:

1. When either titanium or zirconium was used as the initial bath constituent, there was a net loss of molten metal from the bath. While about 25 % of all titanium fed into the reactor in the form of $TiCl_4$ was collected in the bath as free titanium atoms, more than twice as much was removed from the bath due to chlorination reactions. There was no vapourization of metal from the bath.

2. When aluminum was used as the initial bath constituent, about 60 % of all titanium fed to the reactor in the form of $TiCl_4$ was collected in the bath. There were a little more than three moles of aluminum removed from the bath for every mole of titanium collected. The aluminum was removed due to chlorination reactions and there was minimum metal vapourization observed.

3. A thermodynamic analysis of the Al – $TiCl_4$ reaction suggests that significant amounts of liquid titanium metal can be produced through the high temperature reduction of $TiCl_4$ with Al. At atmospheric pressure, the titanium yield depends on the reaction temperature and the Al/$TiCl_4$ molar feed ratio. At a reaction temperature of 2 200 K and a molar ratio of 3,0, about 90 % of all Ti fed into the reactor as $TiCl_4$ can be converted to liquid Ti metal.

REFERENCES

Akashi, K., S. Ohno, R. Ishizuka, and T. Yoshida, "The Characteristics of Titanium Microcrystals Formed from a Mixture of Titanium Tetrachloride and Hydrogen in an Argon Plasma Jet", Communications - Symposium International de Chimie des Plasmas, P. Fauchais (ed.), 3rd, Paper S.4.6., Limoges, France (1977).

Akashi, K., M. Nishimura, and R. Ishizuka, "The Vapor Phase Reactions in Plasma Jet Augmented by Inductive Coupling of r.f. Power with d.c. Arc", Conference Proceedings International Symp. on Plasma Chemitrsy, S. Veprek and Hertz J. (ed.), 4th, Zurich, Switz, 1, pp. 224-9 (1979).

Atamanov, V. M., A. I. Zhuzhunashyili, G. B. Leyadnyi, Yu. F. Nasedkim, V. A. Nikiforov, and N. N. Timchenko, "Reduction of Metals in Steady-Stage Plasma-Beam Discharge Plasma", Zhurnal Tekhnicheskos Fiziki, 4, 49, (11) 2311-20 (1979).

Behnke, J.F., H. Lange, and H. E. Wagner, "Dissociation of Titanium Tetrachloride to Titanium in Hollow Cathode Discharges, Part I. Determination of the Dissociation Degree", Polish Journal of Chemistry, S6, (7-8-9), 1175-9 (1983).

Choi, H. K. and W. H. Gauvin, "Operating Characteristics and Energy Distribution in Transferred Plasma Arc Systems", Plasma Chemistry and Plasma Processing, Vol. 2, No. 4, pp.361-87 (1982).

Chou, T. S. and E. Pfender, "Spot Formation at the Anode of High Intensity Arcs", Warme und Stoffubertragung, Vol. 6, 2, 69 (1973).

Ciba Ltd., British Patent 1, 141, 775 (1969).

Dinulescu, H. A., and E. Pfender, "Analysis of the Boundary Layer of a High Pressure - High Current Arc", J. Appl. Phys., Vol. 51, p. 3149 (1980).

DiPietro, W. O., G. R. Findlay, and J. H. Moore, National Research Corp., AECD-3276, Final Report (December 30, 1948 through May 20, 1950).

Down, M. G., "Titanium Production by a Plasma Process", Westinghouse Research and Development Center, Pittsburgh PA., Final Technical Rept. 15 May 1980 - 15 Sept. 1981, 68P (May 1982).

Ecker, G., "Electrode Components of the Arc Discharge", Ergebuisse der Exakten Naturwiss, Vol. 33, 1 (1961).

Egi, K., "Reduction of Titanium and Zirconium Tetrachloride with Aluminum Alloy Catalysts", Japanese Patent 15796 (28 Feb., 1973).

Finkelnburg, W. and H. Maeker, "Elektrische Bogen und Thermisches Plasma", Handbuch der Physik, Vol. 22, Springer-Verlag, Berlin (1956).

Gyula, E., "Production of a Master Alloy from an Aluminum-Titanium Alloy by Reduction of Titanium Tetrachloride-with Aluminum", Ontöde, Vol. 17, No. 4, pp. 110-2 (1966).

Ingraham, T.R., K.W. Downes, and P. Marier, "The Production of Titanium Trichloride by Arc-Induced Hydrogen Reduction of Titanium Tetrachloride", Can. J. Chem., 35, 850 (1957).

Kikukawa, N., M. Makino, H. Matsumoto, and M. Horie, "Study on the Reduction of Titanium Compounds in a Hydrogen Plasma Jet", Kogai Shigen Kenkynsho Iho, Vol. 13, No. 2, pp. 13-22 (1983).

Maecker, H., "Ergebuisse derExakten Naturwiss", Vol. 25, 293 (1951).

Miller, R. C., and R. J. Ayen, "Reactions of Titanium Tetrachloride in a Radio-Frequency Plasma Torch", I. and E. C. Process Design and Development, Vol. 8, p. 371 (1969).

Newham, I. W., and J. A. Watts, "The Preparation of the Anhydrous Zirconium Trihalides", J. Amer. Chem. Soc., 82, 2113 (1960).

Ohno, S., R. Ishizuka, and K. Akashi, "The Formation of Titanium from Titanium Tetrachloride Introduced into an Argon Plasma Jet", Koon Gakkaishi S, (5) pp. 218-28 (1979).

Pfender, E., and E.R.G. Eckert, "Plasma Heat Transfer and Anode Phenomena in High Intensity Arcs", Research Proposal Submitted to the National Science Foundation (Nov. 1976).

Tsantrizos, P., and W. H. Gauvin, "Operating Characteristics and Energy Distribution in a Nitrogen Transferred Arc Plasma", The Canadian Journal of Chemical Eng., Vol. 60, No. 6, pp. 822-30 (1982).

Voest-Alpine, European Patent 134780 (March 20, 1985).

Westinghouse Electric Corp., United States Patent N . 4,080,194 (21 March, 1978).

APPENDIX I

TITANIUM CHEMISTRY

A complete review of the physical and chemical properties of titanium, its compounds and alloys has recently been published by the International Atomic Energy Agency (Kubaschewski and Komarek, 1983). The properties that are of particular interest to this project are briefly reviewed in this section.

1. Titanium

Titanium has five naturally occuring isotopes, with mass numbers ranging from 46 to 50. The percentage isotopic abundance of these isotopes, together with the atomic masses of the individual nuclides in atomic mass units (^{12}C scale) are listed in Table I (Friedlander et al, 1964). Also, in this table are the directly measured nuclear spins of the various nuclides and their thermal neutron cross-sections. The thermal neutron cross-section for the naturally occurring mixture of isotopes is 5.8 barn and the atomic weight is 47.90.

Titanium metal is dimorphic with a transformation temperature of 882.5°C. Below this temperature it exists in its α-Ti form in a hexagonal lattice, but above it in its β-Ti form in a cubic lattice. It is a silvery, ductile metal offering a rare combination of properties.

TABLE I. NUCLIDES OF TITANIUM

Nuclide	%	Isotopic Mass	Nuclear Spin	Cross-Sections for Thermal Neutrons (barn)
^{46}Ti	7.93	45.953	-	0.6
^{47}Ti	7.28	46.952	5/2	1.7
^{48}Ti	73.94	47.948	-	8.3
^{49}Ti	5.51	48.948	7/2	1.9
^{50}Ti	5.34	49.945	-	0.14

Source: Friedlander et al, 1964.

It is less dense than iron, much stronger than aluminium and almost as corrosion-resistant as platinum. Certain of its properties, such as its tensile strength, may be improved by alloying with aluminium. The $\alpha \rightarrow \beta$ transformation temperature is also higher for the aluminium alloy. Other useful alloys can be formed with molybdenum , manganese and iron. Some physical properties of titanium are listed in Table II (Clark et al, 1975).

Although titanium is considered to be physiologically inert, it exhibits tremendous affinity for oxygen, nitrogen and hydrogen at elevated temperatures. It is not attacked by mineral acids at low temperatures, or by hot aqueous alkali, but it dissolves in HF, HCl, H_2SO_4 and H_3PO_4. It is also attacked by four organic acids, namely oxalic, formic, trichloroacetic and trifluoroacetic, in hot concentrated solutions. It is also reactive to aluminium trichloride. The metal in powder form burns in air, and is the only element to burn in nitrogen. The corrosive action of the above compounds can be traced to their ability to attack the otherwise very stable oxide film which protects the metal surface. The extent of the attack can generally be reduced by the addition of an oxidizing agent such as nitric acid, which restores the oxide film and thus passifies the metal surface. Titanium reacts with many metals and non-metals (such as Al, Sb, Be, Cr, Fe and B) forming interstitial or intermetallic compounds.

TABLE II. PROPERTIES OF TITANIUM

Atomic Weight	47.90
Electronic Structure	$1S^2-2S^2-2p^6-3S^2-3p^6-3d^2-4$
Atomic Number	22
Ground State	$^3F_2$
Melting Point (°C)	1,677
Heat of Fusion, ΔH_{mole} (kcal $mole^{-1}$)	3.7
Boiling Point (°C)	3,277
Heat of Vaporization, ΔH_v (kcal $mole^{-1}$)	102.5 (at 3,277°C)
Transition Temperature, $\alpha \rightarrow \beta$ (°C)	882.5
Heat of Transition, ΔH_t (kcal $mole^{-1}$)	0.950
Lattice Parameters (Å), α-Ti	a=2.95030, c=4.68312
β-Ti	3.3065
Absolute Entropy, $S°_{298.15}$ (cal $mole^{-1}$ K^{-1})	7.33
Ionization Potential (eV), I1	6.82
I2	13.57
I3	27.47
I4	43.24
Atomic or Ionic Radius (Å), α-Ti (25°C)	1.45
β-Ti (900°C)	1.43
Ti^+	0.94
Ti^{2+}	0.76
Ti^{3+}	0.69
Ti^{4+}	0.64
Density (g/cc), α-Ti (25°C)	4.506
β-Ti (900°C)	4.400
Magnetic Susceptibility, $10^6 \chi_A$, 25°C (cgsu)	153
Electric Resistivity, 20°C (micro-ohm-cm)	42.0
Thermal Conductivity, 50°C (W/cm°C)	0.154
Heat of Atomization, ΔH_{f298} (kcal/gatom)	112.6
Thermal Neutron Absorp. Cross-Sect. (barn)	5.8

Source: Clark, R.J.H., et al. 1975.

ii. Titanium Halides

A detailed description of the chemistry of titanium and its halides is offered by Clark (1968). Some properties of titanium halides are summarized in Table III. Titanium tetrachloride, first synthesized in 1825, is of major industrial importance as an intermediate in the manufacture of most titanium products including titanium metal, synthetic rutile and various organo-titanium compounds. Some of its properties are listed in Table IV. It is rapidly hydrolysed in moist air to yellowish-white oxychlorides and hydrogen chloride. It can be reduced to the trichloride by hydrogen and to elementary titanium by various metals, such as sodium and magnesium.

TABLE III. PROPERTIES OF TITANIUM HALIDES

Compound S°(298)	M.W.	Colour	M.P. (°C)	B.P. (°C)	ρ (20°C) (gm.cm^{-3})	$\Delta H_f{}^{\circ}{}_{298}$ (kcal.mole^{-1})	$S^{\circ}{}_{298}$ (e.u.)
TiF_4	123.89	White	-	284	2.798	-394.2	32.0
$TiCl_4$	189.71	Colourless	-24	136.4	1.702	-192.6	81.5
$TiBr_4$	367.54	Orange	39	233	3.25	-147.9	57.6
TiI_4	555.50	Dark-brown	150	377	4.40	- 92.2	-
TiF_3	104.89	Blue	930	-	2.98	-338.1	-
$TiCl_3$	154.26	Red-violet	425	-	2.66	-172.3	33.4
$TiBr_3$	287.63	Blue-Black	400	-	4.24	-130.6	42.2
TiI_3	428.60	Violet	350	-	-	- 80	46.0
$TiCl_2$	118.81	Black	1,035	1,500	3.13	-122.4	24.3
$TiBr_2$	207.72	Black	400	-	4.41	- 95.3	29.5
TiI_2	301.70	Black	480	-	4.99	- 61	32.5

<u>Source:</u> Clarc, R.J.H., 1968.

TABLE IV. PROPERTIES OF TITANIUM TETRACHLORIDE

Molecule	$TiCl_4$ (covalent liquid)
Molecular Symmetry	T_d, 43m (tetrahedral)
r (Ti-CI), (Å)	2.170 ± 0.002
Angle CI-Ti-CI	109.5°
Viscosity, (dyne.sec.cm^{-2})	0.007921 (20°C)
Specific heat, Cp (cal.mole^{-1})	
Liquid	36.5 (20°C)
Vapour	24.1 (136°C)
Vapour Pressure (mm)	$\log_{10}P = 6.79094 - 1348.56(T+208.52)^{-1}$ (at 90° - 142°C)
Latent Heat of Vaporization, ΔH_{298} (kcal.mole^{-1})	10.06

<u>Source</u>: Clark, R.J.H., 1968.

REFERENCES

Clark, R. J. H. et al, "The Chemistry of Titanium, Zirconium and Halnium", Pergamon Texts in Inorganic Chemistry, Vol. 19, Perganon Press (1975).

Clark, R. J. H., "The Chemistry of Titanium and Vanadium: An Introduction to the Chemistry of the Early Transition Elements", Elsevier, Amsterdam (1968).

Friedlander, G., J. W. Kennedy, and J. M. Miller, "Nuclear and Radiochemistry", 2nd ed., John Wiley and Sons, New York (1964).

Kubaschewski, O., and H. L. Komarek, "Titanium: Physico-Chemical Properties of its Compounds and Alloys", International Atomic Energy Agency, Atomic Energy Review, Special Issue No. 6, Vienna (1983).

APPENDIX II

CONTRIBUTIONS TO KNOWLEDGE

The author considers the following results from this thesis as contributions to knowledge:

1. The stabilization and characterization of a transferred-arc plasma which utilizes a plasmagas rich in a metal tetrahalide.
2. The use of tantalum carbide, both thoriated and non-thoriated, for a cathode in a transferred-arc reactor.
3. The reduction of titanium tetrachloride to titanium metal in a plasma reactor using aluminium as the reducing agent.
4. The demonstration of thoria mobility in the thoriated tungsten alloy during its operation as a cathode in a transferred-arc reactor.
5. The demonstration of a thermionic-cathode erosion mechanism based on the vapourization ond redeposition of material on the cathode's surface.

APPENDIX III

RECOMMENDATIONS FOR FUTURE RESEARCH

Areas in need of further research relevant to the present thesis are:

1. The characterization of longer (3 to 30 cm) titanium tetrachloride transferred-arcs.

2. The production of a dense (close to theoretical density) tantalum carbide rod which can be used as a cathode in plasmas utilizing a chloride-rich plasmagas.

3. Further research on the phenomena occurring on the surface of thoriated tungsten cathodes during their operation in a transferred-arc reactor.